Multinuclear NMR spectroscopy of transition metal complexes.

Thesis

MULTINUCLEAR NMR SPECTROSCOPY OF TRANSITION METAL COMPLEXES

by

Ruth Anne Grieves

Submitted for the Degree PhD.

Chemistry

1985

All the work described in this thesis is my own unless stated to the contrary and has not been submitted for any other degree or qualification at any University or other institution.

Date of Submission: 8.8.85
Date of Award: 14.3.86

Abstract

^{95}Mo n.m.r. spectroscopic data for a variety of inorganic and organometallic compounds have been obtained, extending the known chemical shift range to -2953 ppm ($[Mo(\eta\text{-}C_5H_5)_2H_3]^+$) (chapter 6) to 4185 ppm ($[Mo_2(O_2CCF_3)_4]$ in pyridine) (chapter 8). Results from photoelectron spectroscopy, electronic spectroscopy and ^{13}C n.m.r. have been used to interpret ^{95}Mo chemical shift differences (chapters 4-9). Initial investigations have suggested a correlation between temperature independent paramagnetism and molybdenum deshielding (chapter 12). The following trends in molybdenum shielding have been noted:

Greater π-delocalisation of a polyhapto-benzene, an increase in the size of a polyhapto ring or an increase in the chain length of an acyclic polyene deshields the molybdenum (chapters 4,5,7);

Protonation of a molybdenum species leads to increased metal shielding if the protonation involves stabilisation of an electron pair previously localised on the metal, to form a metal-hydrogen σ-bond (chapters 6,7);

Trends in molybdenum shielding with varying group V ligands observed for substituted molybdenum carbonyl compounds have been seen in other types of organometallic molybdenum compounds (chapter 7);

For molybdenum-molybdenum bonded dimers with similar ligands preliminary studies indicate that molybdenum shielding decreases

$Mo\overset{1}{-}Mo > Mo\overset{2}{-}Mo > Mo\overset{3}{-}Mo > Mo\overset{4}{-}Mo$ (chapter 8).

Molybdenum-molybdenum sulphur bridged dimers and clusters have a large chemical shift dispersion and their study by ^{95}Mo n.m.r. suggests that the technique may be useful in catalytic and enzymatic investigations (chapter 9).

Piano-stool compounds often give narrow molybdenum n.m.r. signals presumably related to a low electric field gradient about the metal. When the resonances are sharp molybdenum-phosphorus coupling may be resolved, the variations in magnitude of which may be traced to changes in the Fermi contact term (chapters 4,5).

Direct observation of ^{183}W resonances of organometallic compounds presents several problems but the use of the DEPT pulse sequence greatly enhances the sensitivity enabling signals to be obtained for tungsten hydrides (chapter 11).

Acknowledgements

I would like to thank Dr. Joan Mason, Dr. Jenny Green and Dr. Malcolm Green for their help and guidance;

Gordon Howell for his assistance and patience in obtaining spectra on the Jeol FX90Q;

Drs. O. Howarth and E. Curzon for obtaining spectra on the SERC high field service Bruker 400 n.m.r. spectrometer at Warwick University;

Dr. S. Swithenby and his assistants for the magnetic susceptibility measurements;

Mr. G. Wilkinson, the glassblower at the Inorganic Chemistry Laboratory, Oxford;

Mrs. Anne Earls and Mrs. Shirley Foster for typing this thesis and all my friends at the Open University and Oxford University who have helped me, especially those who lent me samples (as indicated in the text), those who taught me the various synthetic techniques necessary for my work, particularly Olaf Kirchner, Geoff Cloke, Julian Wallis, Dermot O'Hare, Ilse Treurnicht and Ged Parkin, and those who let me stay with them during my trips to Oxford.

My thanks also to Nick Hazel who has been a constant source of support and encouragement.

Contents

List of Tables

List of Figures.

Abbreviations used in this thesis

Ligands

dppe	=	$Ph_2PCH_2CH_2PPh_2$
dppm	=	$Ph_2PCH_2PPh_2$
dmpe	=	$Me_2PCH_2CH_2PMe_2$
dmpm	=	$Me_2PCH_2PMe_2$
2,5 dth	=	$Me_2SCH_2CH_2SMe_2$
ox	=	oxalate
bpy	=	2,2'-bipyridine
phen	=	phenanthrene
bz	=	benzene
fv	=	fulvene
cp	=	η-C_5H_5
Pr^i	=	isopropyl

Physical Measurements etc.

h.o.m.o.	=	highest occupied molecular orbital
l.u.m.o.	=	lowest unoccupied molecular orbital
p.e.s.	=	photoelectron spectroscopy
i.e.	=	ionization energy
i.r.	=	infrared
n.r.	=	not resolved
n.o.	=	not obtained

Note - Throughout this thesis where the h.o.m.o.-l.u.m.o. gap is discussed with reference to nuclear shielding it is assumed that it is that which is appropriate for rotation of charge.

Chapter 1

Introduction: Objectives and Scope of this thesis

Table 1 shows the important n.m.r. parameters for the n.m.r. active molybdenum isotopes. When this work began the majority of published work on ^{95}Mo n.m.r. had focussed on dioxomolybdenum compounds, carbonyl compounds containing group V donor ligands and some organomolybdenum compounds with polyhapto ligands.

The general aims of this research were to develop the use of ^{95}Mo n.m.r. spectroscopy in molybdenum chemistry, particularly organometallic chemistry, including a study of metal-metal bonds (single, multiple and in clusters); to study ^{183}W by direct n.m.r. methods, and to compare the results with ^{95}Mo n.m.r. and to relate the n.m.r. parameters to results from other physical methods, including electronic spectroscopy, p.e.s. and atomic susceptibility (using SQUID) so as to elucidate the factors determining the shielding, linewidths and coupling constants.

With additional access to the specialist facilities available in the laboratories of Drs J.C. and M.L.H. Green, Inorganic Chemistry laboratory, Oxford, it has been possible to synthesise air and moisture sensitive organometallic compounds, including some by metal vapour synthesis, which are difficult or impossible to obtain by other methods. Also they have generously allowed themselves and their students to be used as a source of many molybdenum and tungsten compounds for measurement by metal n.m.r. spectroscopy. Dr. J.C. Green has made available p.e.s. results for some of the molybdenum compounds studied and Dr. S. Swithenby, of the Open University Physics Department, has measured molecular susceptibilities using his SQUID.

	^{1}H	^{13}C	^{95}Mo	^{97}Mo
Resonant Frequency /MHz at 2.3488 T.	100	21.45	6.516	6.653
Natural Abundance /%	99.99	1.11	15.72	9.46
Relative Sensitivity for Equal nos. of Nuclei	1	1.6×10^{-2}	3.2×10^{-3}	3.4×10^{-3}
Receptivity	1	1.8×10^{-4}	5.0×10^{-4}	3.2×10^{-4}
Electrical Quadrupole Moment /10^{-24} cm^2	-	-	-0.019 ± 0.012[a]	0.13
Nuclear Spin	$\frac{1}{2}$	$\frac{1}{2}$	$\frac{5}{2}$	$\frac{5}{2}$

a C.M. Lederer, V.S. Shirley, 'Table of Isotopes', Appendix VII; Wiley, N.Y.(1978).

Table 1 N.m.r. Parameters for the Magnetically Active Isotopes of Molybdenum.

Chapter 2: Literature Survey

^{95}Mo

The first solution ^{95}Mo resonance was reported in 1975.[1] Since then chemical studies on ^{95}Mo n.m.r. have covered several different types of compound and produced a chemical shift range of about 7 000 ppm. The oxidised state of the molybdenum centres of enzymes such as sulphite oxidase and nitrate reductase are believed to have a $[MoO_2]^{2+}$ core so dioxomolybdenum complexes have attracted the attention of ^{95}Mo n.m.r. spectroscopists.[2] The active form of xanthine oxidase is thought to contain an Mo(VI) atom with one terminal oxo and one terminal sulphide group (MoOS) whereas the inactive cyanolysed form of the enzyme is postulated to have two terminal oxo groups (MoO_2). So it is of potential interest that interconversions of dioxomolybdenum compounds of terminal O, S and Se groups can be followed by ^{95}Mo n.m.r.[3]

As a first step in establishing the feasibility of direct observation of ^{95}Mo n.m.r. signals in some biochemical systems it has been shown that it is possible to observe signals of ^{95}Mo-enriched $[MoO_4]^{2-}$ and $[MoS_4]^{2-}$ bound to the protein bovine serum albumin(BSA).[4] Rapid chemical exchange between the free and bound anion means that the observed shift is a weighted average. A plot of $\delta^{95}Mo$ versus [BSA]/[Mo] fits well a simple model of six equivalent binding sites per BSA for $[MoS_4]^{2-}$ but a crude model is inaccurate for $[MoO_4]^{2-}$. However, work defining the ^{95}Mo n.m.r. characteristics of S-donor ligand complexes containing $[MoO]^{4+}$, $[MoN]^{3+}$ and $[Mo(NPh)]^{4+}$ moieties has a less optimistic conclusion. It reports that the relative intrinsic linewidths of the various coordination environments and the effect of steric bulk on the

molecular correlation time have been determined by successively increasing the alkyl chain length of the dithiocarbamato ligands of the complexes and that these results suggest that the observation of ^{95}Mo n.m.r. signals from molybdoenzymes will be difficult.[5] Attention has also been focussed on molybdenum-sulphur clusters. Those of the type Fe_3MoS_4 provide possible models for the molybdenum co-factor of the nitrogenase molybdoferredoxin protein and Mo-S-Cu clusters may provide information on the biological antagonism between molybdenum and copper which leads to a copper deficiency, particularly in ruminant animals.[6] ^{95}Mo n.m.r. has been used to establish the integrity and structures of Cu-Mo-S clusters in solution. Anionic complexes of the general formula $[(XCu)_nMoS_4]^{2-}$ n = 1-4 can be readily distinguished from one another by ^{95}Mo n.m.r. and so this technique provides a simple direct probe for determining the $CuX:MoS_4$ ratio for unknown complexes in solution.[7]

^{95}Mo n.m.r. has been used as an aid in structural problems. For example ^{95}Mo n.m.r. has helped to confirm that solutions of the Mo(IV) aquo ion in acid media contain a high proportion of $[Mo_3O_4(H_2O)_9]^{4+}$ and simple complexes derived from it by substitution of the water ligands.[8]

The wide range of known molybdenum carbonyl compounds has enabled a systematic study of the effects of varying ligands. The narrow signals often observed in such compounds have meant that information on $^{95}Mo-^{31}P$ coupling may be extracted (see Chapter 3.3). Successive substitution of carbonyl by a phosphine or nitrogen donor leads to decreased shielding in the order $[Mo(CO)_6] > [Mo(CO)_5L] > [Mo(CO)_4L_2] > [Mo(CO)_3L_3]$. ^{95}Mo shielding increases with the atomic number of the group V donor atom for a given type of complex.[9,10]

N < P < As < Sb

This is related to nephelauxetic effects (see Chapter 3.1). Transition metal shielding has also been related to the spectrochemical series, ^{95}Mo shielding decreasing in the order PF_3 ∿ phosphite ∿ CO > phosphine > MeCN > pyridine ∿ piperidine > N_2 > NO(linear).[11]

The relationship between the paramagnetic term and transition metal shielding (see Chapter 3.1) has been illustrated by correlations between the highest frequency uv-visible band and the ^{95}Mo chemical shift, for example for the series $[cis\text{-}Mo(CO)_4(PPh_2R)_2]$.[12] However there will only be a correlation if the appropriate band in the uv-visible spectrum is used as shown in a study of complexes containing the unit $[Mo(X)_2]^{2+}$ X = O, CO, NO.[13]

Molybdenum-nitrosyl compounds have been studied partly because the NO^+ ligand is formally isoelectronic with N_2, the substrate of nitrogenase.[13,14]

^{95}Mo chemical shifts are often sensitive to distant substituent changes. For example, in $[Mo(\eta^5\text{-}C_5H_5)(CO)_3CH_2C_6H_4R]$ the ^{95}Mo chemical shift has a range of 40 ppm, shielding increasing from 4-CF_3 substitution to 2,4,6-Me_3 substitution on the benzene ring.[15]

That there are several factors determining the molybdenum and phosphorus chemical shifts is shown by the lack of correlation between $\delta^{95}Mo$ and $\delta^{13}P$ in compounds of the type [$Mo(CO)_5$phosphine] unless the P-donor ligands have a constant cone angle such as in the series $[Mo(CO)_5PPh_2OC_6H_4\text{-}p\text{-}R]$.[16]

The sensitivity of $\delta^{95}Mo$ to small changes in the environment of the molybdenum nucleus has been shown also by the direct

observation of diastereomers by ^{95}Mo n.m.r.[17] and that it is possible to differentiate the two chemically distinct molybdenum environments in the species $[\{Mo(CNCMe_3)_4(N\text{-}N)\}_2(\mu\text{-}CN)X_3]$ N-N = bpy, Me_2bpy, phen.[18]

Studies on organometallic species have included cyclopentadienyl molybdenum carbonyls,[19,20] substituted benzene molybdenum tricarbonyls, where ^{95}Mo shielding was found to decrease with increasing Mo-arene bond strength,[21] molybdenum-carbonyl-polyene compounds[22] and 7-coordinate isocyanide complexes of the type $[Mo(CNR)_{7-n}L_n][PF_6]_2$.[18]

^{183}W

Much work has been done on direct ^{183}W observation in polytungstates and heteropolytungstates.[23] These investigations have included structural characterisation and have used coupling to other nuclei including ^{183}W. 2-D n.m.r. has been used to establish the connectivity of various W atoms via $^{183}W\text{-}O\text{-}^{183}W$ couplings.[31]

^{183}W chemical shifts have been recorded directly for the series $[WO_{4-n}Sn]^{2-}$ n = 0-4 and related silver or copper cyanide complexes[24] and two ditungsten tetracarboxylate quadruply bonded compounds.[25] The shifts of the former series were found to parallel those of the molybdenum analogues.

Direct observation of ^{183}W is difficult and time consuming so indirect methods such as double and triple resonance experiments have been used. These make use of the resolvable coupling to ^{183}W of ^{1}H, ^{13}C, ^{19}F and ^{31}P.[26,27,28] Mononuclear organotungsten species with cyclopentadienyl and carbonyl ligands and carbonyl-phosphine compounds are amongst those studied in this way. Again, the trends in ^{183}W shielding follow those found in ^{95}Mo n.m.r.[29]

It has been demonstrated that the use of $Cr(acac)_3$ as a relaxation agent helps in the direct observation of ^{183}W signals of $[W(CO)_5L]$ (where L = CO or phosphine).[30]

References for Chapter 2

1 R.R. Vold, R.L. Vold, J. Magn. Reson., 1975, 19, 365.

2 M. Minelli, K. Yamanouchi, J.H. Enemark, P. Subramanian, B.B. Kaul, J.T. Spence, Inorg. Chem., 1984, 23, 2554.

3 M. Minelli, J.H. Enemark, K. Wieghardt, M. Hahn, Inorg. Chem., 1983, 22, 3952.

4 S. Bristow, C.D. Garner, S.K. Hagyard, G.A. Morris, J.R. Nicholson, C.F. Mills, J. Chem. Soc. Chem Commun., 1985, 479.

5 M. Minelli, C.G. Young, J.H. Enemark, Inorg. Chem., 1985, 24, 1113.

6 S.R. Acott, C.D. Garner, J.R. Nicholson, W. Clegg, J. Chem. Soc. Dalton Trans., 1983, 713.

7 M. Minelli, J.H. Enemark, J.R. Nicholson, C.D. Garner, Inorg. Chem., 1984, 23, 4384.

8 S.F. Gheller, T.W. Hambley, R.T.C. Brownlee, M.J. O'Connor, M.R. Snow, A.G. Wedd, J. Am. Chem. Soc., 1983, 105, 1527.

9 E.C. Alyea, A. Somogyvari, Proceedings of the Climax Fourth International Conference on the Chemistry and uses of Molybdenum (H.F. Barry and P.C.H. Mitchell eds.) Climax Molybdenum Company, Ann Arbor, Michigan, 1982, p46.

10 A.F. Masters, G.E. Bossard, T.A. George, R.T.C. Brownlee, M.J. O'Connor, A.G. Wedd, Inorg. Chem., 1983, 22, 908.

11 S. Donovan-Mtunzi, M. Hughes, G.J. Leigh, H. Modh. Ali, R.L. Richards, J. Mason, J. Organomet. Chem., 1983, 246, C1.

12 G.M. Gray, C.S. Kraihanzel, Inorg. Chem., 1983, 22, 2959.

13 M. Minelli, J.L. Hubbard, J.H. Enemark, Inorg. Chem., 1984, 23, 970.

14 M. Minelli, J.L. Hubbard, D.L. Lichtenberger, J.H. Enemark, Inorg. Chem., 1984, 23, 2721.

15 R.T.C. Brownlee, A.F. Masters, M.J. O'Connor, A.G. Wedd, H.A. Kimlin, J.D. Cotton, Org. Magn. Reson., 1982, 20, 73.

16 G.M. Gray, R.J. Gray, D.C. Berndt, J. Magn. Reson., 1984, 57, 347.

17 M. Minelli, T.W. Rockway, J.H. Enemark, H. Brunner, M. Muschiol, J. Organomet. Chem., 1981, 217, C34.

18 M. Minelli, J.H. Enemark, A. Bell, R.A. Walton, J. Organomet. Chem., 1985, 284, 25.

19 J.Y. Le Gall, M.M. Kubicki, F.Y. Petillon, J. Organomet. Chem., 1981, 221, 287.

20 M.M. Kubicki, R. Kergoat, J.Y. Le Gall, J.E. Guerchais, J. Douglade, R. Mercier, Aust. J. Chem., 1982, 35, 1543.

21 A.F. Masters, R.T.C. Brownlee, M.J. O'Connor, A.G. Wedd, Inorg. Chem., 1981, 20, 4183.

22 S. Dysart, I. Georgii, B.E. Mann, J. Organomet. Chem., 1981, 213, C10.

23 W.H. Knoth, P.J. Domaille, D.C. Roe, Inorg. Chem., 1983, 22, 198.

24 S.F. Gheller, T.W. Hambley, J.R. Rodgers, R.T.C. Brownlee, M.J. O'Connor, M.R. Snow, A.G. Wedd, Inorg. Chem., 1984, 23, 2519.

25 D.J. Santure, J.C. Huffman, A.P. Sattelberger, Inorg. Chem., 1985, 24, 371.

26 W. McFarlane, A.M. Noble, J.M. Winfield, J. Chem. Soc.(A), 1971, 948.

27 H.C.E. McFarlane, W. McFarlane, D.S. Rycroft, J. Chem. Soc. Dalton Trans., 1976, 1616.

28 I.J. Colquhoun, W. McFarlane, R.L. Keiter, J. Chem. Soc. Dalton Trans., 1984, 455.

29 G.T. Andrews, I.J. Colquhoun, W. McFarlane, S.O. Grim, J. Chem. Soc., Dalton Trans., 1982, 2353.

30 R.L. Keiter, D.G. Vander Velde, J. Organomet. Chem., 1983, 258, C34.

31 C. Brevard, R. Schimpf, G. Tourne, G.M. Tourne, J. Am. Chem. Soc., 1983, 105, 7059.

Chapter 3: Theoretical Background

Section 1: Shielding Theory[1]

By using perturbation theory Ramsey (1950) developed equations for the averaged nuclear magnetic shielding as the sum of two molecular terms

$$\sigma = \sigma_d + \sigma_p$$

σ_d represents the shielding due to "free" circulation of charge about the nucleus induced at the Larmor angular velocity by the magnetic field. This circulation opposes the applied field.

σ_p represents circulations of the valence electrons which reinforce the applied field. They are brought about by the partial unquenching of the orbital angular momentum of the valence electrons in the magnetic field.

$$\sigma_d = \frac{\mu_o e^2}{12\pi m} \langle o|\sum_j r_j^{-1}|o\rangle$$

$$\sigma_p = \frac{-\mu_o e^2}{12\pi m^2} \sum \left[\frac{\langle o|\sum_j \underline{L}_j|n\rangle\langle n|\sum_j (\underline{L}_j \underline{r}_j^{-3})|o\rangle + \text{c.c.}}{(E_n - E_o)} \right]$$

μ_o = permeability of free space

e = electronic charge

m = electronic mass

E_n = energy of the nth excited state

$\underline{L}$ = angular momentum vector of the jth electron

$\underline{r}$ = position vector of the jth electron

c.c. = complex conjugate

Ramsey's shielding terms are summed over the whole molecule. However local (atomic) shielding terms, initiated by Saika and Slichter, are more convenient, easier to calculate, and more

easily compared for the same nucleus in different molecules. The longer range diamagnetic and paramagnetic contributions to the shielding of the nucleus of interest roughly cancel so the use of local shielding terms is possible.

$$\sigma^{AA} = \sigma_d^{AA} + \sigma_p^{AA} + \Sigma\sigma^{AB}$$

The diamagnetic and paramagnetic terms are confined to electrons on the atom A, and $\Sigma\sigma^{AB}$ sums the contribution from other atoms B. For proton shielding variations in σ_d^{AA}, σ_p^{AA} and $\Sigma\sigma^{AB}$ are all important because of the small range of proton shifts and the proximity of circulations on neighbouring atoms. Other nuclei have much larger chemical shift ranges, σ_d^{AA} does not vary greatly from its free atom value and σ^{AB} terms are relatively small, usually difficult to calculate and are neglected.

An effective excitation energy can be used instead of the sum over excited states as in the Karplus-Pople (1963) expression for the shielding of second row elements, derived from Ramsey's theory of shielding.

$$\sigma_p^A = \frac{-\mu_o \mu_B^2}{2\pi(\Delta E)} \langle r^{-3} \rangle \Sigma Q$$

$$\mu_B = \text{Bohr magneton} = \frac{e\hbar}{2m}$$

The Q terms express the imbalance of charge in the valence shell and are obtained from the charge densities and bond orders.

Jameson and Gutowsky (1964) introduced a more general expression

$$\sigma_p^A = \frac{-2\mu_o \mu_B^2}{(\Delta E)} [\langle r^{-3} \rangle_{np} P_i + \langle r^{-3} \rangle_{nd} D_i]$$

P_i and D_i represent the imbalance of the valence electrons in the p and d orbitals resepectively of the atom A.

This expression gives the same results as that of Griffith and Orgel (1957). They used Ramsey's shielding theory, Saika and Slichter's local term approximation and crystal field theory to develop an expression for the paramagnetic term for d^6 (low spin) Co(III) complexes.

$$\sigma_p = \frac{-\mu_o}{4\pi} \frac{4\mu_B^2 \langle r^{-3} \rangle_{3d}}{3\Delta_o} \langle o|\underline{L}^2|o\rangle$$

$\langle r^{-3} \rangle_{3d}$ is a quantum mechanical average of the inverse cube of the d electron radius

Δ is the octahedral crystal field splitting ($t_{2g} - e_g$)

Deshielding of the nucleus is due to circulations of t_{2g} electrons via e_g orbitals (unoccupied in the ground state). This idea is supported by the close correlation found between δ^{59}Co and the spectrochemical series of the ligands, and the temperature dependence of the chemical shifts. Increasing the temperature increases the population of the higher vibrational modes which tends to reduce Δ_o. In accord with this a small decrease in shielding with increasing temperature has been found with ^{59}Co, ^{195}Pt and ^{103}Rh, for example.

Buckingham and Stephens extended Griffith and Orgel's work to estimate the effects of the d-electron currents on a proton attached to a transition metal at a distance R from the metal nucleus. They examined d^6 octahedral and d^8 square planar complexes (the latter's excitation energies are shown below).

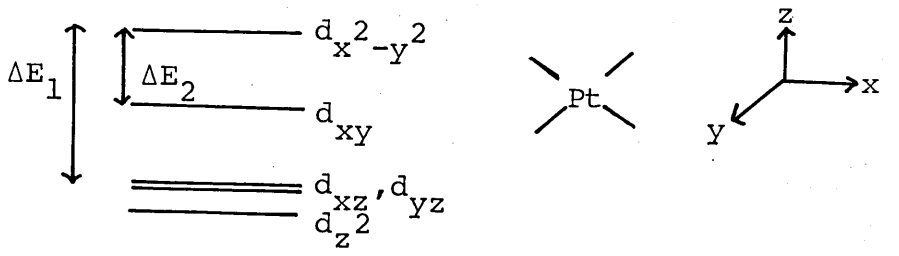

When R = O their equations give the transition metal shielding.

The most important limitation of Griffith and Orgel's approach is the neglect of covalent bonding. To make some allowance for covalency either an orbital reduction factor, $k_{\sigma\pi}$, between the t_{2g} and e_g orbitals of the crystal field model or a C_m^2 factor, where C_m is the coefficient of the metal orbital in the molecular orbital, have been introduced into the equation for σ_p.

Some values of k have been obtained for Co(III) complexes. Since the relative importance of $\langle r^{-3} \rangle_{nd}$ is greatest near the nucleus, where it is least affected by the ligands, it is taken as effectively constant. Values of k in Co(III) complexes of ligands of the first three rows of the Periodic Table were estimated as 0.85, 0.72 and 0.67 respectively.

Smaller radial terms ($k^2 \langle r^{-3} \rangle_{nd}$ or $C_m^2 \langle r^{-3} \rangle_{nd}$) in complexes compared to free ions are related to nephelauxetic effects in optical spectroscopy. The electron circulation is farther away from the metal nucleus and so the paramagnetic term is smaller. This may be the result of π-delocalisation of d electrons onto the ligands. Smaller radial terms (increased shielding) are also found where there are heavier, more polarisable, ligand atoms.

The results from shielding theory, using local shielding terms, of use in rationalising the chemical shift of a transition metal are:

(1) σ_d does not vary greatly for a given nucleus in different compounds so changes in σ_p are responsible for variations in shielding;

(2) shielding is reduced by circulations of valence electrons which reinforce the applied field. Thus it is reduced when:

(a) The electron circulation is nearer to the nucleus i.e. a larger radial term $\langle r^{-3} \rangle_{nd}$. This is linked with atomic charge and with nephelauxetic effects of ligands.

(b) The effective excitation energy for the rotation of charge is lower, i.e. a smaller ΔE term. This is linked with the spectrochemical series in transition metal chemistry.

(c) There is charge imbalance in the valence shell.

Section 2: Linewidths

While the quadrupolar nature of the isotope ^{95}Mo allows fast data accumulation, line broadening is a problem.

The linewidth at half height is given by

$$W_{\frac{1}{2}} = \frac{1}{\pi T_2}$$

where T_2 = transverse (spin-spin) relaxation time.

For mobile isotropic fluids in which the extreme narrowing conditions are fulfilled.

i.e. $\omega^2 \tau_c^2 \ll 1$

ω is the Larmor precession frequency in rad s^{-1}

τ_c is the correlation time

$T_1 = T_2 = T_q$

T_1 = longitudinal (spin-lattice) relaxation time

T_q = quadrupolar relaxation time

$$T_q = \frac{3}{40} \frac{(2I + 3)}{I^2(2I - 1)} \chi^2 \left(1 + \frac{\eta^2}{3}\right) \tau_c$$

For ^{95}Mo $(I = \frac{5}{2})$

$$T_q = \frac{3}{125} \chi^2 \left(1 + \frac{\eta^2}{3}\right) \tau_c$$

τ_c is the correlation time;

χ is the nuclear quadrupole coupling constant (NQCC) $= \frac{e^2qQ}{\hbar}$ (frequency units);

Q is the nuclear quadrupole moment (1.9×10^{-26} cm^2 for ^{95}Mo);

eq is the electric field gradient (efg) at the nucleus due to asymmetry in the valence shell;

η is the asymmetry parameter.

$$\eta = (q_{yy} - q_{xx})/q_{zz}$$

q_{xx}, q_{yy}, q_{zz} ($|q_{zz}| \geq |q_{yy}| \geq |q_{xx}|$) are the components of the electric field gradient.

By definition $\eta < 1$

For axial symmetry $\eta = 0$

Small changes in χ are significant because it occurs as its square; however changes in η are less significant since $\eta < 1$ and the term involved is $(1 + \frac{\eta^2}{3}) \cdot \tau_c$, the correlation time for the tumbling motion which mediates the relaxation process, roughly corresponds to the average time for the molecule to

rotate through one radian. When these motions are anisotropic, as in a flat or rod shaped molecule for example, τ_c is a weighted average for rotation about the different axes, an effective correlation time. For a spherical molecule of volume V

$$\tau_c = \frac{V\eta'}{kt} \qquad \text{(Debye-Stokes-Einstein theory)}$$

where η' is the viscosity

$$W_{\frac{1}{2}} \propto \eta'$$

As τ_c is inversely dependent on the temperature (though the kT term and the exponential decrease of η' with increasing temperature) the linewidth decreases sharply with increase in temperature. For example the linewidth of the $[MoO_2(acac)_2]$ ^{95}Mo resonance in MeOH varied from 73 Hz at 41 ^{o}C to 270 Hz at -34 ^{o}C.[2]

It is thought that the high viscosity of the 4 M acid solutions used made it difficult to observe ^{95}Mo signals in Mo(IV) aq systems at 0.01 - 0.05 M concentrations at room temperature. These problems were overcome by examining ^{95}Mo enriched samples at 50 ^{o}C.[3] Non spherical or asymmetric molecules may tumble more slowly so increasing τ_c and hence $W_{\frac{1}{2}}$. The NQCC is small for highly symmetrical molecules such as $[Mo(CO)_6]$ resulting in narrow lines. This term is affected by:

(1) rotational reorientation of the NQCC;

(2) collisions with solvent molecules;

(3) vibrationally induced electric field gradients.

χ will be large when the molecule has substituents of different polarities. However, it has been shown that the electric field gradient may be small in an apparently irregular environment.[4]

Relaxation times for ^{95}Mo range from 7 s in $[Mo(CO)_6]$ to 180 μs in $[Mo_2(O_2CBu^n)_4]$[5], the variation accounted for by the factors discussed here.

The charge imbalance terms in approximate shielding theory should increase with the electric field gradient. In accord with this some increase in δ with $W_{\frac{1}{2}}$ has been observed. However there are cases where the opposite relationship has been noted because a change in the energy term or the radial term swamps the effect of a change in the charge imbalance term. For example in the series $[MoXY(ONHR)_2]$ X = O, S, Se, Y = O, S [6] δ increases (O < S < Se) while the linewidth decreases (O > S > Se). The variation in shielding is ascribed to changes in ΔE. As the X and Y groups become less electronegative and the M-X and M-Y bonds then less polarised, the efg would decrease so decreasing $W_{\frac{1}{2}}$. However a corresponding decrease in Q and so increase in shielding is overborne by a decrease in ΔE.

So the factors affecting the linewidth for a given nucleus are:

(1) efg (measured by NQCC);

(2) size and shape of the molecule;

(3) temperature;

(4) viscosity of the sample solution;

(5) solvent-solute interactions.

Section 3: Coupling Constants

For two directly bound nuclei j and k the reduced coupling constant is given by

$$K_{jk} = K_{jk}^{(1)} + K_{jk}^{(2)} + K_{jk}^{(3)}$$

$K_{jk}^{(1)}$ arises from the interaction of nuclear spin and electron orbital motion

$K_{jk}^{(2)}$ arises from the interaction of nuclear spin and the dipole moments of the electrons

$K_{jk}^{(3)}$ represents the Fermi contact interaction. This is the major factor accounting for variations in the coupling constant. It requires a finite electron density at the nucleus and so only involves s electrons. Pople and Santry calculated it as

$$K_{jk}^{(3)} = (\frac{2}{3}\mu_o\mu_B)^2 \langle s_j|\delta(r_j)|s_j\rangle\langle s_k|\delta(r_k)|s_k\rangle \pi_{s_j s_k}$$

s_j and s_k are the valence shell s functions. The integrals $\langle s|\delta|s\rangle$ represent s electron density at the nucleus and π_{s_j,s_k} is the mutual polarisability of the atoms j and k and is the change in electron density in the s-orbital of one atom which arises when the energy of the other s-orbital changes. The sign of K depends on π_{jk} and this is determined by the relative energies of the various electronic excited states.

Absolute values of coupling constants increase with the electronegativity of substituents on either nucleus for given oxidation states and coordination numbers. This is because there is greater p character in the bonds to the electronegative substituents leaving greater s character at the coupled nuclei and the electronegative substituent

increases the effective nuclear charge causing orbital contraction. Both these factors increase the Fermi contact interaction term and so K increases. For example $^{1}J(^{95}Mo-^{31}P)$ in $[MO(CO)_5(phosphine)]$ complexes increases in the order $PR_3 < PAr_3 < P(NMe_2)_3 < P(OR)_3 < PCl_3 < PF_3$.[7]

Couplings between ^{95}Mo and ^{31}P, ^{17}O[8], ^{14}N[9], ^{13}C[10] and ^{1}H[11] have previously been observed. Values of $^{1}J(^{95}Mo-^{31}P)$ are generally of the order of a few hundred Hz and trends in $^{1}J(^{95}Mo-^{31}P)$ have been compared with $^{1}J(^{183}W-^{31}P)$ for corresponding compounds. Alyea et. al.[12] had only limited success when attempting to correlate $^{1}J(^{95}Mo-^{31}P)$ with pKa values for phosphines. The σ-donor properties of phosphines have been related to their basicities towards the proton, and studies have shown an inverse relationship between the ^{31}P coupling constant to ^{183}W (^{103}Rh and ^{195}Pt and a direct relationship to that of ^{199}Hg) with pKa. It was suggested that a synergic model of phosphine-metal bonding might give better correlations. In the case of tungsten a direct relationship had been observed between the coupling constant to ^{31}P and the C-O stretching vibrations, or the average Cotton-Kraihanzel force constants, for monosubstituted tungsten carbonyls. Preliminary results have shown that molybdenum follows this pattern.

Masters et. al.[11] obtained a linear relationship between $^{1}J(^{95}Mo-^{31}P)$ and $^{1}J(^{183}W-^{31}P)$ using 9 examples of $[Mo(CO)_5(PR_3)]$ (M = Mo,W) and concluded that common effects were operating. They suggest that the proposed correlation between a shorter W-P bond distance and a higher $^{1}J(^{183}W-^{31}P)$, where R = Ph,OPh, may apply for molybdenum systems too from comparison of the metal-phosphorus coupling constants in the corresponding molybdenum and tungsten compounds (where R = Ph,OPh and Bu^n_3, OBu^n_3).

Using more examples, McFarlane et. al.[13] using M(0) carbonyl derivatives, found that the experimental ratio $^{1}J(^{183}W\text{-}^{31}P)/^{1}J(^{95}Mo\text{-}^{31}P)$ in corresponding compounds is 1.76:1 which yields a ratio for the reduced coupling constants ($K_{xy} = J_{xy}\ 4\pi^2/h\gamma_x\gamma_y$) of 2.76:1. The magnitude of this ratio is attributed almost wholly to the smaller 5s electron density at the nucleus for molybdenum. Any deviations from this value of the reduced coupling constant ratio are small so indicating that the nature of the bonding is similar in corresponding compounds.

($^{95}Mo\text{-}^{31}P$) coupling was first observed in 1976 as satellites at the base of the proton decoupled ^{31}P spectra of $Mo(CO)_5L$[14] (L = phosphine ligand). It was thought that the coupling was between ^{31}P and both the naturally occurring Mo isotopes having spin $\frac{5}{2}$ (all other naturally occurring Mo isotopes having I=0). However it was later pointed out that the rate of ^{97}Mo quadrupolar relaxation is much too great for the detection of discrete satellites associated with this nucleus.[15]

The n.m.r. spectrum of a spin ½ nucleus bonded to a spin $\frac{5}{2}$ nucleus will consist of 6 lines of equal intensity, but only if the spin-lattice relaxation time (T_1) of the quadrupolar nucleus is long compared to the inverse of the coupling constant.[16] The line shape becomes more complex when these values are comparable. A series of lineshapes ~~have~~ has been calculated as a function of T_1 and J.

The general result is that as T_1 decreases the total width of the multiplet decreases and the lines acquire different widths until the individual components of the multiplet become unresolvable and a broad absorbance results.

Ultimately T_1 is much shorter than $1/J$ and the signal is a sharp singlet. $^1J(^{55}Mn-^{13}C)$ has been observed in the ^{13}C spectra for the series $[Mn(RNC)_6][BF_4]$ R = Et, Pr^i, Bu^t, cyclohexyl. Poorer resolution was obtained as the size of the R group increased.[17] It has been observed (see Chapter 7) for arene-molybdenum phosphine derivatives that only where a relatively sharp ^{95}Mo signal is observed are ^{95}Mo satellites observed for the ^{31}P resonance.

References for Chapter 3

1 J. Mason, Adv. Inorg. Chem. Radiochem., 1979, 22, 199.

2 S.F. Gheller, T.W. Hambley, P.R. Traill, R.T.C. Brownlee, M.J. O'Connor, M.R. Snow, A.G. Wedd, Aust. J. Chem., 1982, 35, 2183.

3 S.F. Gheller, T.W. Hambley, R.T.C. Brownlee, M.J. O'Connor, M.R. Snow, A.G. Wedd, J. Am. Chem. Soc., 1983, 105, 1527.

4 J.W. Akitt, W.S. MacDonald, J. Magn. Reson., 1984, 58, 401.

5 R.T.C. Brownlee, M.J. O'Connor, B.P. Shehan, A.G. Wedd, J. Magn. Reson., 1985, 61, 516.

6 M. Minelli, J.H. Enemark, K. Wieghardt, M. Hahn, Inorg. Chem., 1983, 22, 3952.

7 S. Donovan-Mtunzi, M. Hughes, G.J. Leigh, H. Modh. Ali, R.L. Richards, J. Mason, J. Organomet. Chem., 1983, 246, C1.

8 O. Lutz, W. Nepple, A. Nolle, Z. Naturforsch., 1976, 31a, 1046.

9 M. Minelli, J.L. Hubbard, K.A. Christensen, J.H. Enemark, Inorg. Chem., 1983, 22, 2652.

10 B.E. Mann, J. Chem. Soc., Dalton Trans., 1973, 2012.

11 A.F. Masters, G.E. Bossard, T.A. George, R.T.C. Brownlee, M.J. O'Connor, A.G. Wedd, Inorg. Chem., 1983, 22, 908.

12 E.C. Alyea, A. Somogyvari, Proceedings of the Fourth International Conference on the Chemistry and Uses of Molybdenum (H.F. Barry & P.C.H. Mitchell, eds.) Climax Molybdenum Company, Ann Arbor, Michigan, 1982, p.46.

13 G.T. Andrews, I.J. Colquhoun, W. McFarlane, S.O. Grim, J. Chem. Soc., Dalton Trans., 1982, 2353.

14 D.S. Milbrath, J.G. Verkade, R.J. Clark, Inorg. Nucl. Chem. Lett., 1976, 12, 921.

15 G.T. Andrews, W. McFarlane, Inorg. Nucl. Chem. Lett., 1978, 14, 215.

16 M. Suzuki, R. Kubo, Mol. Phys., 1963, 7, 201.

17 R.M. Nielson, S. Wherland, Inorg. Chem., 1984, 23, 3265.

Chapter 4: Substituted-Benzene Molybdenum Compounds

Section 1: Sandwich Compounds

^{95}Mo spectral data for a selection of bis(monosubstituted-arene) molybdenum compounds is shown in Table 4.1.1. The ^{95}Mo chemical shift is sensitive to the substituent on the ring, a range of over 250 ppm was found.

The electronic spectra of a representative sample of these compounds are shown in Figure 4.1.1. Little work has been done on the electronic spectra of bis-arene systems.[3] The only reported uv-visible spectrum for bis-arene compounds of Group VIB is that of $[Cr(\eta\text{-}C_6H_6)_2]$.[4] This consists of a broad band (ε = 25) at 640 nm and a stronger peak at 320 nm (ε = 8 000). The former was thought most likely to represent at least two d-d transitions with peaks at higher energies representing Laporte allowed transitions. The spectra of the bis-substituted benzene molybdenum compounds in this study are qualitatively similar, they generally consist of a broad complex band at long wavelengths with low extinction coefficient, assigned as d-d transitions and then to shorter wavelengths, there is a stronger band, with extinction coefficient of the order 10^2 - 10^3, rising to an absorption around 200 nm. The broadness and complexity of the low frequency absorptions precludes any detailed comparisons of the spectra but it may be noted that as the ^{95}Mo ~~chemical shifts~~ nuclei of these bis-substituted benzene molybdenum compounds become less shielded so the position of the bands in the electronic spectra move to longer wavelengths. This suggests a decrease in the h.o.m.o. - l.u.m.o. gap, in accordance with the dependence of $\delta^{95}Mo$ on the energy term from shielding theory. (see note under Abbreviations)

Table 4.1.1: Spectral data for bis-(monosubstituted arene) molybdenum compounds

	Solvent	δ^{95}Mo /ppm	$W_{\frac{1}{2}}$ /Hz	I.E. (eV) a_1	e_2	$e_1(\pi)$
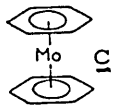 c	C_6H_5Me /C_6D_6	-1362	50	5.52	6.59	9.47, 10.15[a]
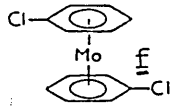 f	C_6H_5Me /C_6D_6	-1342	50			
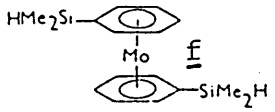 f	C_6H_5Me	-1332	120	5.45	6.62	9.16[b]
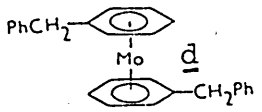 d	C_6H_5Me /C_6D_6	-1272	205			
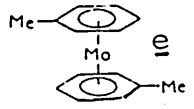 e	C_6H_5Me	-1270	55	5.32	6.33	9.05, 9.75[a]
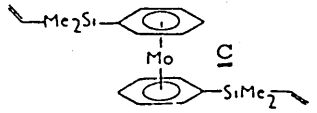 c	40/60 petrol	-1266				
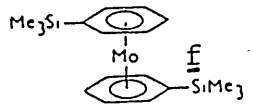 f	C_6D_6	-1246	215			
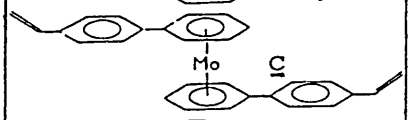 c	THF	-1107	200	sample decomposition[b]		
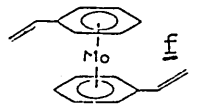 f	C_6H_5Me	-1098	60	5.48	6.60	8.69, 9.46[b]

a ref 1, b ref 2,

c compound supplied by I.Treurnicht

d compound supplied by P.R.Brown

e compound supplied by P.Newman

f compound supplied by author

Figure 4.1.1. Electronic Spectra of some Bis-(substituted benzene) Molybdenum Compounds.

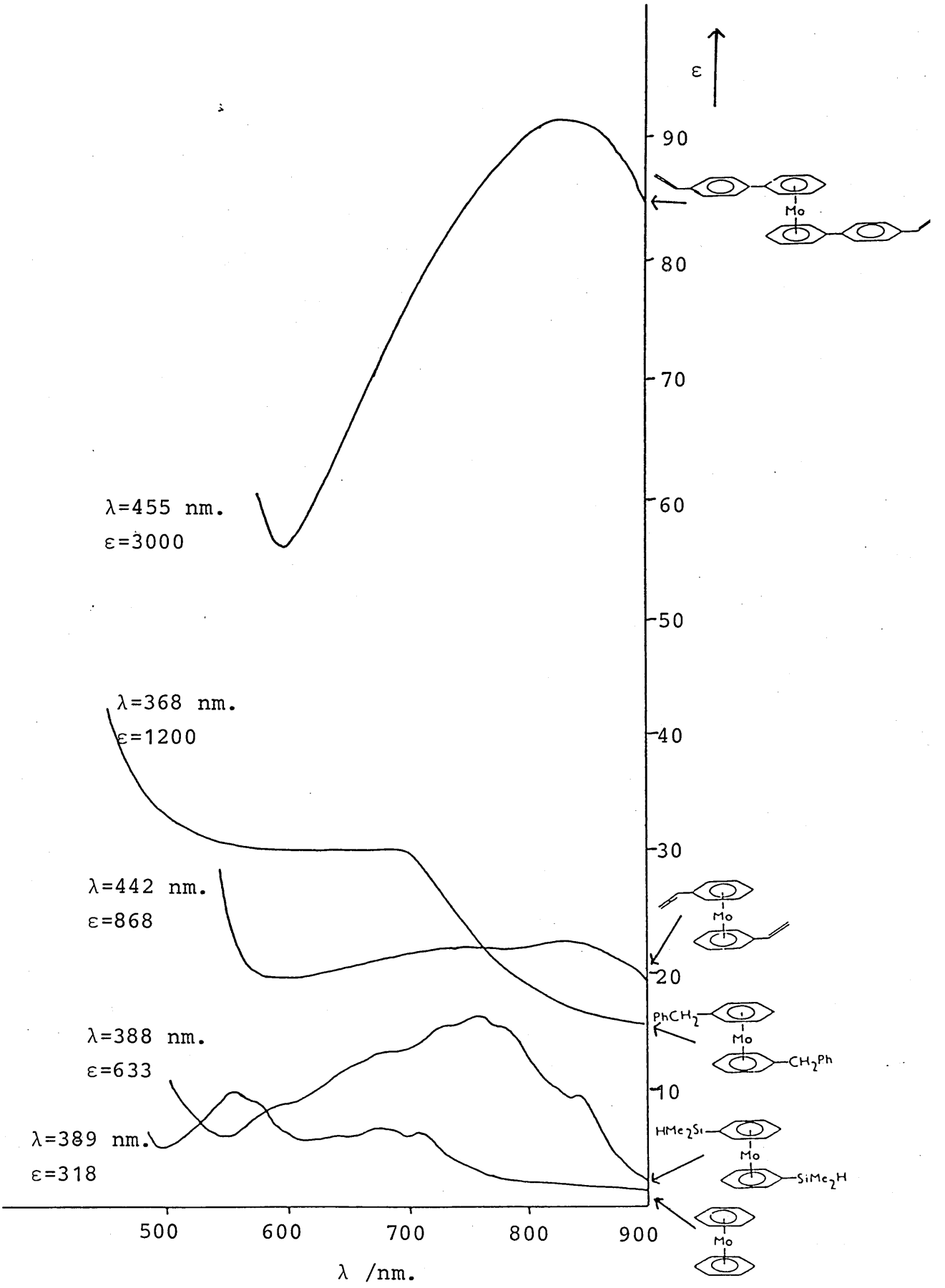

From p.e.s. studies m.o. diagrams have been proposed for bis-arene molybdenum compounds,[1] that for bis-benzene molybdenum is shown in Figure 4.1.2. There are two main factors determining the ionization energies of the metal based molecular orbitals, the a_1 and e_2 levels.[1]

(a) donor ability of the ligand which will be related to the energy of the e_1 ligand orbital relative to the metal acceptor orbital;

(b) the relative energies of the ligand acceptor and metal donor orbitals. The upper e_2 orbitals of the ligand are the lowest unoccupied orbitals and so important in electron withdrawal from the metal.

The a_1 level is mainly non-bonding and so will be primarily sensitive to the effective nuclear charge on the metal.

Extended Hückel calculations have been carried out on bis-benzene molybdenum and bis-styrene molybdenum[2]. There is greater 2 $p\pi$ delocalisation in bis-styrene molybdenum relative to bis-benzene molybdenum so there is a decrease in the π-π^* separation. As a result the metal based e_1^* orbital lowers in energy while the e_2 orbital becomes higher in energy so there is a decrease in the metal h.o.m.o. - l.u.m.o. gap as shown in the correlation diagram, Figure 4.1.3. This agrees with the observed decrease in shielding of the molybdenum in these compounds.

From the plot of i.e. vs $\delta^{95}Mo$ for these bis-arene molybdenum compounds (Figure 4.1.4) the energy of the e_1 donor bond to the metal decreases with a decrease in ^{95}Mo shielding. If this meant a reciprocal increase in the energy of the e_1^* metal based l.u.m.o. then the metal h.o.m.o. - l.u.m.o. gap could be

Figure 4.1.2. Frontier Molecular Orbital Diagrams for Bis-benzene molybdenum and Bis-styrene molybdenum[1,2]

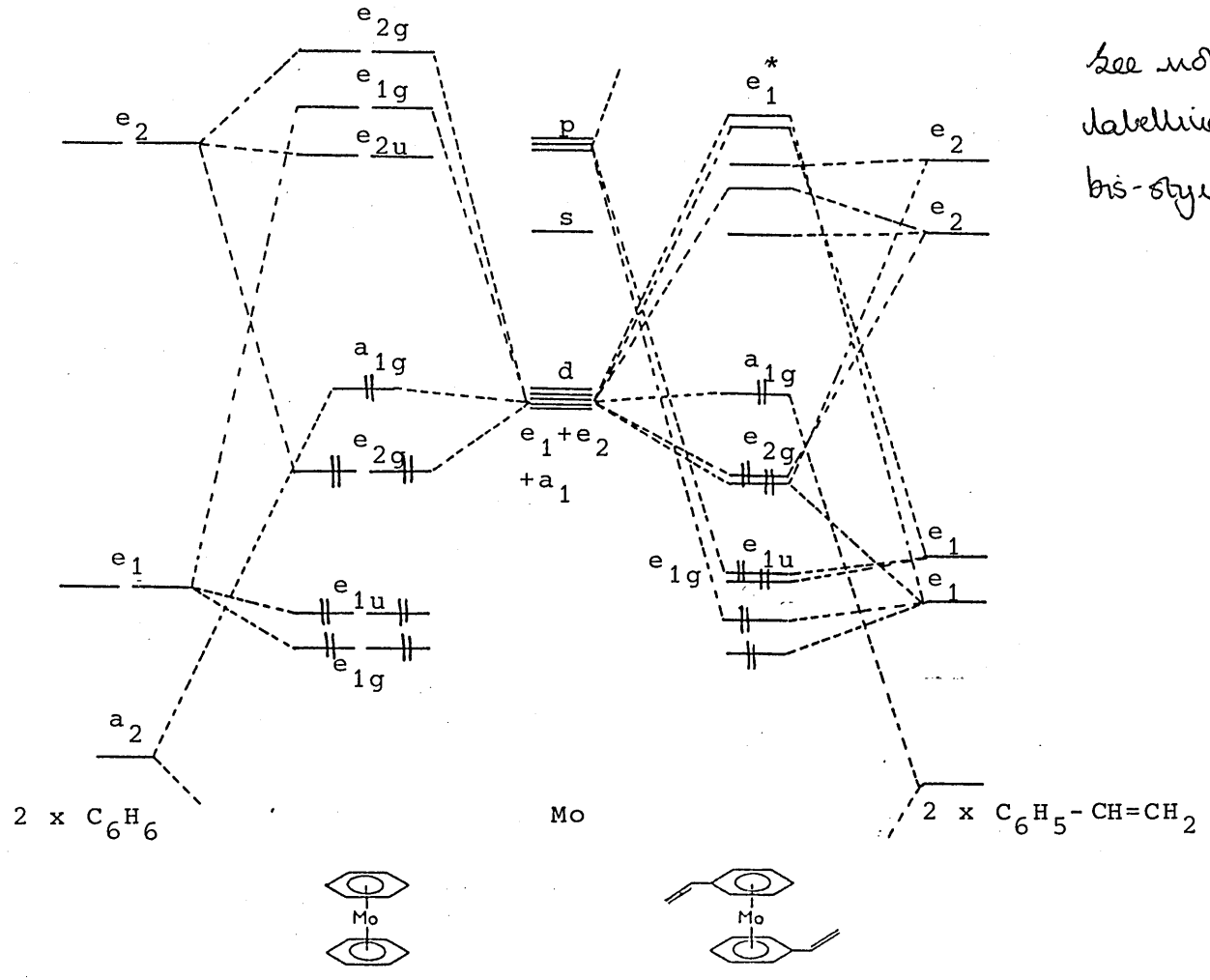

See note p28 concerning labelling of orbitals of bis-styrene molybdenum.

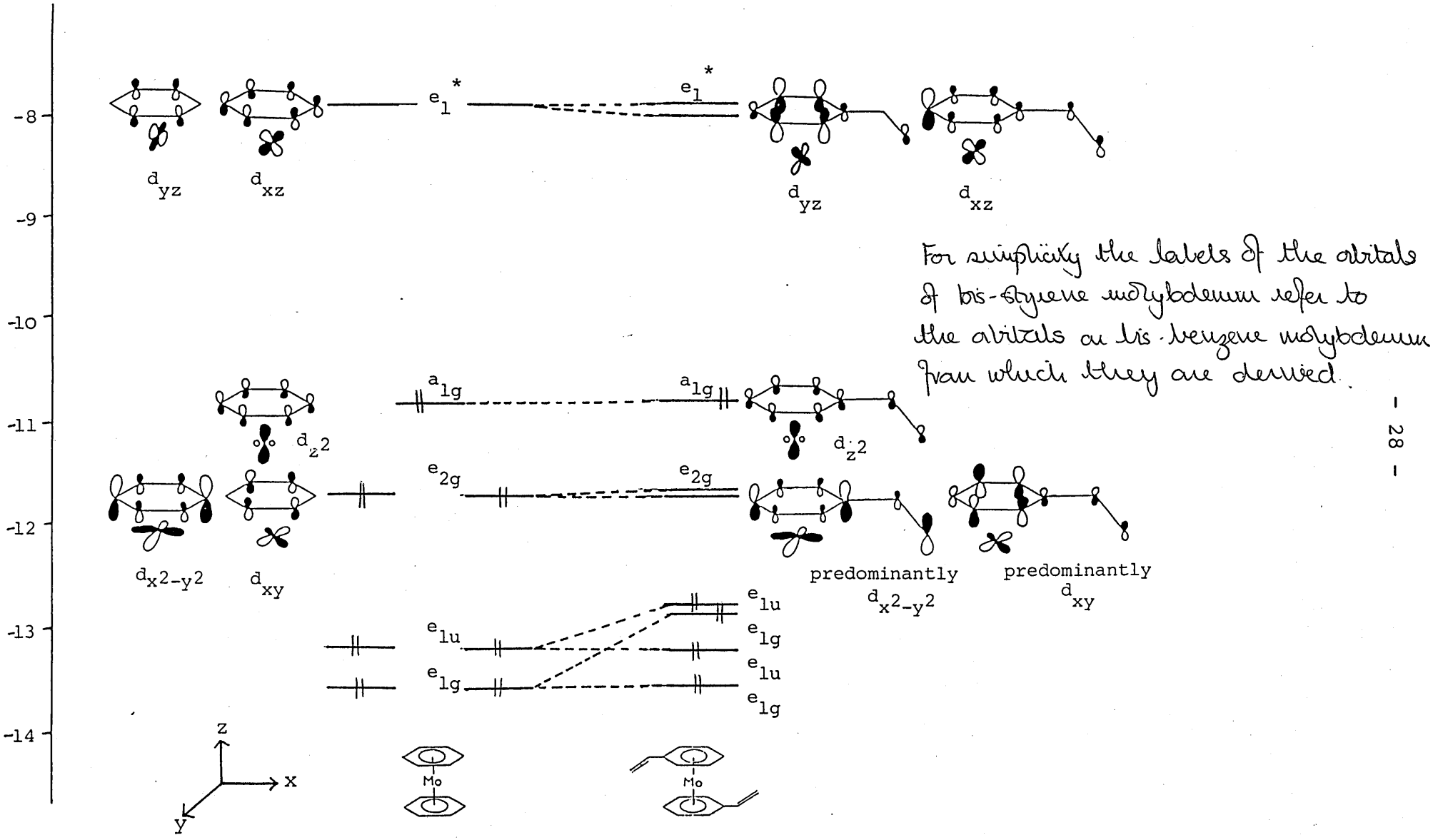

For simplicity the labels of the orbitals of bis-styrene molybdenum refer to the orbitals on bis-benzene molybdenum from which they are derived.

Figure 4.1.3. Correlation Diagram showing metal based m.o.s for Bis-benzene molybdenum and Bis-styrene molybdenum[2]

Figure 4.1.4. Ionization Energy versus δ^{95}Mo for Bis-(substituted benzene) Molybdenum Compounds.

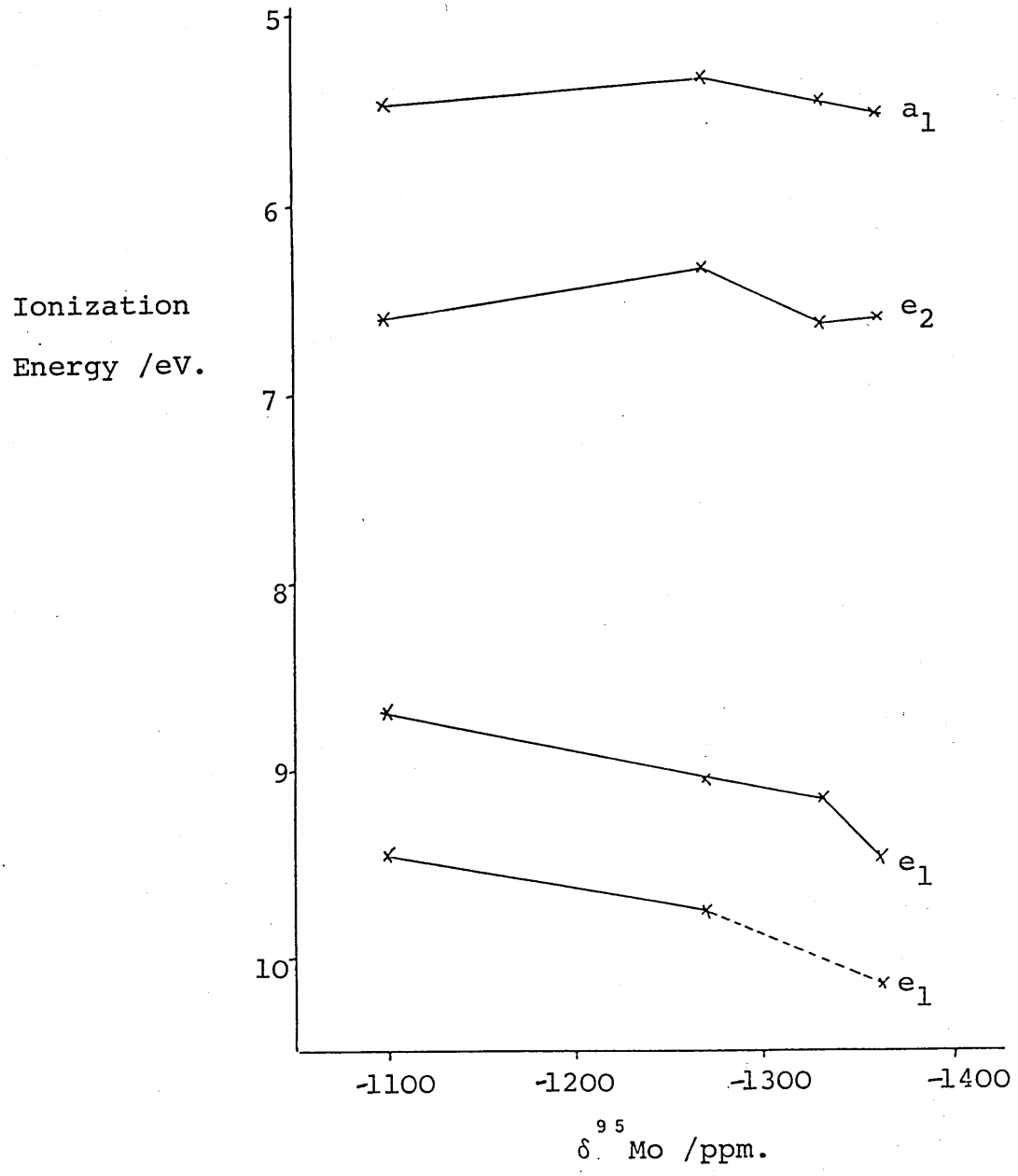

imagined to decrease and so cause the observed decrease in ^{95}Mo shielding. Only small differences in the energies of the metal based h.o.m.o. e_2 and a_{1g} orbitals are observed.

Comparison of ^{13}C data for these compounds is made difficult by localised substituent effects.

The linewidths of the substituted bis-arene molybdenum compounds are reasonably small. Although some changes in linewidth may be due to factors such as the viscosity of the individual sample solutions the linewidth tends to increase with a larger substituent. For example $[Mo(\eta\text{-}C_6H_5Me)_2]$ gave a linewidth of 55 Hz and $[Mo(\eta\text{-}C_6H_5CH_2Ph)_2]$ 205 Hz. The linewidth of the $[Mo(\eta\text{-}C_6H_6)_2]$ is 50 Hz but $[Mo(arene)L_3]$ derivatives have been shown to give much sharper lines (as low as 6 Hz) suggesting that conditions for a low electric field gradient around the molybdenum are more nearly met in such compounds.

Section 2: Substituted-Benzene Molybdenum Tricarbonyl Compounds

Table 4.2.1 shows n.m.r. data for a series of substituted benzene molybdenum tricarbonyl compounds. These results show how the ^{95}Mo chemical shift is sensitive to small changes in the molecule. The ^{95}Mo chemical shifts where the arene is monosubstituted by an alkyl group i.e. PhMe, $PhCH_2CH_2Br$, $PhBu^n$, $PhBu^t$ lie close together. It is of interest to note that the latter two arenes give molybdenum compounds with different ^{95}Mo chemical shifts. [Mo(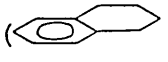)$(CO)_3$] has a ^{95}Mo chemical shift close to those of the $[Mo(xyl)(CO)_3]$ compounds. The molybdenum in $[Mo(\eta^6\text{-naphthalene})(CO)_3]$ is deshielded relative to the mono-ring arene molybdenum analogues. This may be due to the greater 2 pπ delocalisation in naphthalene relative to benzene leading to a decrease in the

Table 4.2.1 N.m.r. data for Substituted Benzene Molybdenum Tricarbonyl Compounds

Subistuted Benzene	$\delta^{95}Mo$ in CH_2Cl_2	$W_{\frac{1}{2}}$/Hz	$\delta^{13}CO$ in $CDCl_3$	$\delta C^{17}O$ in $CDCl_3$
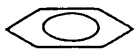 d	-2099	6	192	
 d	-2064	8	221.4	
 d	-2059	6		
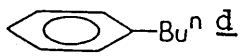 d	-2053	7		
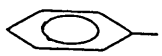 d	-2034 a	5	221.4	361
 d	-1988 a	9	221.1	362
 d	-1984	⩽32		
	-1979 a	5		
 d	-1971 a	7	223.1 b	367
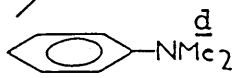 d	-1969	⩽30		
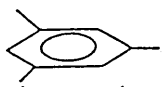 d	-1907 a	8	223.7 b	361
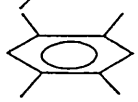 d	-1889	8	224.4 b	
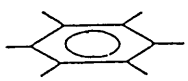 c	-1812	25	225.9 b	
 d	-1402	<30		

a ref 5

b ref 7

c compound supplied by author

d compound supplied by E.C.Alyea

π-π^* separation and the interaction of arene with the $[Mo(CO)_3]$ moiety then resulting in a lowering of the h.o.m.o. - l.u.m.o. gap at the metal centre.

The ^{95}Mo shielding decreases with increasing substitution of the benzene ring in these arene molybdenum tricarbonyl compounds (Figure 4.2.1). Similarly the ^{13}CO shielding decreases slightly with increasing ring substitution. This would follow an increase in π-donation from the ring to the metal and increase in back-bonding to the carbonyl. The π^* state of CO is stabilised by metal bonding so ΔE decreases compared to free CO. For the series $[Mo(C_6Me_xH_{6-x})(CO)_3]$ x = 1,2,3 the decrease in ^{95}Mo shielding was related to an increase in the Mo-arene bond strength.[5] Such an increase in bond strength may decrease the radius and then shielding theory would predict a decrease in shielding in accord with the results.

For this series of methyl substituted benzene molybdenum tricarbonyl compounds the ^{95}Mo and ^{13}CO chemical shift changes are not reflected in ^{17}O resonance, from the limited number of shifts reported here. It has been noted previously that the $C^{17}O$ resonance of substituted metal carbonyls does not correlate as well as the ^{13}CO resonance with variation in substituent on the metal.[8]

Piano stool compounds of the type $[Mo(arene)(CO)_3]^q$ have been shown to give relatively sharp signals in ^{95}Mo resonance. It has been suggested in the case of the substituted-benzene molybdenum tricarbonyl compounds that there is a very small electric field gradient around the molybdenum atom in these compounds, probably because the bonding electrons occupy positions near the magic angle to the axis.[6] However the linewidths of the bis-arene molybdenum compounds are greater.

Figure 4.2.1 $\delta^{13}CO$ versus $\delta^{95}Mo$ for the Series $[Mo(C_6H_nMe_{6-n})(CO)_3]$

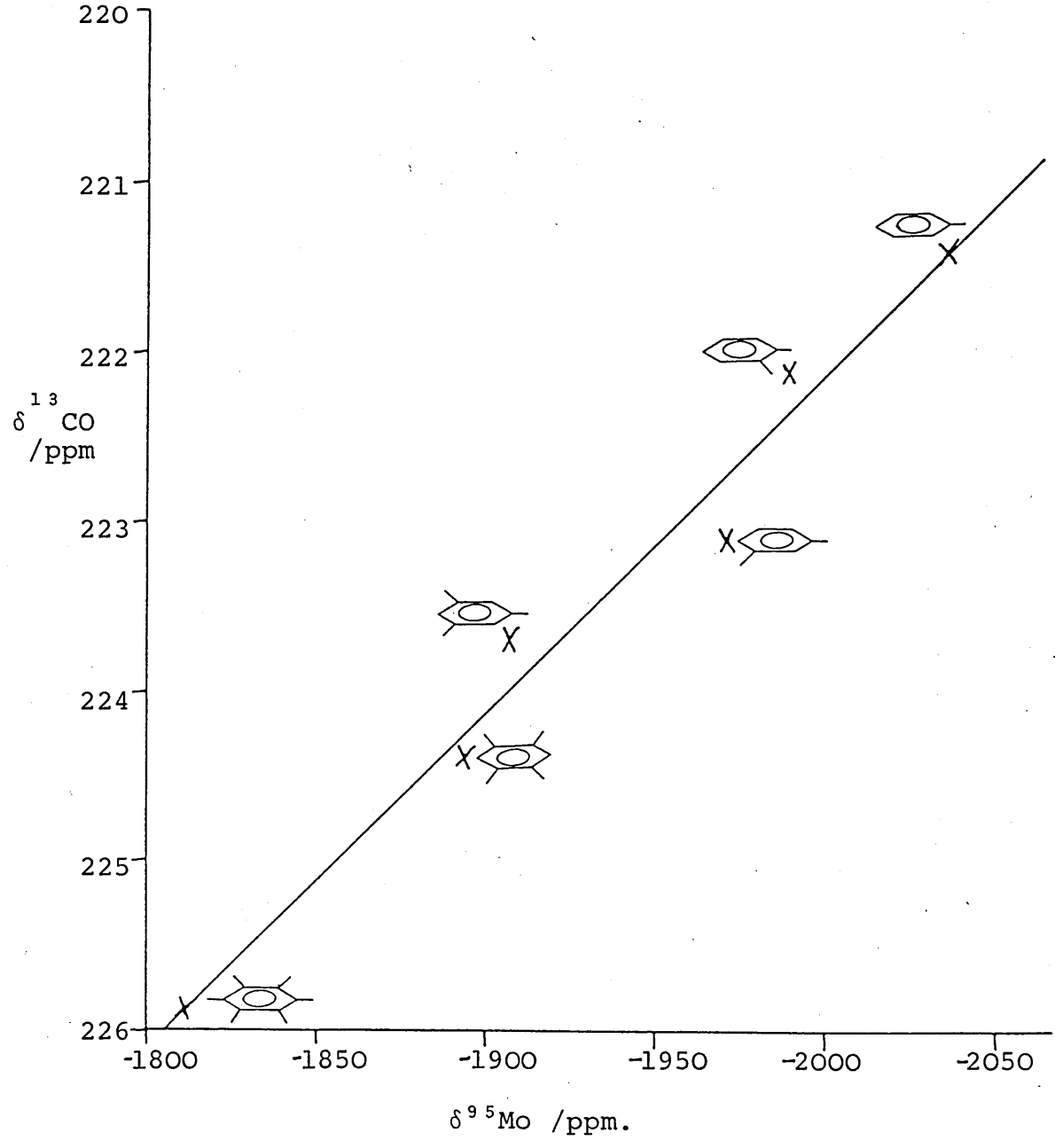

For example that of $[Mo(C_6H_6)_2]$ is 50 Hz (solvent viscosity at 25 ^{o}C 0.602 cP), compared with 6 Hz for $[Mo(C_6H_6)(CO)_3]$ (solvent viscosity at 25 ^{o}C 0.393 cP).

References for Chapter 4

1. S. Evans, J.C. Green, S.E. Jackson, B. Higginson, J. Chem. Soc., Dalton Trans., 1974, 304.
2. G.J. Wilson, Part II Thesis, Oxford, 1984.
3. K.D. Warren, Structure and Bonding, 1976, 27, 92.
4. R.D. Feltham, J. Inorg. and Nucl. Chem., 1961, 16, 197.
5. A.F. Masters, R.T.C. Brownlee, M.J. O'Connor, A.G. Wedd, Inorg. Chem., 1981, 20, 4183.
6. J.W. Akitt, W.S. MacDonald, J. Magn. Reson., 1984, 58, 401.
7. B.E. Mann, B. Taylor, "^{13}C NMR Data for Organometallic Compounds", Academic, 1981.
8. D. Cozak, I.S. Butler, J.P. Hickey, L.J. Todd, J. Magn. Reson., 1979, 33, 149.

Chapter 5: Polyhapto-ring Molybdenum Compounds

Section 1: $[MoL(CO)_3]^q$ Compounds

N.m.r. data for compounds of the type $[MoL(CO)_3]^q$ where L is a carbocyclic ligand are given in table 5.1.1. Comparison of complexes where L = C_nH_n (n = 5,6,7) shows a decrease in the ^{95}Mo shielding with increase in ring size. This may be traced to a change in the energy term and the radial term of shielding theory. The interaction diagram for $[M(C_6H_6)(CO)_3]$ in Figure 5.1.1 shows that the major metal-arene interactions occur between

(i) the e_{1g} benzene orbitals and the 2e orbitals of the C_{3v} $Mo(CO)_3$ unit, the latter containing major contributions from d_{xz} and d_{yz} orbitals (ligand → metal donation) and

(ii) the e_{2g} benzene orbitals and the 1e orbitals of the C_{3v} $Mo(CO)_3$ unit, the latter containing significant $d_{x^2-y^2}$ and d_{xy} character (metal → ligand donation)[2].

Figure 5.1.2 shows that as the size of the ring increases the ring e_{1g} and the metal based 2e orbitals move further apart in energy leading to poorer overlap and a lowering of the metal based antibonding orbital[12]. So increasing ring size results in a decrease in the h.o.m.o. - l.u.m.o. gap at the metal. Deshielding would also occur with an increase in the radial term such as results from an increase in the positive charge on the complex from $[Mo(C_5H_5)(CO)_3]^-$ to $[Mo(C_7H_7)(CO)_3]^+$ (although the charge is not localised on the metal).

Comparison of $[Mo(\eta^6\text{-}L)(CO)_3]$ compounds shows a decrease in ^{95}Mo shielding in the order

$$L = C_6H_6 > C_7H_8 > C_8H_{10} > C_8H_8$$

Table 5.1.1 Spectroscopic Data for Half-Sandwich Molybdenum Tricarbonyl Compounds

	δ^{95}Mo	$W_{\frac{1}{2}}$/Hz	Solvent	Solvent Viscosity /cp.25° C	δ^{13}CO in $CDCl_3$	$\delta C^{17}O$ in $CDCl_3$
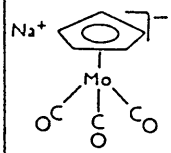	-2120 [a]	21	CH_2Cl_2	0.393		
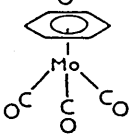 d	-2099	6	CH_2Cl_2	0.393		
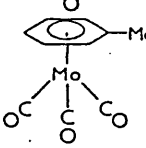 d	-2034	5	CH_2Cl_2	0.393	221.4	361
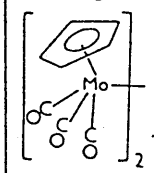	-1856 [e]	150	$CDCl_3$	0.542	218.6 [b]	
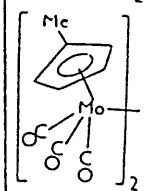 c	-1831	160	CH_2Cl_2	0.393		397
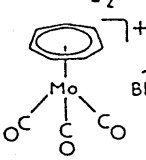 c	-1807	10	$(CH_3)_2CO$	0.316	206.3 [b]	
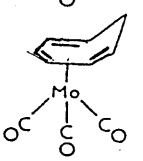 c	-1702 -1690	12 12	$(CH_3)_2CO$ CH_2Cl_2	0.316 0.393	217.9(2) [b] 229.2(1)	373
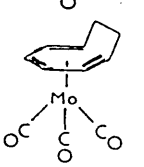 c	-1632	34	C_6H_5Me	0.552	216.6(2) [b] 228.4(1)	
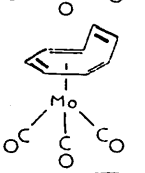 c	-1502	60	C_6H_5Me	0.552	213.5(2) [b] 228.2(1)	
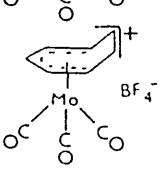 c	-1355	50	$(CH_3)_2CO$	0.316		

a ref 3 b ref 4 c compound supplied by author
d compound supplied by E.C.Alyea e ref 5

Figure 5.1.1a. Derivation of the Fragment Orbitals for a C_{3v}-ML_3 Unit[1]

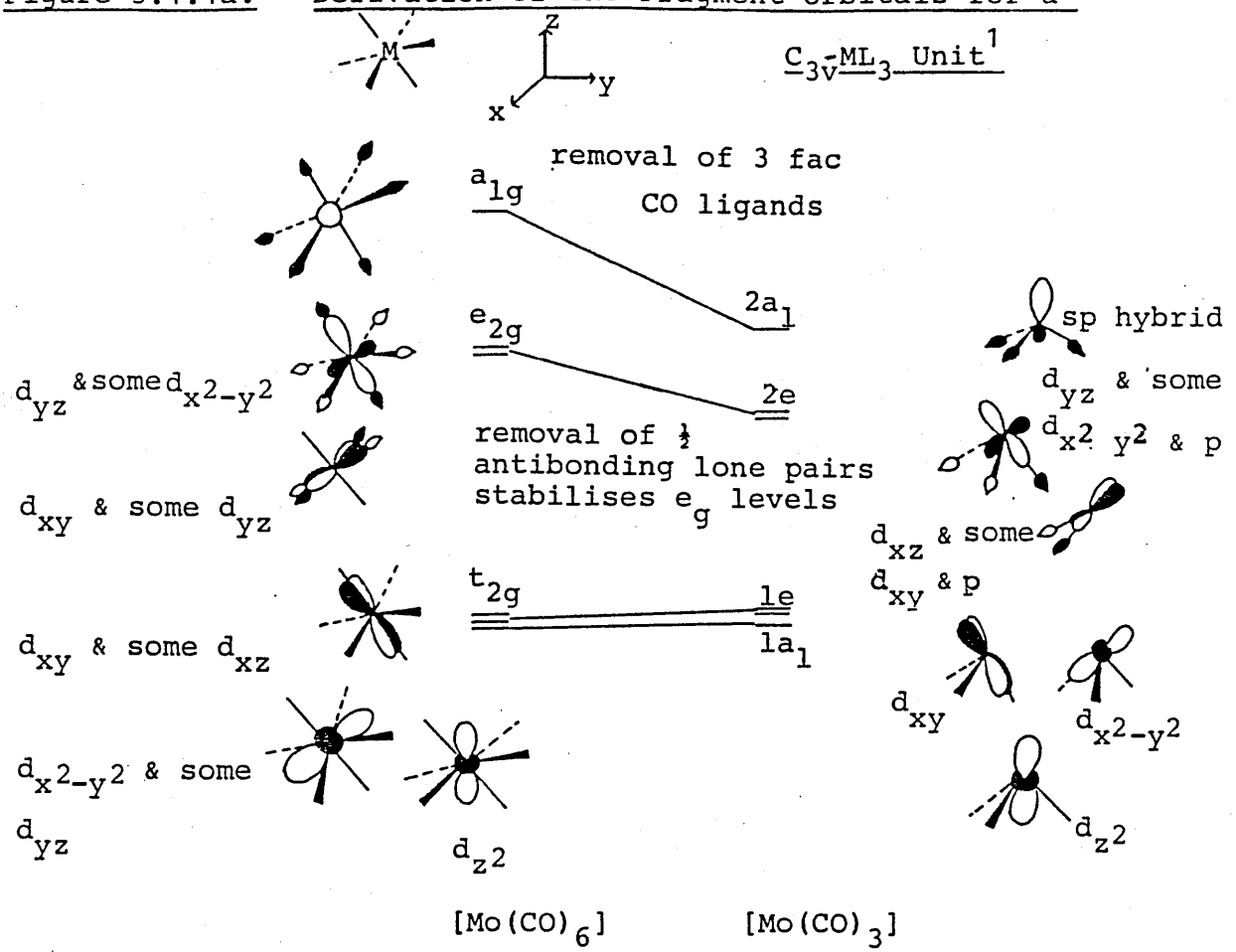

Figure 5.1.1b. Interaction Diagram for $[M(C_6H_6)(CO)_3]^2$

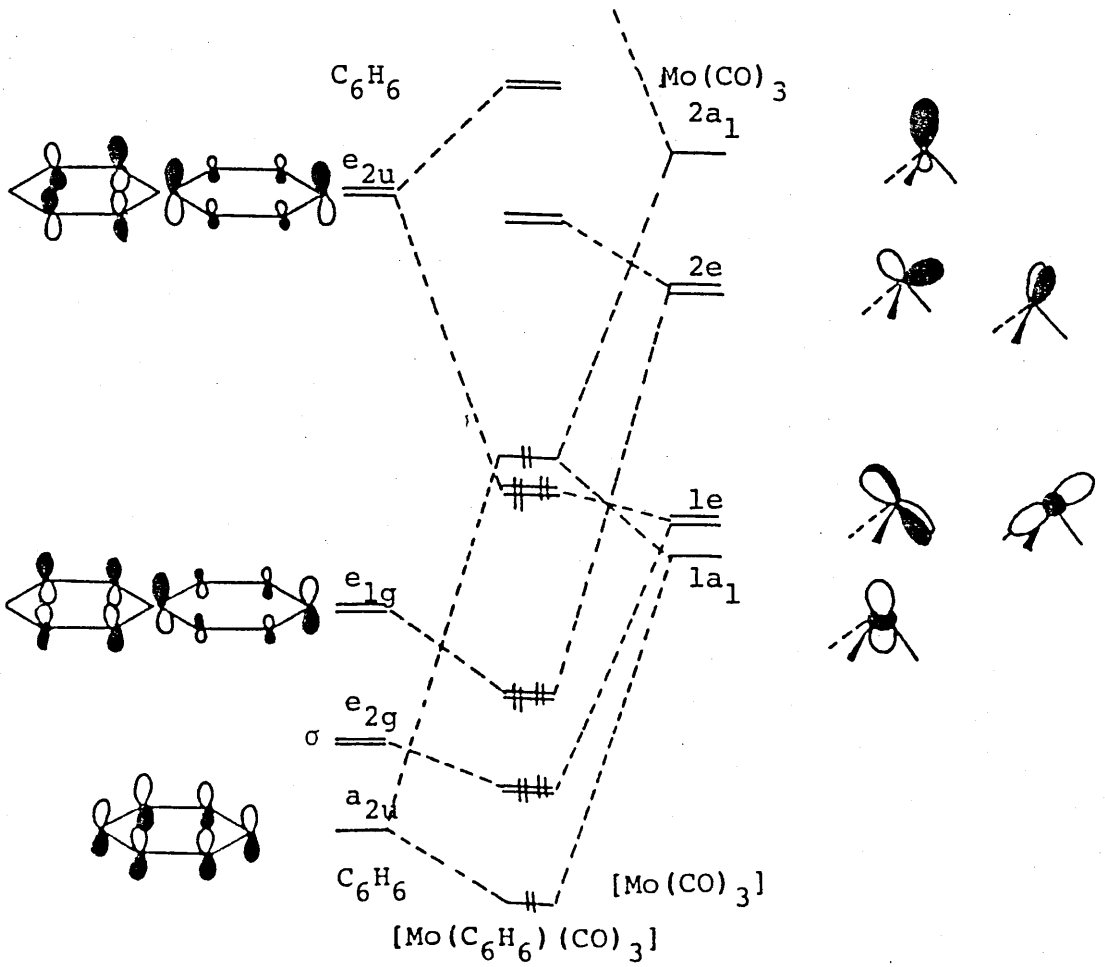

Figure 5.1.2. Energies and nodal properties of C_nH_n molecules[12]

(z-axis is perpendicular to the plane of the paper)

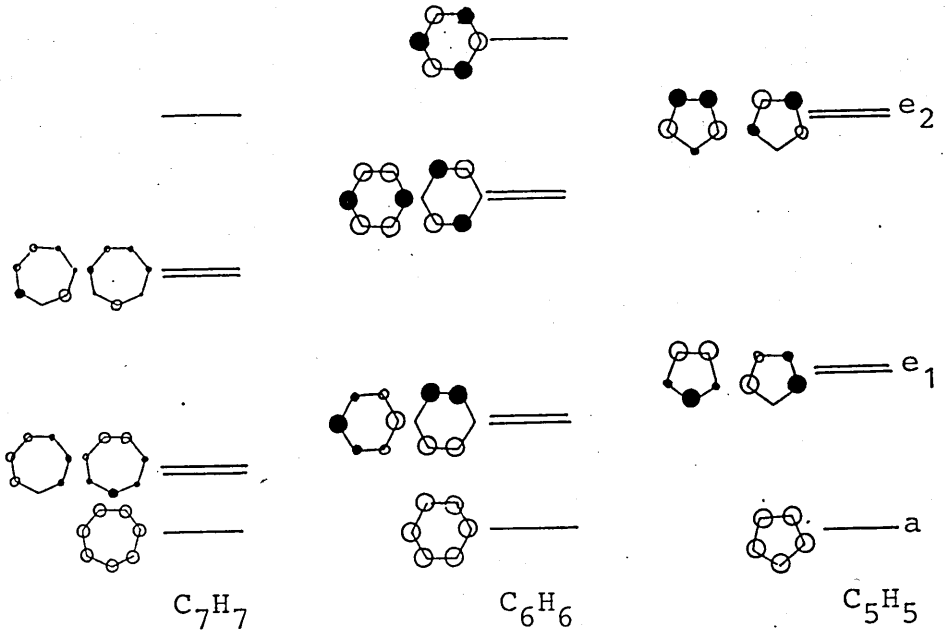

Figure 5.1.3.

δ^{95}Mo versus δ^{13}CO for compounds of the type $[Mo(\eta^6\text{-}L)(CO)_3]$

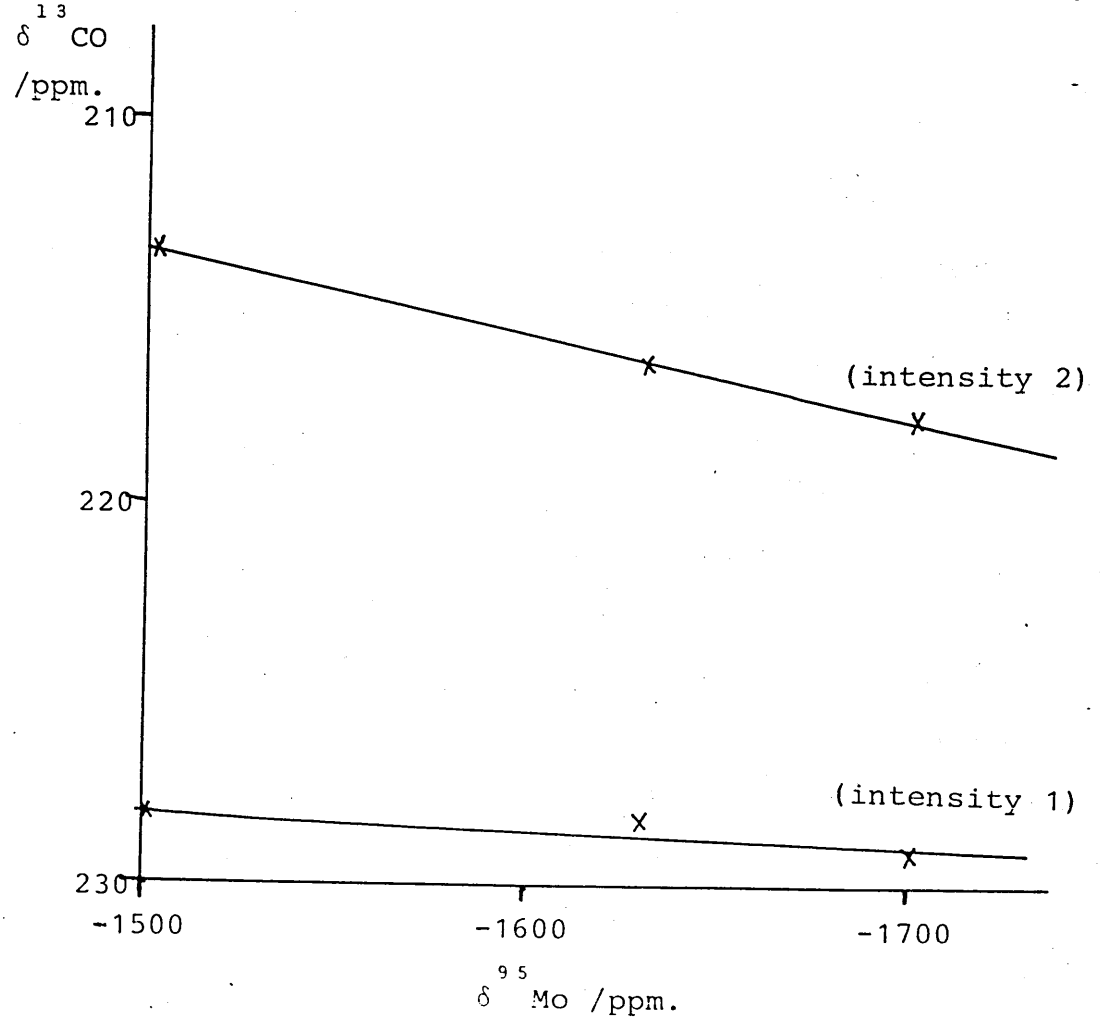

This ordering is also illustrated in the ^{95}Mo shielding

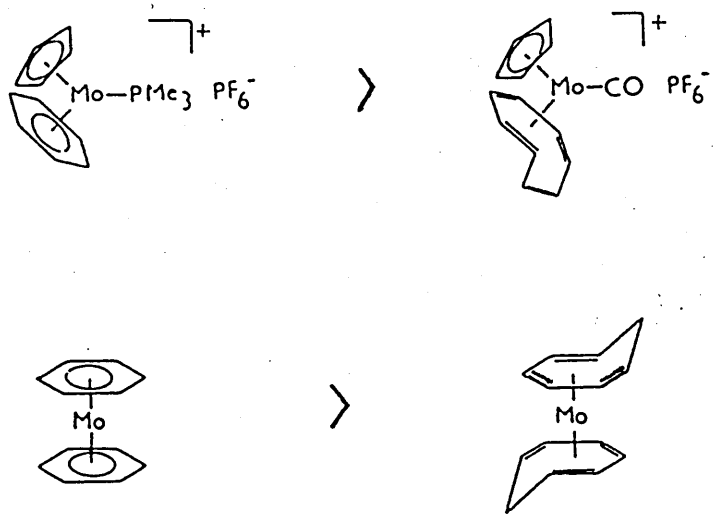

A change in the Mo-L bonds may be transmitted to the Mo-CO bonds and result in a variation in the ^{13}CO resonance. In the series $[Mo(\eta^6\text{-}L)(CO)_3]$ where L is a non-aromatic carbocyclic ligand there is a decrease in the shielding of the molybdenum nucleus with a slight increase in the ^{13}CO shielding, Figure 5.1.3. (Note that for each such compound there are two ^{13}CO resonances with intensity ratio 2:1). X-ray structural data[6,7] indicate that C_7H_8, C_8H_{10} and C_8H_8 are best regarded as $(\eta^2)_3$ ligands. In the case of the methyl-substituted benzene molybdenum tricarbonyl compounds it was suggested (Chapter 4) that an increase in π-donation from the ring to the metal brought about an increase in backbonding to the carbonyl and hence a decrease in the ^{13}CO shielding. Then an order of increasing π-donation would be $\eta^6\text{-}C_8H_8 < \eta^6C_8H_{10} < \eta^6C_7H_8$. An increase in π-donation would tend to raise the metal based l.u.m.o. so increasing the h.o.m.o. - l.u.m.o. gap causing the observed increase in ^{95}Mo

shielding in the series $[Mo(\eta^6\text{-}L)(CO)_3]$. A possible explanation of this variation in π-donating ability may be that as the ring size increases there is poorer overlap between the π-orbitals of L and the metal d orbitals. In a study of rhodium-olefin complexes[8] the ^{103}Rh shielding was found to decrease with increasing ring size or C-C-C bond angle of a series of 1,3 diene systems. It was noted that the p,d overlap is expected to be less efficient in 1,4- and 1,5-diene rhodium complexes and deshielding was observed.

It has been noted that the greater ^{13}C coordination shifts for η^6-cycloheptatriene in $[Mo(\eta^6\text{-}C_7H_8)(CO)_3]$ compared to those for benzene derivatives in $[Mo(\eta^6\text{-arene})(CO)_3]$ imply stronger metal-triene bonding than metal-arene bonding.[10] The ^{95}Mo chemical shifts obtained are then consistent with the trends in chemical shift and bond strength observed for the compounds $[Mo(C_6Me_xH_{6-x})(CO)_3]$ (chapter 4).

The deshielding of the ^{95}Mo nucleus in $[Mo(C_7H_9)(CO)_3]^+$ relative to other $[MoL(CO)_3]^q$ complexes may be at least partly due to it being a 16-electron species as opposed to an 18-electron species. This factor has been used to explain the deshielding of ^{91}Zr in $[Zr(\eta^5\text{-}C_5H_5)(\eta^3\text{-}CH_2CHCR_2)(CH_2{=}CR\text{-}CR{=}CH_2)]$ relative to $[Zr(\eta^5\text{-}C_5H_5)_2](CH_2{=}CR\text{-}CR{=}CH_2)$.[9]

Section 2: Sandwich Compounds

Table 5.2.1 shows spectroscopic data for a variety of sandwich complexes of molybdenum.

Table 5.2.1 Spectroscopic data for sandwich compounds

Sample	Solvent	δ^{95}Mo	$W_{\frac{1}{2}}$/Hz	Ionization Energies/eV			
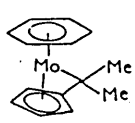 a	C_6H_5Me + C_6D_6	-1923	40				
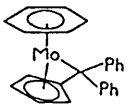 a	C_6H_5Me	-1922	300	6.04 6.55,7.45 8.78,9.79	a_{1g} (d_{z^2}) e_2 (d_{xy},$d_{x^2-y^2}$) ligand		f
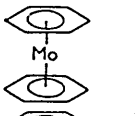 b	C_6H_5Me	-1362	50	5.52 6.59, 9.47,10.15	a_{1g} (d_{z^2}) e_2 (d_{xy},$d_{x^2-y^2}$) e (d_{xz},d_{yz})		g
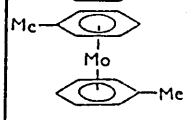 c	C_6H_5Me	-1270	55	5.32 6.33 9.05,9.75	a_1 e_2 e_1		g
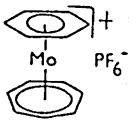 d	CH_2Cl_2	-487	150				
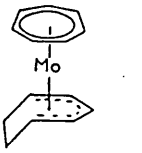 e	C_6H_5Me + C_6D_6	-469	170	5.62 7.04 7.56,7.85 9.18	a_1		h
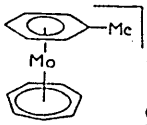 d	CH_2Cl_2	-457	150				
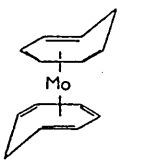 c	C_6H_5Me	358	100	decomposes at room temperature			

a compound supplied by A.Izquierdo
b compound supplied by I.Treurnicht
c compound supplied by P.Newman
d compound supplied by M.L.H.Green laboratory
e compound supplied by R.C.Tovey
f ref 11
g ref 12
h ref 13

Replacing one of the benzene rings of $[Mo(C_6H_6)_2]$ with either dimethylfulvene or diphenylfulvene gives the purple compounds $[Mo(C_6H_6)(fulvene)]$.[14] The molybdenum centres in $[Mo(C_6H_6)(C_5H_4CR_2)]$ (R = Me,Ph) are more shielded than that in $[Mo(C_6H_6)_2]$. Comparison of the m.o. diagrams for these types of molecule derived from p.e.s. data (Figure 5.2.1) show that in $[Mo(C_6H_6)(C_5H_4CR_2)]$ the d_{z^2} orbital is stabilised relative to that in $[Mo(C_6H_6)_2]$. This results in an increase in the metal h.o.m.o. - l.u.m.o. gap. The substitution of phenyl for methyl groups in the fulvene compounds does not affect the ^{95}Mo chemical shift. This observation may be rationalised by referring to the crystal structure of the phenyl derivative.[14] The fulvene ligand is considered to be η^5,η^1 bonded to the molybdenum and the phenyl rings adopt a propeller-like conformation such that the $p\pi$ - $p\pi$ conjugative interaction with the exocyclic carbon of the fulvene ligand will be minimal.

However in the iron-cyclopentadienyl-fulvene sandwich the ^{57}Fe chemical shift is sensitive to the substituents on the exocyclic carbon on the fulvene C_6.[15]

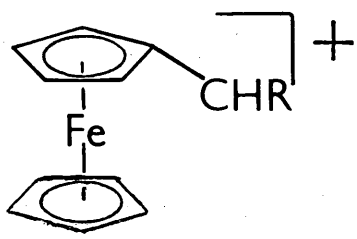

	$\delta^{57}Fe$
R = H	-524
Me	-219
Ph	221

In the case of the ferrocenyl compound C_6 is only semi-bridging so it may be imagined that changing the substituents would

Figure 5.2.1. Molecular Orbital Diagrams for $[Mo(bz)_2]$ and $[Mo(bz)(fv)]$[11]

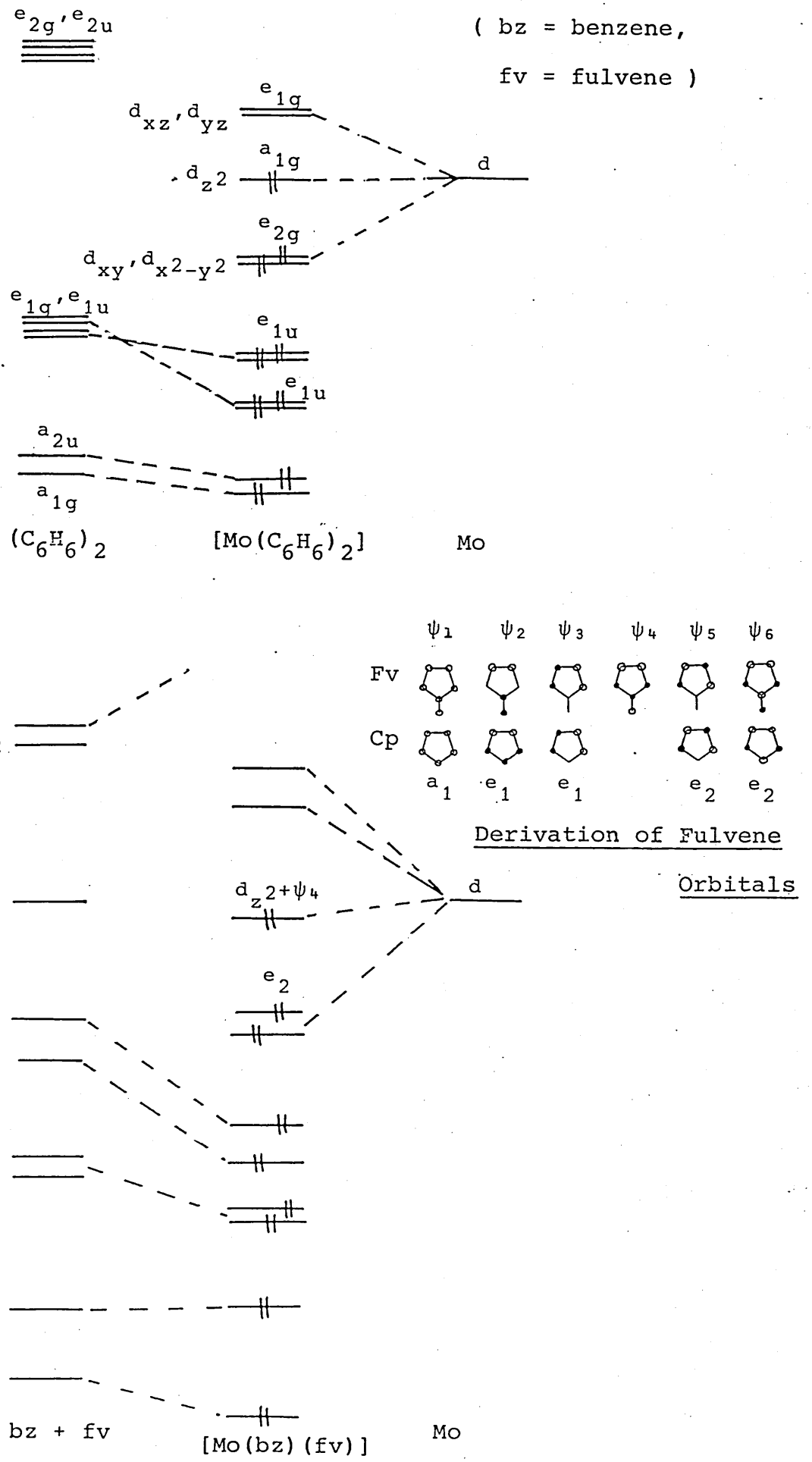

vary the interaction with the metal d-orbitals and hence the ^{57}Fe shielding.

The increase in linewidth observed for the molybdenum resonance on substitution of diphenylfulvene for dimethylfulvene in these compounds is probably due to an increase in molecular size reducing the tumbling rate in solution.

The metal centre in $[Mo(\eta\text{-}C_6H_6)(\eta\text{-}C_7H_7)]^+$ is less shielded than that in $[Mo(\eta\text{-}C_6H_6)_2]$. An m.o. diagram for a mixed ring sandwich complex is shown in Figure 5.2.2. A simple Hückel treatment of isolated rings predicts that the e-type ring m.o.'s are progressively stabilised with increase in ring size (Figure 5.1.2). Owing to these energy differences the orbitals of the two rings mix less with each other and to differing extents with the metal orbitals. On grounds of energy separation interaction of e_1 orbitals with a metal is likely to decrease with increase in ring size while that of the e_2 orbitals is likely to increase. The metal based h.o.m.o's are a_1 (mainly non-bonding d_{z2}) and e_2 (derived from d_{x2-y2} and d_{xy}) and the metal based l.u.m.o. is e_1 (d_{yz} and d_{xz}). The effect of replacing one of the benzene rings of $[Mo(\eta\text{-}C_6H_6)_2]$ with C_7H_7 may then result in a lowering of the metal-based h.o.m.o. - l.u.m.o. gap because of the change in the extend of mixing of the ligand orbitals with each other and with the metal orbitals. Also the positive charge will reduce the d-electron radius and so lead to deshielding of the molybdenum.

$[Mo(\eta^6\text{-}C_7H_8)_2]$ is deshielded relative to $[Mo(\eta\text{-}C_6H_6)_2]$ by 1720 ppm. The metal-ring bond in the former is much weaker than the latter so a low excitation energy may be responsible for the appreciable deshielding.[16] $[Mo(\eta^6\text{-}C_7H_8)]$ is unstable at

room temperature converting to $[Mo(\eta^7\text{-}C_7H_7)(\eta^5\text{-}C_7H_9)]$ a reaction which has been observed by ^{95}Mo n.m.r.

Figure 5.2.2. Molecular Orbital Diagram for $[Mo(C_6H_6)(C_7H_7)]^{+12}$

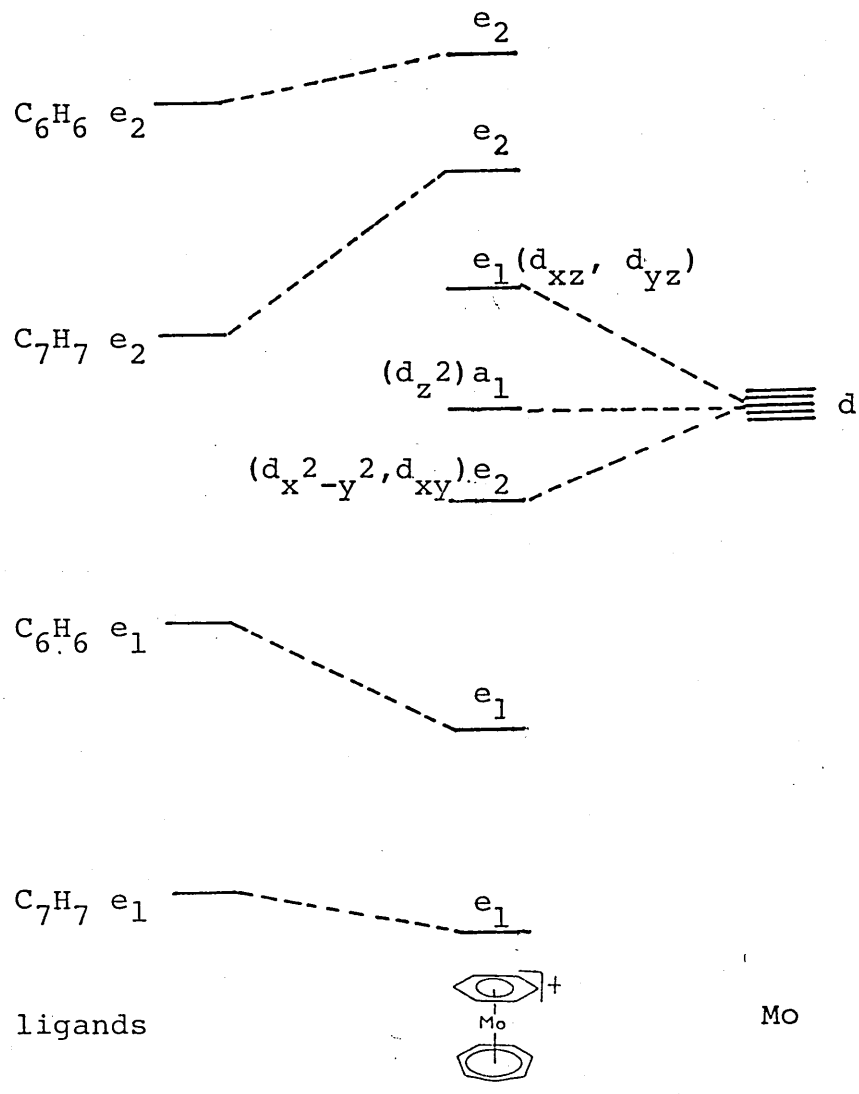

Section 3: A Comparison of Sandwich and Half-Sandwich Compounds

As illustrated in the preceding sections deshielding of the molybdenum nucleus is observed with increasing ring size and by replacement of a closed aromatic system with an open π-system. This is also observed in ^{57}Fe resonance[15] where an order of shielding $\eta^5-C_5H_5 > \eta^6-C_6H_6 > \eta^5-C_6H_7$ may be deduced from a study of iron-sandwich compounds and for ^{59}Co resonance[17] where the order is $\eta^4-C_4H_4 > \eta^5-C_5H_5 > \eta^4-C_8H_{12}$, as deduced from a report on cyclopentadienyl cobalt diene compounds and the relationship between $\delta^{59}Co$ and catalytic activity.

Of the compounds studied the ^{95}Mo shielding is greater in the polyhapto-ring molybdenum tricarbonyl compounds than in molybdenum sandwich compounds. This is related to the CO being a stronger ligand with better backbonding to the (lower lying) π* CO orbital than is the case with these unsaturated carbocycles.

The coordination shift of benzene in $[Mo(\eta-C_6H_6)_2]$ is -53.3 ppm and in $[Mo(\eta-C_6H_6)(CO)_3]$ is -34.6 ppm. The suggestion that the Cr-CO bond strength is greater in $[Cr(\eta C_6H_6)(CO)_3]$ than in $[Cr(CO)_6]$ is supported by bond enthalpy calculations[18], bond lengths obtained from x-ray structural analysis and i.r. studies[26], the latter showing that the Cr-CO bond in substituted benzene chromium tricarbonyl compounds has greater multiple π-bonding character than in the hexacarbonyl. Replacing $[(CO)_3]$ in $[Cr(CO)_6]$ with a benzene ring increases the electron density on the chromium and so there may be increased back donation to the remaining carbonyl ligands. This would increase the [Cr-CO] bond strength. The existence of a considerable dipole moment indicates electron withdrawal from the arene by $[Cr(CO)_3]$. Bond enthalpy calculations[19] and

bond lengths obtained from x-ray structural analysis suggest that benzene forms a stronger bond to chromium in $[Cr(\eta\text{-}C_6H_6)_2]$ than in $[Cr(\eta\text{-}C_6H_6)(CO)_3]$. Going from $[Cr(\eta\text{-}C_6H_6)(CO)_3]$ to $[Cr(\eta\text{-}C_6H_6)_2]$ there is an increase in shielding of the arene carbons of 19.4 ppm. Calculations[20] have shown that the shift to higher shielding observed for the ^{13}C of the arene ring on coordination to a transition metal must be explained with reference to all three terms in the Pople-Karplus expression. It has been suggested[21] that the greater ^{13}C coordination shift of (C_6H_6) observed with $[Cr(\eta\text{-}C_6H_6)_2]$ relative to $[Cr(\eta\text{-}C_6H_6)(CO)_3]$ may be explained in terms of a variation in the degree of metal → arene backbonding. M.o. calculations, p.e. and i.r. spectroscopic studies indicate that there is more metal to arene backbonding in $[Cr(\eta\text{-}C_6H_6)]_2$ than in the half-sandwich complexes, where metal to arene backbonding is minimal where the two π-acids (CO and C_6H_6) are competing for electron density.[28] The available data for the molybdenum analogues (Table 5.3.1) indicates that similar arguments may be used here to explain the coordination shifts of the arene rings bound to a molybdenum atom.

This may be extended to rationalise the differences in the ^{13}C chemical shifts shown for sandwich and half-sandwich compounds of molybdenum in Table 5.3.2. When two rings are in competition, that which has the smaller coordination shift to lower frequencies is then the poorer π-acceptor. However when the carbocyclic ring attached to the molybdenum is cyclo-heptatriene there is no appreciable difference in the ^{13}C resonances of the ring in the half-sandwich carbonyl compound and the sandwich compound. This is consistent with there being no strengthening of the metal-ring bond on replacement of the carbonyl ligands by η^6-cycloheptatriene.

Table 5.3.1.

	$[Mo(CO)_6]$	$[Mo(1,3,5\text{-}C_6H_3Me_3)(CO)_3]$	$[Mo(C_6H_6)_2]$
δ^{95} Mo	-1862	-1907	-1362
ν(C-O) cm^{-1}	2004[d]	1972,1900[a]	-
$\bar{D}$(Mo-arene) /kJ mol^{-1}	-	280[b]	211[c]
Dipole moment in cyclohexane	-	6.21[a]	-

a ref 22, b ref 23, c ref 24, d ref 25

Table 5.3.2.

	δ^{95}Mo	δ^{13}C(benzene/ toluene)	δ^{13}C(C_7H_7)	δ^{13}C other
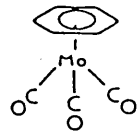	-2099	94.1		
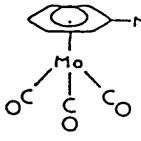	-2034	113.7,96.6,94.4, 91.3,21.1.		
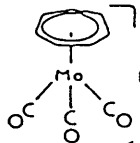	-1807		100.0[c]	
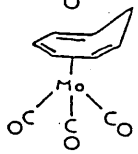	-1702			61.3 $C^{1,6}$ 98.1 $C^{3,4}$ 103.7 $C^{2,5}$
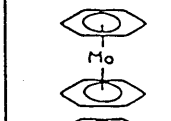	-1362	75.4		
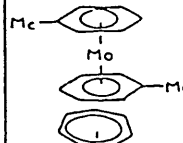	-1270	89.6,78.6,75.9, 75.0,21.6.		
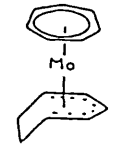	-469		83.9[b]	37.4(2),82.5(2)[b] 91.3(1),102.6(2)
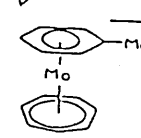	-457	100.7,98.1,97.1, 20.3.	86.8	
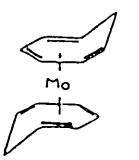	358			52(broad),95,106[a]

a ref 16 b ref 26 c ref 4

The linewidths of the bis-ring compounds are greater than those of the ring-molybdenum tricarbonyl compounds as is generally observed for bis-ring compounds versus "piano stool" complexes.

References for Chapter 5

1 T.A. Albright, Tetrahedron, 1982, 38, 1339.

2 T.A. Albright, P. Hofmann, R. Hoffmann, J. Am. Chem. Soc., 1977, 99, 7546.

3 A.F. Masters, R.T.C. Brownlee, M.J. O'Connor, A.G. Wedd, Inorg. Chem., 1981, 20, 4183.

4 B.E. Mann, B. Taylor, "^{13}C NMR Data for Organometallic Compounds" Academic, 1981.

5 B.E. Mann, S. Dysart, I. Georgii, J. Organomet. Chem., 1981, 213, C10.

6 J.D. Dunitz, P. Pauling, Helv. Chim. Acta, 1960, 43, 2188.

7 J.S. McKechnie, I.C. Paul, J. Am. Chem. Soc., 1966, 88, 5927.

8 E. Maurer, S. Rieker, M. Schollbach, A. Schwenk, T. Egolf, W. von Philipsborn, Helv. Chim. Acta, 1962, 65, 26.

9 R. Benn, A. Rufinska, J. Organomet. Chem., 1984, 273, C51.

10 B.E. Mann, J. Chem. Soc., Chem. Commun., 1971, 976.

11 C.E. Davies Part II Thesis, Oxford, 1983.

12 S. Evans, J.C. Green, S.E. Jackson, B. Higginson, J. Chem. Soc., Dalton Trans., 1974, 304.

13 J.C. Green, R.C. Tovey, personal communication.

14 M.L.H. Green, A. Izquierdo, J.J. Martin-Polo, V.S.B. Mtetwa, C.K. Prout, J. Chem. Soc., Chem. Commun., 1983, 538.

15 A.A. Koridze, N.M. Astakhova, P.V. Petrovskii, J. Organomet. Chem., 1983, 254, 345.

16 P. Newman, personal communication.

17 H. Bonnemann, W. Brijoux, R. Brinkmann, W. Meurers, R. Mynott, W. von Philipsborn, T. Egolf, J. Organomet. Chem., 1984, 272, 231.

18 M.J. Calhorda, C.F. Frazão, J.A. Martin -Simões, J. Organomet. Chem., 1984, 262, 305.

19 J.A. Connor, J.A. Martin-Simões, H.A. Skinner, T. Zafarini-Moattar, J. Organomet. Chem., 1979, 179, 331.

20 D.A. Brown, J.P. Chester, N.J. Fitzpatrick, I.J. King, Inorg. Chem., 1977, 16, 2497.

21 V. Graves, J.J. Lagowski, Inorg. Chem., 1976, 15, 577.

22 C. Barbeau, J. Turcotte, Can. J. Chem., 1976, 54, 1612.

23 D.L.S. Brown, J.A. Connor, C.P. Demain, M.L. Lueng, J.A. Martin -Simões, H.A. Skinner, M.T. Zafarani-Moattar, J. Organomet. Chem., 1977, 142, 321.

24 E.O. Fischer, A. Reckziegel, Chem. Ber., 1961, 94, 2204.

25 L.H. Jones, R.S. McDowell, M. Goldblatt, Inorg. Chem., 1969, 8, 2349.

26 E.M. Van Dam, W.N. Brent, M.P. Silvon, P.S. Skell, J. Am. Chem. Soc., 1975, 97, 465.

Chapter 6: Bent Sandwich Compounds

Table 6.1 shows ^{95}Mo n.m.r. data for a variety of bent sandwich compounds.

Comparing $[Mo(\eta\text{-}C_5H_5)(\eta^6\text{-}C_8H_8)CO]^+$ with $[Mo(\eta\text{-}C_5H_5)(\eta\text{-}C_6H_6)PMe_3]^+$ where CO and PMe_3 are both strong field ligands, $(\eta^6\text{-}C_8H_8)$ deshields the molybdenum relative to $(\eta^6\text{-}C_6H_6)$. Similarly the molybdenum nucleus in $[Mo(\eta\text{-}C_6H_6)(CO)_3]$ is more shielded than in $[Mo(\eta^6\text{-}C_8H_8)(CO)_3]$ (see Section 3.1). The Mo nucleus in $[Mo(\eta\text{-}C_5H_5)(\eta\text{-}C_6H_6)(PMe_3)]^+$ is shielded relative to that in $[Mo(\eta\text{-}Pr^iC_5H_4)(\eta\text{-}C_6H_6)(NCMe)]^+$ in accord with results obtained in Mo-carbonyl derivatives with N and P donor ligands and this has been related to the spectrochemical series.[2]

The orbital structure of $[M(\eta\text{-}C_5H_5)_2L_n]$ compounds has been studied by Green, Green, Prout, Dahl and Hofmann using crystallography[3], electron paramagnetic resonance[4], photoelectron spectroscopy[5] and m.o. calculations[6]. Derivation of the frontier molecular orbitals of the $[Mo(\eta\text{-}C_5H_5)_2]$ fragment (D_{5d} metallocene) was followed by a consideration of the changes brought about by bending the structure and the interaction of such a moiety with ligands, Figure 6.1. Figure 6.2 shows the effect of protonation on the molecular orbitals of $[Mo(\eta\text{-}C_5H_5)_2H_2]$. The third proton interacts with the h.o.m.o. of the $[Mo(\eta\text{-}C_5H_5)_2H_2]$ species lowering the energy of the latter, increasing the h.o.m.o. - l.u.m.o. gap and so further increasing shielding of the molybdenum nucleus in $[Mo(\eta\text{-}C_5H_5)_2H_2]$ on protonation.

Figure 6.3 compares the m.o.'s of $[Mo(\eta\text{-}C_5H_5)_2CO]$ and $[Mo(\eta\text{-}C_5H_5)_2H_2]$. The ability of CO to interact with a suitable

Table 6.1 Spectroscopic data for Bent Sandwich Molybdenum Complexes

Sample	Solvent	δ^{95}Mo	$W_{\frac{1}{2}}$/Hz.	^{13}C	Ionization Energies /eV (with C_{2v} assignments) $3a_1$ $2b_1$ $2a_1 + 1b_2 + 1b_1 + 1a_2$
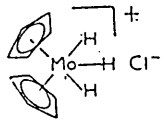 d	dil. HCl_{aq}	-2953	300	90.8	
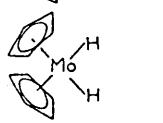 c	toluene	-2507	300	75.4	6.4 8.9 9.5[g]
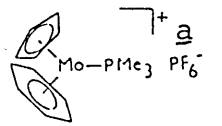 a	acetone	-2170	~350	-	
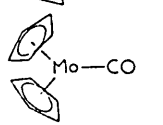 f	THF	-1964	150	-	5.9 6.8 8.8 9.3 9.6 [g]
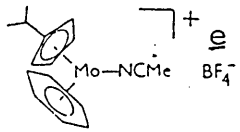 e	acetone	-1805	~550	-	
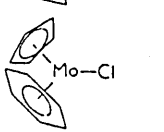 b	toluene	-1750	br.	-	
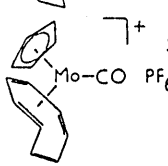 a	acetone	-1683	650	-	

Notes for Table 6.1.

a compound supplied by M.L.H.Green laboratory

b compound supplied by A. Izquierdo

c compound supplied by J.N.Verpeaux

d $[MoCp_2H_2]$ dissolved in HCl_{aq}, ref 1

e compound supplied by V.Patel

f compound supplied by author

g ref 5

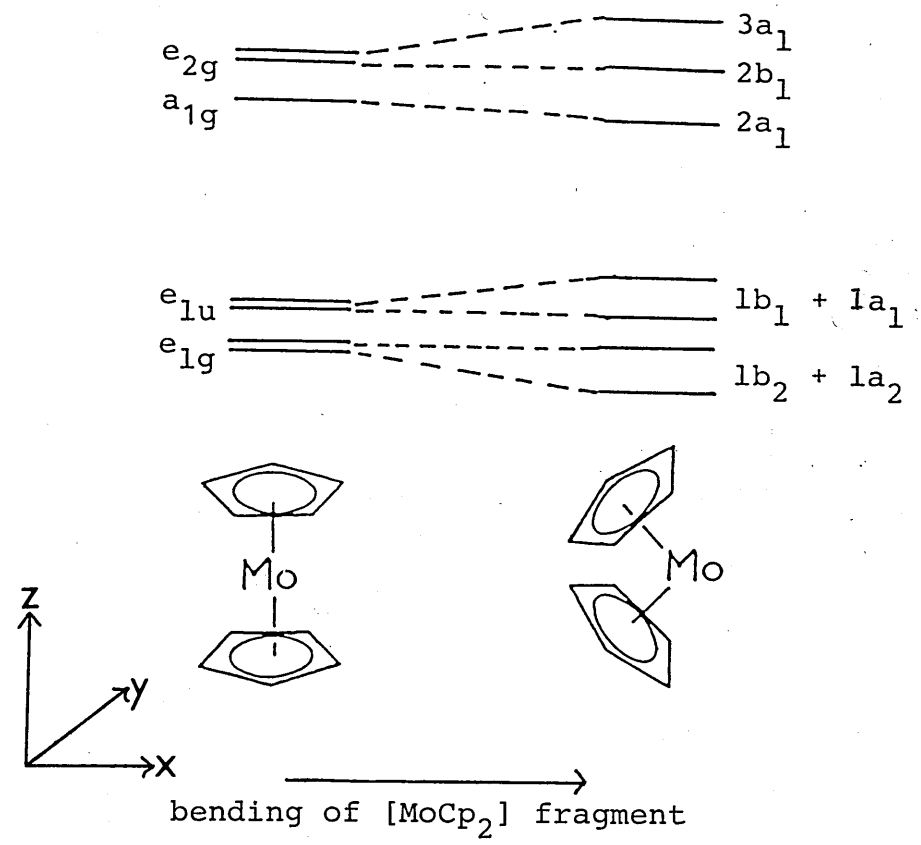

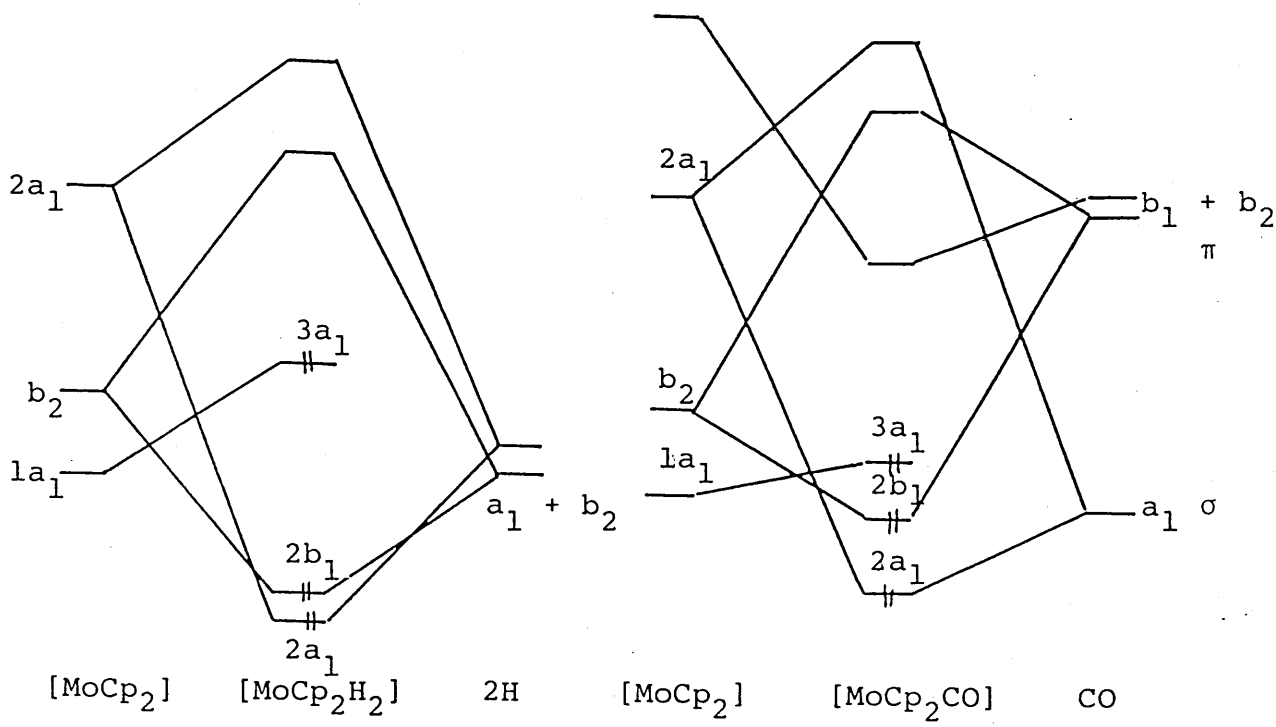

Figure 6.1 Molecular Orbital Diagrams for $[MoCp_2]$ Moieties.

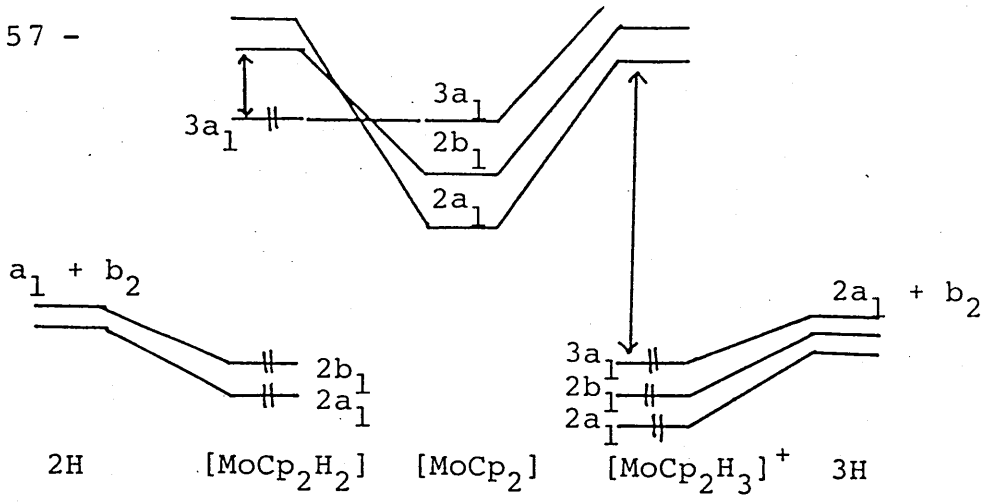

Figure 6.2 Protonation of $[MoCp_2H_2]$

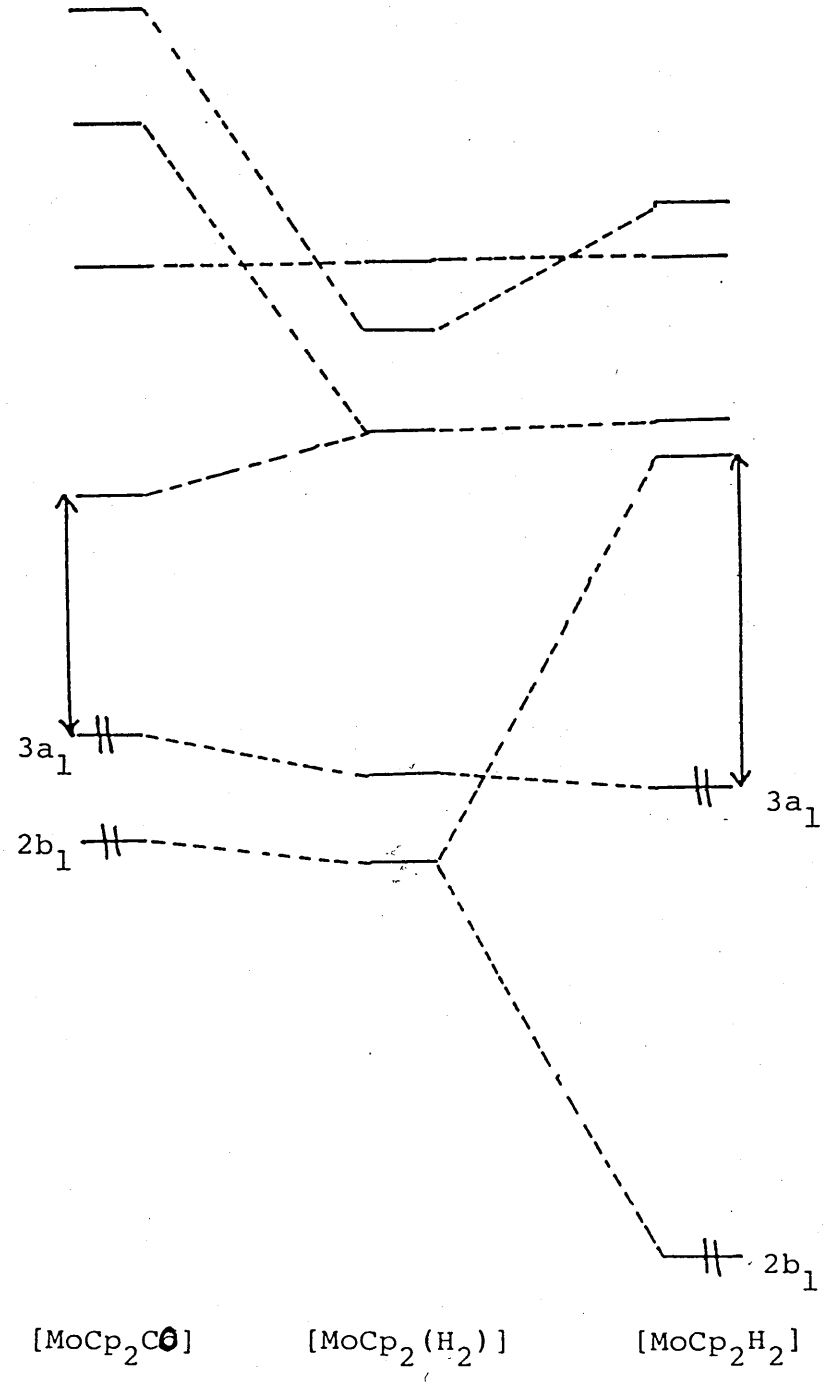

Figure 6.3 A Comparison of the Molecular Orbitals of $[MoCp_2H_2]$ and $[MoCp_2CO]$.

metal based orbital of molybdenum via its π^* orbitals results in a lowering of the b_1 orbital relative to that in $[Mo(\eta\text{-}C_5H_5)_2H_2]$ as shown in the p.e. data in Table 6.1. This suggests that the b_1 bonding or antibonding orbital is important in the electronic transitions associated with deshielding of the molybdenum nucleus because the lowering of the energy for such an electronic transition results in decreased shielding.

In this series of $[Mo(\eta\text{-}C_5H_5)_2]$ complexes low energy paramagnetic circulations, such as would shield the ^{95}Mo nucleus are possible from the partly $d\pi$, partly non-bonding orbital(s).

^{95}Mo shielding decreases with increasing number of $d\pi$/non-bonding electron pairs, thus:

$$MoCp_2H_3^+(0) > MoCp_2H_2(1) > MoCp_2CO(2)$$

It may be noted that these bent sandwich complexes give quite broad lines which, when combined with the limited solubility of some $[Mo(\eta\text{-}C_5H_5)_2]$ compounds, limits their study without resorting to high field n.m.r. techniques.

References for Chapter 6

1 M.L.H. Green, J.L. McCleverty, L. Pratt, G. Wilkinson, J. Chem. Soc., 1961, 4854.

2 S. Donovan-Mtunzi, M. Hughes, G.J. Leigh, H. Modh. Ali, R.L. Richards, J. Mason, J. Organomet. Chem., 1983, 246, C1.

3 J.C. Green, M.L.H. Green, C.K. Prout, J. Chem. Soc., Chem. Commun., 1972, 421.

4 J.L. Petersen, L.F. Dahl, J. Am. Chem. Soc., 1974, 96, 2248.

5 J.C. Green, S.E. Jackson, B. Higginson, J. Chem. Soc., Dalton Trans., 1975, 403.

6 J.W. Lauher , R. Hoffmann, J. Am. Chem. Soc., 1976, 98, 1729.

7 G.L. Geoffroy, M.G. Bradley, Inorg. Chem., 1978, 17, 2410.

Chapter 7: Benzene-Molybdenum Half Sandwich Complexes

Section 1: Benzene-molybdenum-allyl Complexes

η^3-allyl metal complexes are of interest as intermediates in the metal catalysed transformations of 1,3 dienes[1].

Table 7.1.1 shows n.m.r. data for a variety of Mo-benzene-allyl derivatives.

It is generally observed for molybdenum-arene species that methylation of the arene deshields the molybdenum. The chemical shifts of $[Mo(\eta\text{-}C_6H_6)(\eta\text{-}^3C_3H_5)_2]$ and $[Mo(\eta\text{-}C_6H_5Me)(\eta^3\text{-}C_3H_5)_2]$ illustrate this point. A large deshielding is observed when an η^3-allyl group in $[Mo(\eta\text{-}C_6H_6)(\eta^3\text{-}C_3H_5)_2]$ is replaced by an acetate group. Replacement of a benzene ring in $[Mo(\eta\text{-}C_6H_6)_2]$ with two $(\eta^3\text{-}C_3H_5)$ groups causes an increase in the shielding of the molybdenum of 64 ppm. Similarly for $[Mo(\eta\text{-}C_6H_5Me)_2]$ replacement of one ring by two allyl groups causes an increase of 116 ppm. The decrease in ^{95}Mo shielding when $[C_3H_5]$ in $[Mo(\eta\text{-}C_6H_6)(\eta^3\text{-}C_3H_5)_2]$ is replaced by $[CH_2{=}CH\text{-}CH{=}CH_2]$ may be related to the lowering of the m.o.'s of acyclic polyenes with increase in chain length.[2] (Figure 7.1.1)

The series of [Mo(Bz)(allyl)] cations measured in ^{95}Mo resonance provide further illustrations of trends previously seen in molybdenum carbonyl derivatives.[3,4] (However, in contrast, shielding decreases on replacement of a P-ligand 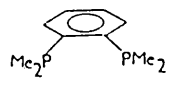 by an As-ligand ).

(a) For molybdenum carbonyl phosphine compounds $[Mo](R_2P(CH_2)_nPR_2)$ a ^{95}Mo shielding increase n = 1 < 2 accompanies a ^{31}P shielding decrease n = 2 > 1.

Table 7.1.1 N.m.r. data for molybdenum benzene allyl derivatives

Compound	Solvent	Solvent viscosity at 25° C/cP	$\delta^{95}Mo$	$W_{\frac{1}{2}}$ Hz	$^1J(^{95}Mo-^{31}P)$ from ^{95}Mo resonance Hz	$\delta^{31}P$	$^1J(^{95}Mo-^{31}P)$ from ^{31}P resonance Hz	$\delta^{13}C$ (arene)	$\delta^{13}C$ -CH-	$\delta^{13}C$ CH_2-	$\delta^{13}C$ other
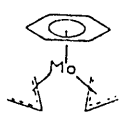 b	benzene	0.608	-1426	10				93.5	91.6	36.9	
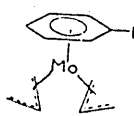 b	toluene	0.558	-1386	14				102.3,89.5 88.8,20.1	91.3	38.1	
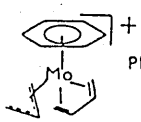 + j PF_6^-	benzene	0.608	-1354	⩽30				100.0	113.9	[108.4,50.2,43.8]	
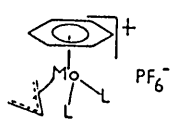 PF_6^-											
L⌒L = dmpe e	acetone	0.316	-1255	13	156	48.7	153	96.2	72.4	35.5	17.9[$J(^{13}C-^{31}P)$=14 Hz. 11.5[$J(^{13}C-^{31}P)$=13 Hz.
[1,2-$(PMe_3)_2$ d $-C_6H_4$]	acetone	0.316	-1250	⩽20	156	45.2	n.r.	97.1	75.3	35.1	131.8,129.3,128.9, 17.8. (P ligand)
L = $P(OMe)_3$ d	acetone	0.316	-1098	6	261	165.6	n.r.	98.2	80.4	38.8	

continued.....

Table 7.1.1 N.m.r. data for molybdenum benzene allyl derivatives

Compound	Solvent	Solvent viscosity at 25° C/cP	$\delta^{95}Mo$	$W_{\frac{1}{2}}$ Hz	$^1J(^{95}Mo-^{31}P)$ from ^{95}Mo resonance Hz	$\delta^{31}P$	$^1J(^{95}Mo-^{31}P)$ from ^{31}P resonance Hz	$\delta^{13}C$ (arene)	$\delta^{13}C$ -CH-	$\delta^{13}C$ CH_2-	$\delta^{13}C$ other
L⌒L = [1,2-$(AsMe_2)_2$-C_6H_4] d	acetone	0.316	-1080	12				95.3	71.1	32.2	131.6,130.1,13.7,9.4 (As ligand)
dmpm c	acetone	0.316	-1063	11	134	-10.6	133	96.7	74.5	36.2	18.5[$J(^{13}C-^{31}P)$=14 Hz. 11.9[$J(^{13}C-^{31}P)$=12 HZ.
L = PMe_3 h	acetone	0.316	-978	7	153	2.5	152	96.5	78.1	40.6	19.5[$J(^{13}C-^{31}P)$=14 Hz.
L⌒L = dpr^ipe f (arene = toluene)	acetone	0.316	-823	22	149	71.1	143				
L⌒L = dppe c	acetone	0.316	-936	⩽39	161	68.3	153	98.9	76.6	38.7	134.8,132.9,131.5, 129.9 (P ligand)
= dppm c	acetone	0.316	-795	⩽34	144	14.1	135	98.3	76.9	38.3	132.7,131.3,129.7, 43.6 (P ligand)
= 2,5 dth b	acetone	0.316	-348	100				97.8	76.7	43.4	37.8($S-CH_2-$) 20.5($S-CH_3$)
= H_2N⌒NH_2 b	acetone	0.316	-111	50				97.8	77.8	43.8[a]	45.4 [a]
= [1,2-$(NH_2)_2$-C_6H_4] b	acetone	0.316	25	100				98.1	79.3	44.0	127.8,126.6
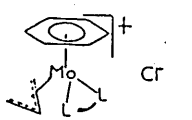 b	water	1.0	39	100				101.0	87.0	51.8	157.2,139.4,126.3, 124.8 (bpy ligand)
L⌒L = bpy											

continued.....

Table 7.1.1 N.m.r. data for molybdenum benzene allyl derivatives

Compound	Solvent	Solvent viscosity at 25° C/cP	$\delta^{95}Mo$	$W_{\frac{1}{2}}$ Hz	$^1J(^{95}Mo-^{31}P)$ from ^{95}Mo resonance Hz	$\delta^{31}P$	$^1J(^{95}Mo-^{31}P)$ from ^{31}P resonance Hz	$\delta^{13}C$ (arene)	$\delta^{13}C$ -CH-	$\delta^{13}C$ CH_2-	$\delta^{13}C$ other
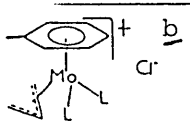 b L L = bpy	water	1.0	44	170				107.5,97.4 96.5, 19.6	86.2	52.3	157.0,139.4,126.5, 124.8(bpy ligand)
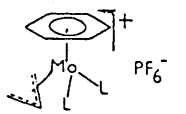 c L L = 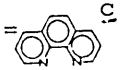	acetone	0.316	54	⩽50				100.0	85.2	50.3	156.6,137.4,128.0, 124.8
= bpy b	acetone	0.316	61	39				100.1	86.6	50.9	156.4,154.5,138.4, 125.4,123.9(bpy ligand)
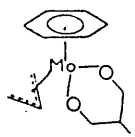 g	toluene	0.558	641	120							
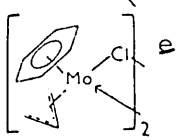 e	THF		834	80							

a assignments from decoupling experiment, b compound supplied by author, compound supplied by N.Copley, d compound supplied by H.Bunting, compound supplied by A.Izquierdo f compound supplied by V.C.Gibson, g compound supplied by I.Treurnicht, h compound supplied by C.MacAteer, j compound supplied by M.L.H.Green laboratory.

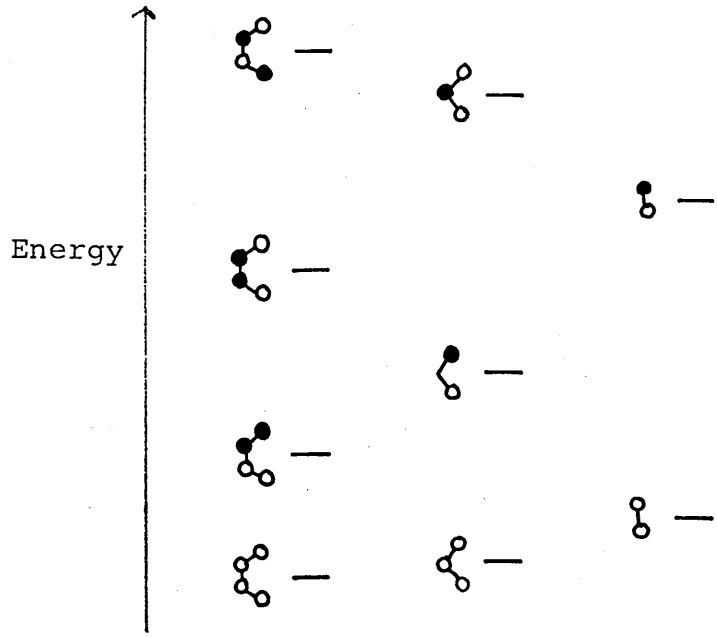

Figure 7.1.1. Relative energies and nodal characteristics of the π-orbitals of acyclic polyenes[2]

(b) $^{1}J(^{95}Mo-^{31}P)$ does not vary greatly but increases slightly with $\overline{Mo-P-P}$ ring size and increases on replacement of PR_3 with $P(OR)_3$.

(c) Shielding decreases for the derivatives dmpe > dppe (i.e. replacing a stronger ligand, an alkyl phosphine, with a weaker aryl phosphine) and for dmpe > $(PMe_3)_2$. (i.e. replacing a bidentate ligand with two similar monodentate ligands).

When comparing ^{95}Mo shielding, generally larger differences in chemical shifts occur when there are no carbonyl ligands present. This may be due to the synergic nature of the bonding of the carbonyl ligand enabling it to partly 'compensate' for the effects of other ligands and also its high position in the spectrochemical series resulting in high effective shielding of the ^{95}Mo nucleus.

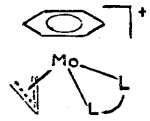

$\overset{\frown}{L\ L}$ = dppe, $\delta^{95}Mo$ = -936 ppm.

$\overset{\frown}{L\ L}$ = bpy, $\delta^{95}Mo$ = 61 ppm.

$\Delta\delta$ = 997 ppm.

$[Mo(CO)_4dppe]$ $\delta^{95}Mo$ = -1782 ppm.[4]

$[Mo(CO)_4bpy]$ $\delta^{95}Mo$ = -1190 ppm.[4]

$\Delta\delta$ = 592 ppm.

The difference in shielding of dppe and bpy derivatives is ascribed largely to nephelauxetic effects.

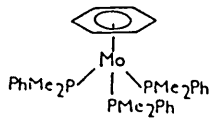

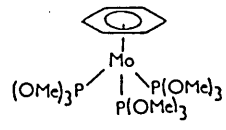

$\delta^{95}Mo$ = -1807 ppm. $\longleftrightarrow$ $\delta^{95}Mo$ = -1375 ppm.

$\Delta\delta$ = 432 ppm.

$[Mo(CO)_3(P(OMe)_3)_3]$ $\delta^{95}Mo$ = -1756 ppm.[4]

$[Mo(CO)_3(PMe_2Ph)_3]$ $\delta^{95}Mo$ = -1427 ppm.[5] $\Delta\delta$ = 327 ppm.

The differences in shielding of $[P(OMe)_3]$ and $[PMe_2Ph]$ derivatives are ascribed largely to spectrochemical effects.

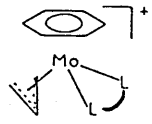

$L\frown L$ = dppm, $\delta^{95}Mo$ = -795 ppm.
$L\frown L$ = dppe, $\delta^{95}Mo$ = -936 ppm.
$\Delta\delta$ = 141 ppm.

$[Mo(CO)_4dppm]$ $\delta^{95}Mo$ = -1552 ppm.[4]
$[Mo(CO)_4dppe]$ $\delta^{95}Mo$ = -1782 ppm.[4]
$\Delta\delta$ = 230 ppm.

Differences in ^{95}Mo shielding between these two molybdenum-carbonyl derivatives have been related to deformations of inter-bond angles. Carbonyls, as good π-acceptors, (and moderate σ donors) withdraw electron density from the metal so the metal orbitals contract due to the greater effective nuclear charge. Such orbital contraction means that angle strain is felt to a greater extent than in the molybdenum-benzene derivatives. Benzene is a good π donor and poor acceptor so pushing electron density onto the metal orbitals causing expansion and so angle strain is lessened.

Figures 7.1.2-4 show graphs of ^{95}Mo versus $\delta^{13}C_6H_6$, δ^{13} -CH- and $\delta^{13}CH_2$- for the series of compounds $[Mo(\eta\text{-}C_6H_6)(\eta^3\text{-}C_3H_5)(L_2)]^+ PF_6^-$. $\delta^{13}C_6H_6$ varies only slightly with $\delta^{95}Mo$ but as the ^{95}Mo shielding decreases there is a trend towards decreased shielding of the carbons of the allyl group. The decreased shielding of a molybdenum centre on exchange of a P-ligand for an N-ligand is well known and is ascribed to nephelauxetic effects. The first two π MOs of the $[allyl]^+$ ligand are

Figure 7.1.2. $\delta^{13}C_6H_6$ versus $\delta^{95}Mo$ for the Compounds $[Mo(\eta\text{-}C_6H_6)(\eta^3\text{-}C_3H_5)(L_2)]^+ PF_6^-$

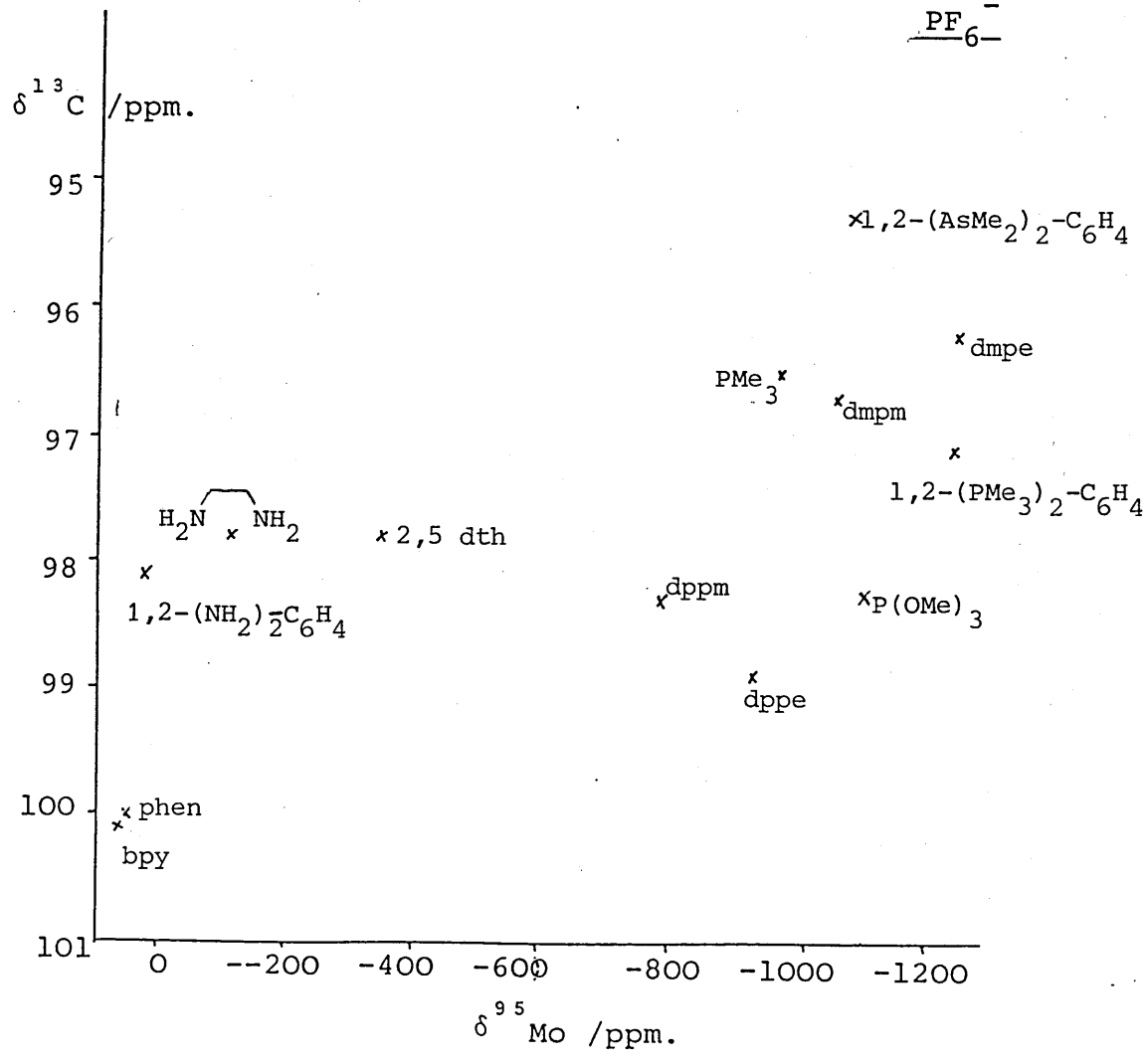

Figure 7.1.3. δ^{13}-CH- versus δ^{95}Mo for the compounds $[Mo(\eta\text{-}C_6H_6)(\eta^3\text{-}C_3H_5)(L_2)]^+PF_6^-$

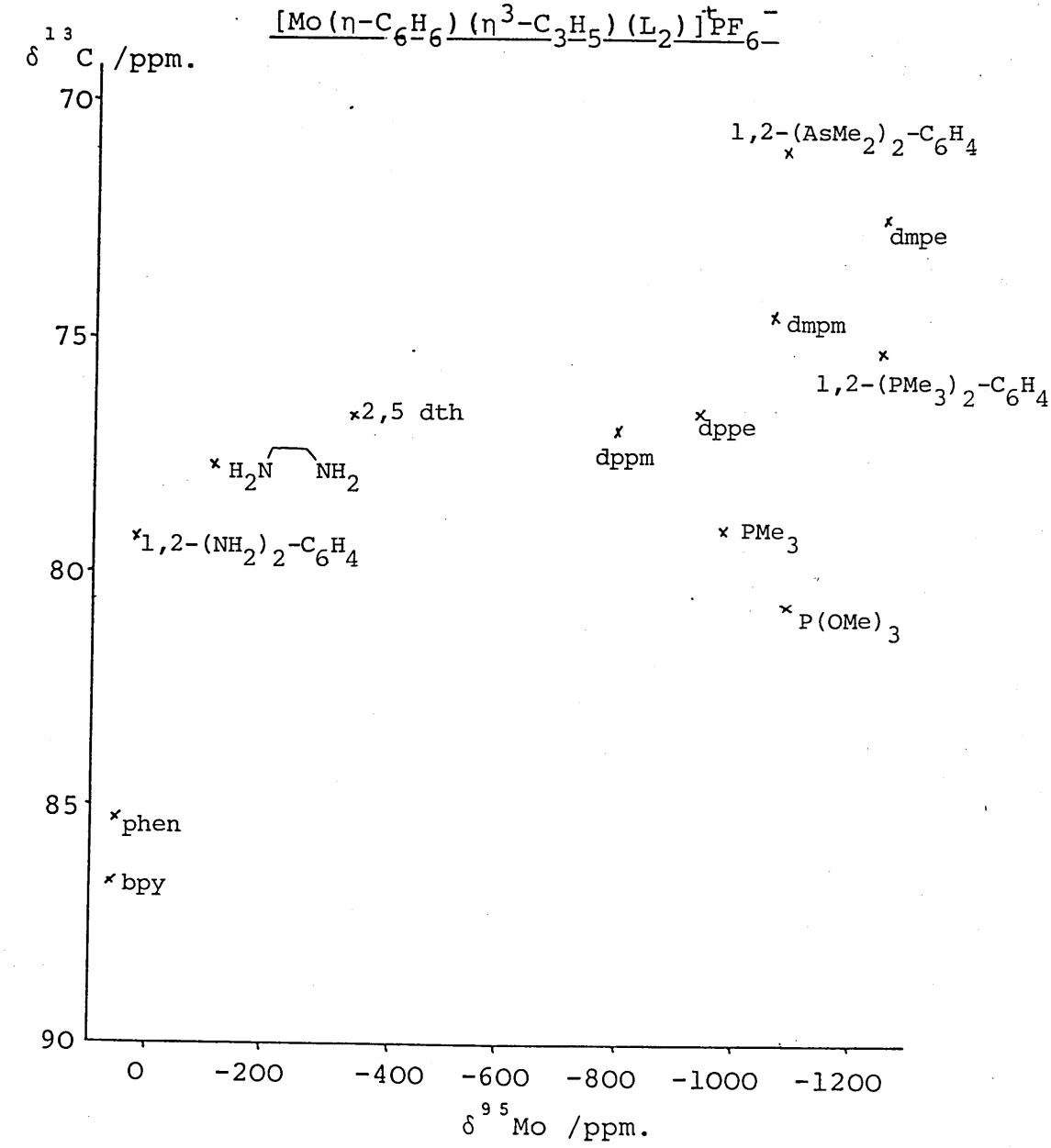

Figure 7.1.4. $\delta^{13}CH_2$- versus $\delta^{95}Mo$ for the compounds $[Mo(\eta\text{-}C_6H_6)(\eta^3\text{-}C_3H_5)(L_2)]^+PF_6^-$

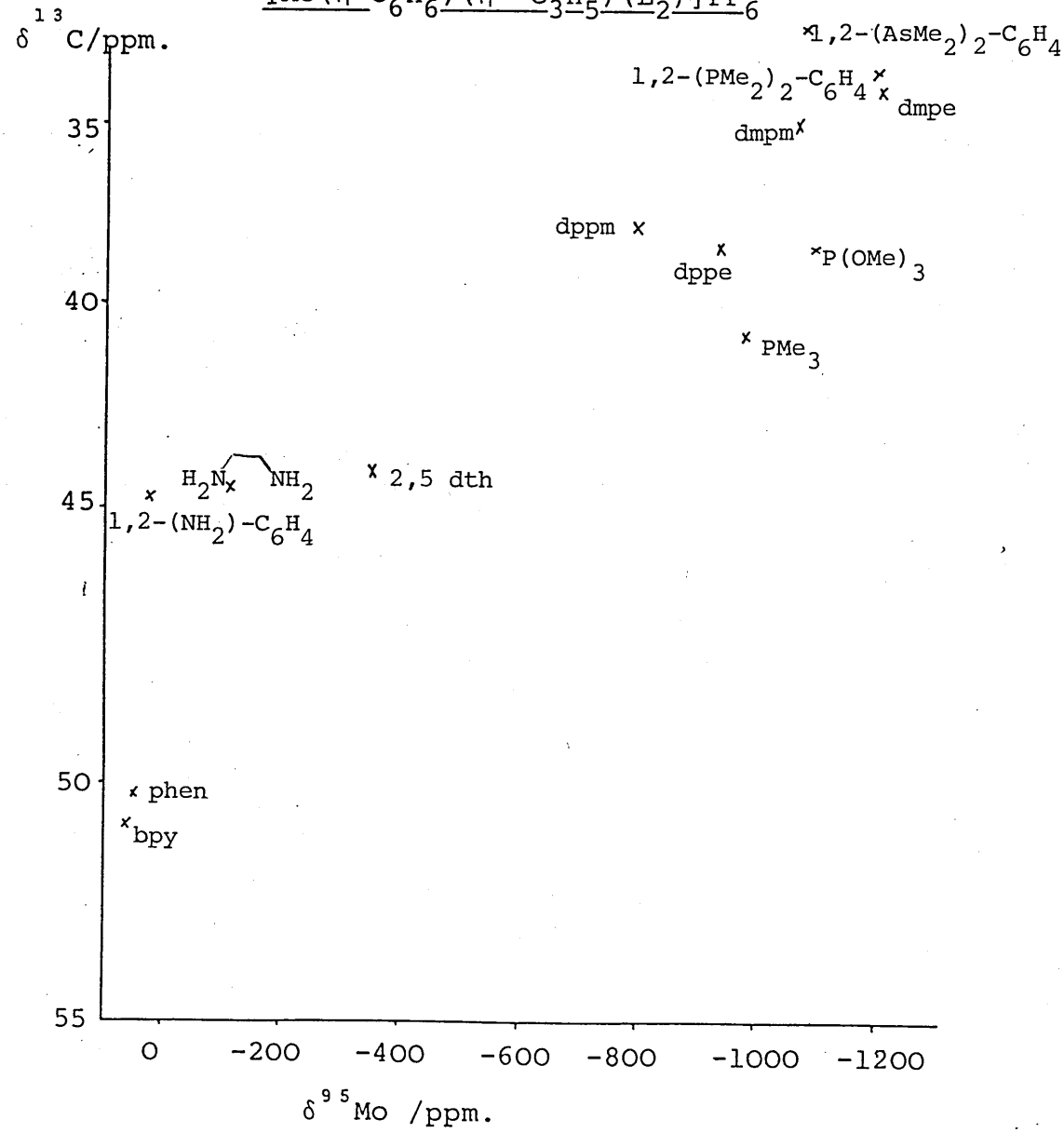

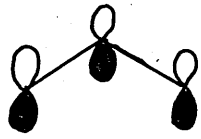

filled

ψ_1

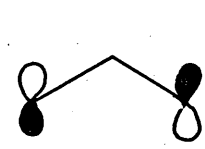

empty

ψ_2

The better correlation of $\delta^{13}CH_2$- with $\delta^{95}Mo$ than of δ^{13}-CH- with $\delta^{95}Mo$ may be related to the l.u.m.o. ψ_2 being situated on the terminal carbon atoms. The contraction of the ^{95}Mo d-orbitals on replacing a P-ligand with an N-ligand will result in poorer overlap of ψ_2(allyl) with the filled d-orbitals and this may tend to decrease the $^{13}CH_2$- shielding.

The linewidths of the compounds in Table 7.1.1 are relatively small. There is a general increase in the linewidth with an increase in molecular size and with loss of symmetry about the metal centre. The broader lines observed for certain substituted molybdenum carbonyl compounds may be due to the presence of unresolved scalar coupling to quadrupolar ligand nuclei, ^{14}N and ^{75}As.[4]

Section 2 Benzene-molybdenum phosphine compounds

Tables 7.2.1 and 7.2.2 give spectral data for molybdenum benzene phosphine piano stool compounds.

It is generally observed that where the linewidth of the ^{95}Mo signal is small molybdenum satellites are discernable in the ^{31}P spectrum. It has been shown that the n.m.r. spectrum of a spin $\frac{1}{2}$ nucleus bonded to a spin $\frac{5}{2}$ nucleus will consist of 6 lines of equal intensity only if the spin lattice relaxation time (T_1) of the quadrupolar nucleus is long compared to the inverse of the coupling constant[6] (see Chapter 3.3) In the systems discussed here $T_1 = T_2 = T_q$. Therefore, in the series $[Mo(\eta\text{-}C_6H_6)(\eta\text{-}C_3H_5)(L_2)]^+$ in acetone solution (see also Section 1)

	$W_{\frac{1}{2}}$/Hz	$^1J(^{95}Mo\text{-}^{31}P)$/Hz from ^{95}Mo spectrum	from ^{31}P spectrum
L_2 = dmpe	13	156	153
$(PMe_3)_2$	7	153	152
$[P(OMe)_3]_2$	6	261	n.r.

a possible reason for the failure to observe ^{95}Mo satellites in the case $L_2 = [P(OMe)_3]_2$ may be the smaller value of $^1/J$. The variation of $^1J(^{95}Mo\text{-}^{31}P)$ with phosphine has been discussed in Section 1. A further illustration of this is given by the $[Mo(\eta\text{-}C_6H_6)(dmpe)(L)]^+$ complexes. When $L = P(OMe)_3$ the ^{95}Mo spectrum is a doublet of triplets but when $L = PMe_3$ it appears to be a quartet.

Table 7.2.1 Benzene-molybdenum triphosphines and related compounds

Sample	Solvent	Solvent Viscosity /cP at 25 °C	δ^{95}Mo /ppm	$W_{\frac{1}{2}}$ /Hz	$^{1}J(^{95}Mo-^{31}P)$ /Hz	δ^{31}P /ppm	$\delta^{13}C_6H_6$ /ppm	δ^{13}C other /ppm
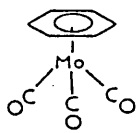 a	CH_2Cl_2	0.393	-2099	6	-	-	94.2 j	
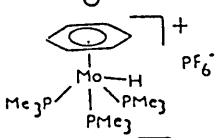 b	$(CH_3)_2CO$	0.316	-1839	65	166			
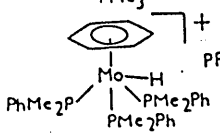 d	$(CH_3)_2CO$	0.316	-1946	500	n.r..	5.7	82.4 h	130.1, 129.4 P-Ph 24.9, 24.5, 24.1, 23.6 P-Me
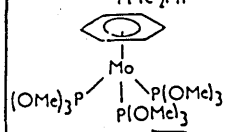 b	C_6H_5Me	0.552	-1807	7	340		79.0 h	
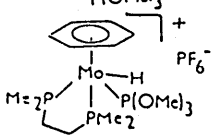 c	$(CH_3)_2CO$	0.316	-1556	30	278 e 156			
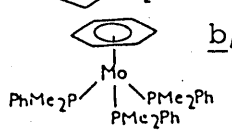 b,d	C_6H_5Me	0.552	-1375	12	220 (216) f	12.7	73.2 h	ca.130(c) P-Ph 25.3, 25.0, 24.8, 24.5 P-Me
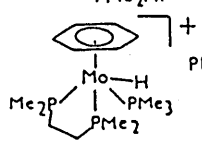 c	$(CH_3)_2CO$	0.316	-1316	⩽50		161		

Notes for Table 7.2.1

a see Chapters 4.2 and 5.1

b compound supplied by C. MacAteer

c compound supplied by P. Newman

d compound supplied by author

e $^{1}J(^{95}Mo-^{31}P_{phosphite})$ = 278 Hz, $^{1}J(^{95}Mo-^{31}P_{phosphine})$ = 156 Hz.

f number in parentheses refers to value obtained from ^{31}P spectrum.

g obscured by solvent peak C_6D_6

h ^{13}C n.m.r. in C_6D_6

j ^{13}C n.m.r. in $CDCl_3$

Table 7.2.2 Benzene-molybdenum diphosphines and related compounds

Sample	Solvent	Solvent Viscosity /cP at 25°C	δ^{95}Mo /ppm	$W_{\frac{1}{2}}$ /Hz	$^{1}J(^{95}Mo-^{31}P)$ /Hz d	δ^{31}P /ppm	$\delta^{13}C_6H_6$ /ppm	δ^{13}C other /ppm
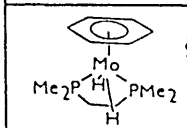 a	C_6H_5Me	0.552	-1909	27	146 (~140)	52.4	80.6 eg	
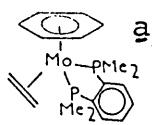 a	C_6H_5Me	0.552	-1909	≤30	195			
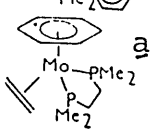 a	C_6H_5Me	0.552	-1825	17	190 (188)	44.2	73.5 eg	
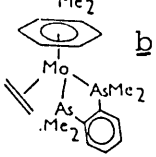 b	C_6D_6	0.608	-1721	25			72.0 e	33.5,15.7, 10.6.
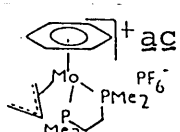 ac	$(CH_3)_2CO$	0.316	-1255	13	156 (153)	48.7	96.2 f	
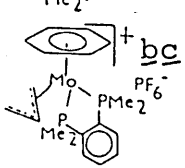 bc	$(CH_3)_2CO$	0.316	-1250	12	156 (n.r.)	45.2	97.1 f	

continued.....

Table 7.2.2 Benzene-molybdenum diphosphines and related compounds

Sample	Solvent	Solvent Viscosity /cP at 25°C	δ^{95}Mo /ppm	$W_{\frac{1}{2}}$ /Hz	$^{1}J(^{95}Mo-^{31}P)$ /Hz d	δ^{31}P /ppm	$\delta^{13}C_6H_6$ /ppm	δ^{13}C other /ppm
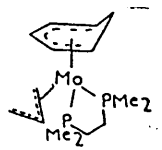 a	C_6H_5Me	0.552	-1272	25	139,183	43.6 50.9		
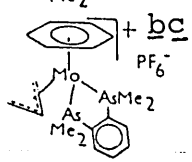 + bc PF_6^-	$(CH_3)_2CO$	0.316	-1080	12			95.3 f	

a compound supplied by M.L.H. Green laboratory

b compound supplied by H. Bunting

c see also chapter 7.1

d numbers in parantheses refer to values obtained from ^{31}P spectrum

e ^{13}C n.m.r. in C_6D_6

f ^{13}C n.m.r. in $(CD_3)_2CO$

g ref. 8

From ^{1}H n.m.r. studies it was deduced that $[Mo(\eta^{5}\text{-}C_6H_7)(dmpe)(allyl)]$ has the structure shown below.[7]

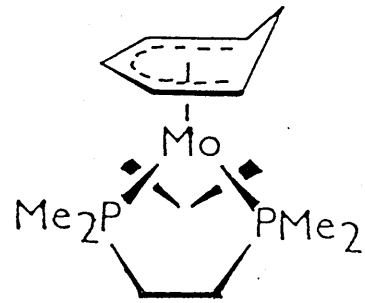

The ^{31}P and ^{95}Mo n.m.r. spectra support this, the former consisting of two doublets and the latter a doublet of doublets, the phosphorus atoms being inequivalent and coupling to the molybdenum atom to differing extents. In an attempt to assign each of the coupling constants, 183 and 139 Hz, to a ^{31}P resonance the ^{31}P spectrum with a high signal to noise ratio was studied but no distinctive ^{95}Mo satellites could be discerned.

From Table 7.2.1 in the series $[Mo(\eta\text{-}C_6H_6)(L)_3]$ ^{95}Mo shielding increases $L = PMe_2Ph < P(OMe)_3 < CO$.

This variation has been related to the spectrochemical series.[3] The benzene carbon shielding increases

$L = CO < P(OMe)_3 < PMe_2Ph$

In Chapter 5.3 it is proposed that the greater shielding of the carbons of the benzene ring in $[Mo(\eta\text{-}C_6H_6)]_2$ than in $[Mo(\eta\text{—}C_6H_6)(CO)_3]$ may be explained in terms of variation in the degree of metal → arene backbonding. Similar arguments may be applied here, the acceptor abilities of the ligands increasing $PMe_2Ph < P(OMe)_3 < CO$.

From the data in Table 7.2.1 ^{95}Mo shielding increases on protonation of molybdenum-benzene triphosphine compounds while the ^{31}P shielding of the phosphine increases and the benzene carbon shielding decreases. The protonation may be viewed as similar to the case of $[Mo(\eta\text{-}C_5H_5)H_2]$ in that a formerly metal based electron pair is used in bonding to the proton (see chapter 6).

^{95}Mo shielding increases $[Mo(\eta\text{-}C_6H_6)(L_2)(\eta\text{-}C_3H_5)]^+$ < $[Mo(\eta\text{-}C_6H_6)(L_2)(\eta\text{-}C_2H_4)]$ and is accompanied by an increase in the benzene carbon shielding. The change in ^{95}Mo shielding may be related to Figure 7.1.1 and the increase in shielding $[Mo(\eta\text{-}C_6H_6)(\eta\text{-}C_3H_5)(\eta\text{-}C_4H_6)]^+$ < $[Mo(\eta\text{-}C_6H_6)(\eta\text{-}C_3H_5)_2]$ (Section 1). Then it may be proposed that ^{95}Mo shielding decreases with increasing chain length of a polyene $\eta\text{-}C_2H_4$ > $\eta\text{-}C_3H_5$ > $\eta\text{-}C_4H_6$. Also the increase in positive charge could result in an increase in the radial term giving a decrease in metal shielding.

References for Chapter 7

1 P.W. Jolly, R. Mynott, Adv. in Organomet. Chem., 1981 19, 257.

2 D.M.P. Mingos, Chapter 19 in Vol. 3 of "Comprehensive Organometallic Chemistry", ed. G. Wilkinson, F.G.A. Stone, E.W. Abel. Pergamon Press, 1982, p61.

3 S. Donovan-Mtunzi, M. Hughes, G. J. Leigh, H. Modh. Ali, R.L. Richards, J. Mason, J. Organomet. Chem., 1983, 246, C1.

4 A.F. Masters, G.E. Bossard, T.A. George, R.T.C. Brownlee, M.J. O'Connor, A.G. Wedd, Inorg. Chem., 1983, 22, 908.

5 E.C. Alyea, A. Somogyvari, Proceedings of the Climax Fourth International Conference on the Chemistry and Uses of Molybdenum, (H.F. Barry and P.C.H. Mitchell eds.) Climax Molybdenum Company, Ann Arbor, Michigan, 1982, p46.

6 M. Suzuki, R. Kubo, Mol. Phys., 1963, 7, 201.

7 M.L.H. Green, L.C. Mitchard, W.E. Silverthorn, J. Chem. Soc. Dalton Trans., 1973, 2177.

8 A. Izquierdo, D.Phil. Thesis, Oxford, 1983.

Chapter 8 Molybdenum-molybdenum Bonded Compounds

Section 1: Mo-Mo Quadruply Bonded Compounds

Table 8.1.1. shows spectroscopic data for some Mo-Mo quadruply bonded compounds. The study of this type of compound in ^{95}Mo resonance is limited by the broad signals observed and the low solubility of certain types of complex. The broad lines are due to a substantial electric field gradient that would be present at the metal centre and the large size of the molecules. T_1 for $[Mo_2(O_2CBu^n)_4]$ has been measured as 180 μs.[8] In compounds of the type $[Mo_2(O_2CR)_4]$ where R = $(CH_2)_6CH_3$,Ph no resonances are observed, possibly due to excessive line broadening.

Molybdenum-molybdenum quadruply bonded compounds have the least shielded molybdenum nuclei of all the types of molybdenum compounds studied so far.

The ^{95}Mo chemical shift of $[Mo_2(O_2CCF_3)_4]$ is solvent dependent. Shielding of the molybdenum decreases as the coordinating power of the solvent increases. The solvent molecules are thought to coordinate axially, a bis-pyridine adduct has been isolated and its crystal structure determined,[9] weakening the metal-metal bond as evidenced from values of Mo-Mo bond distances and ν(Mo-Mo) stretching frequencies, Table 8.1.2. The lowest energy transition in the electronic spectra of dimolybdenum tetracarboxylate compounds has been the centre of much discussion and it has been proposed to be spin-allowed $\delta \rightarrow \delta^*$. The lowest unoccupied orbital is the π^* orbital involving carbon and oxygen p-orbitals and it is considered that the relatively high transition energy of the first band in the electronic spectra might result from a stabilisation of the δ orbital through mixing with the π^* orbital.[13] The

Table 8.1.1 Spectroscopic Data for Molybdenum-molybdenum Quadruply Bonded Compounds

Sample	Solvent	δ^{95}Mo /ppm	$W_{\frac{1}{2}}$Hz	Electronic Spectra λ_{max}/nm	ε(M^{-1} cm^{-1})	Ionization Energies /eV
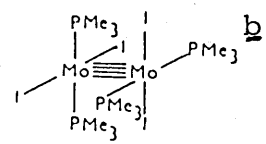 [b]	C_6H_5Me/C_6D_6	2927	850	614[g]	3.5×10^3	n.o.
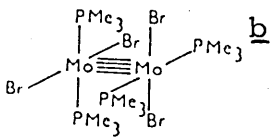 [b]	THF/$(CD_3)_2CO$ C_6H_5Me/C_6D_6	2996 3008	800 840	595[g]	3.6×10^3	6.6 δ 7.8 π [h]
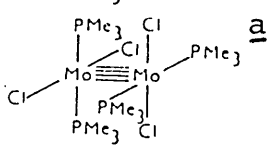 [a]	THF/$(CD_3)_2CO$ C_6H_5Me/C_6D_6	3021 3008	800 800	583[g]	3.4×10^3	6.44 δ 7.70 π [j]
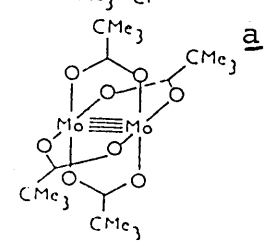 [a]	THF/$(CD_3)_2CO$	3667	870	434[m]	136	6.75 δ 8.54 π [k]
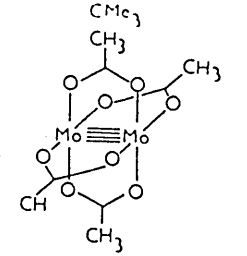	THF	3702[l]	520	441[m]	60	6.92 δ 8.77 π [k]

continued.....

Table 8.1.1 Spectroscopic Data for Molybdenum-molybdenum Quadruply Bonded Compounds

Sample	Solvent	δ^{95}Mo /ppm	$W_{\frac{1}{2}}$Hz	Electronic Spectra λ_{max}/nm	ε(M^{-1} cm^{-1})	Ionization Energies /eV
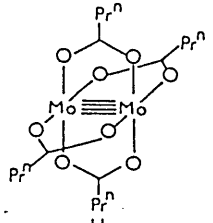	DMF	3730[e]	1400			
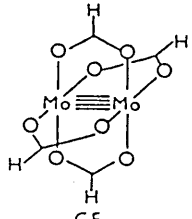 d	HCO_2H	3768[f]	670	439	120	7.60 δ k 9.37 π k
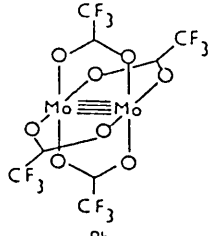 a	$CHCl_3$ THF/$CDCl_3$ THF C_5H_5N/CH_2Cl_2	3874 4021 4026[e] 4185	430 400 250 320	430 436 504		8.67 δ k 10.44 π k
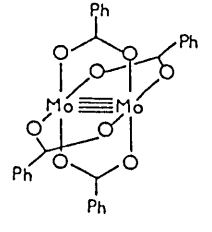 c	THF/$(CD_3)_2CO$	n.o.				

Notes for Table 8.1.1.

a compound supplied by author

b compound supplied by S.K.Habron

c compound supplied by I.Treurnicht

d compound supplied by V.C.Gibson

e measured at 55 C, ref 1

f dubious signal

g ref 2

h ref 3. Decomposition of the sample to give PMe_3, the remaining features of the spectrum are assumed to be the complex

j ref 4

k ref 5

l ref 6

m ref 7

n ref 14

Table 8.1.2 Molybdenum-molybdenum quadruple bond data

Compound	δ^{95}Mo	Mo-Mo Bond Distance /A	ν(Mo-Mo)/cm^{-1} stretching frequency
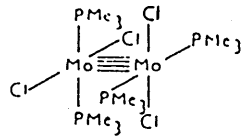	3008	2.13 [a]	342 [d]
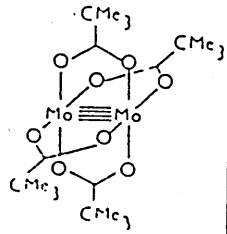	3667	2.008 [b]	-
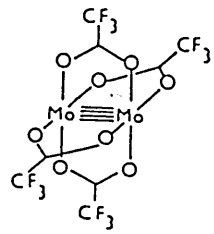	3874	2.09 [b]	397 [c]
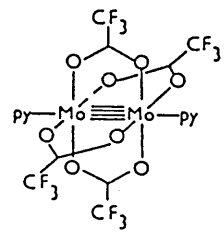	4185	2.129 [c]	367 [c]

a ref 10

b ref 11

c ref 9

d ref 12

increase in wavelength of the first band in the electronic spectra of $[Mo_2(O_2CCF_3)_4]$ with increasing donor power of the solvent is consistent with a decrease in the h.o.m.o. - l.u.m.o. gap and so correlates with the observed decrease in shielding of the molybdenum.

Figure 8.1.1 is a plot of $\delta^{95}Mo$ versus the lowest energy electronic absorption band (δ-δ^*) in molybdenum-molybdenum quadruply bonded compounds. It has been pointed out[14] that for a given metal the overlap of the d orbitals to form a metal-metal bond may be affected by the ligands. For example, the σ-donating ability of the ligands can increase the effective charge on the metal causing expansion of the d orbitals and increased δ overlap. The δ orbitals are more sensitive than the π orbitals to the nature of the ligands because as the ligands approach along the x and y axes (see Figure 8.1.4) they interact directly with the $d_{x^2-y^2}$ orbitals to form M-L σ bonds. The orbitals affected to the next greatest extent are the co-planar d_{xy} orbitals which are used to form the M-M δ bond. Some ligands can act as π donors. The p electrons of halides can repel the filled δ orbital. While influencing the electronic spectra, particularly the δ-δ^* region, these overlap effects may not play an important role in determining bond lengths or bond strengths. These properties are set by the much stronger σ and π interactions which maximise at longer M-M distances than δ interactions. So the lack of correlation observed in Figure 8.1.1 implies that it is not the δ-δ^* transition that is most important in determining the metal shielding in molybdenum-molybdenum quadruply bonded complexes.

Figure 8.1.1. δ^{95}Mo versus λ_{max} from the Electronic Spectra for Molybdenum-molybdenum Quadruply Bonded Compounds

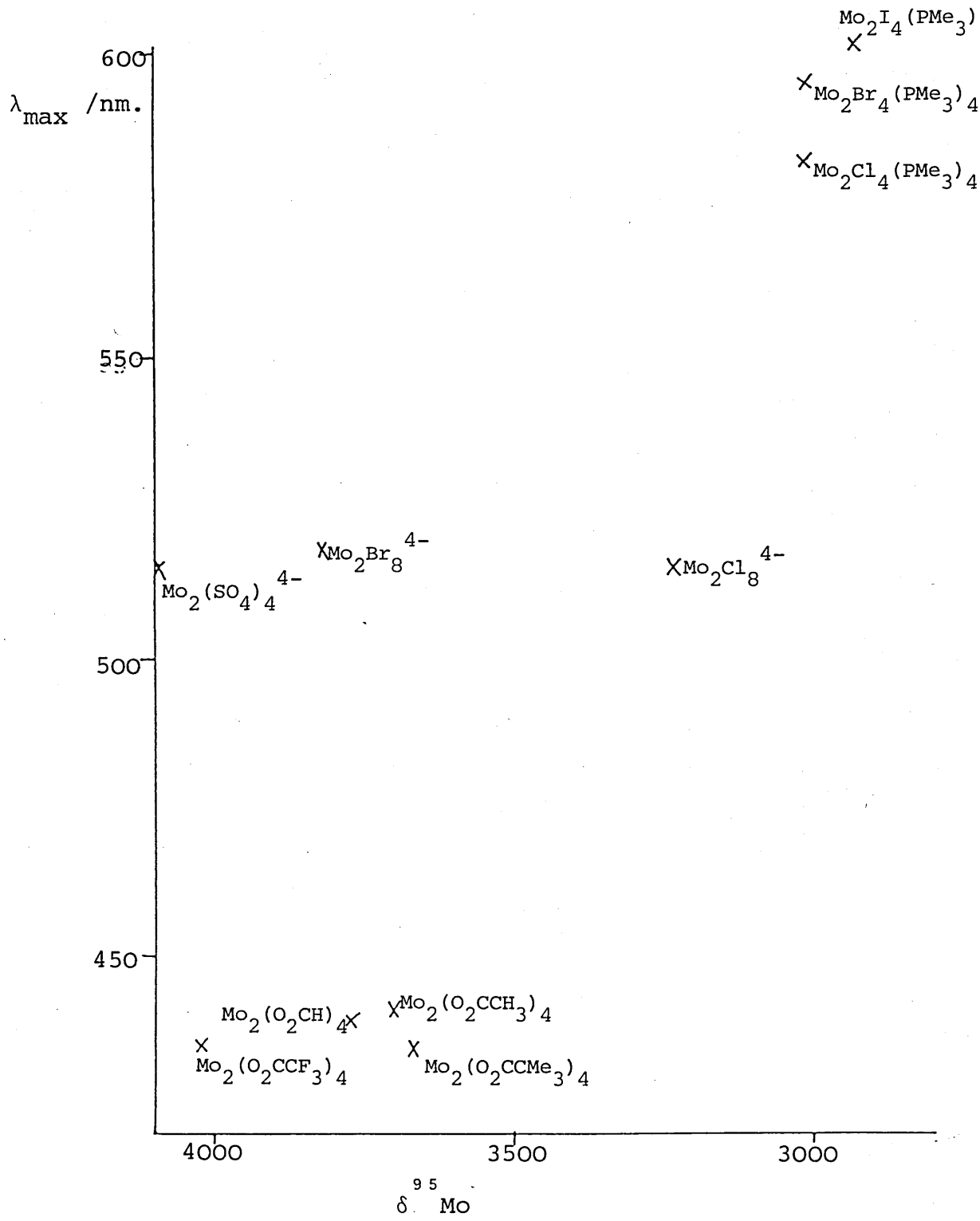

Key to Figure 8.1.1.

Compound	δ^{95}Mo reference	λ_{max} reference
$Mo_2(SO_4)_4^{4-}$	6	14
$Mo_2(O_2CCF_3)_4$	this work	this work
$Mo_2Br_8^{4-}$	6	14
$Mo_2(O_2CH)_4$	this work	14
$Mo_2(O_2CCH_3)_4$	6	14
$Mo_2(O_2CCMe_3)_4$	this work	7
$Mo_2Cl_8^{4-}$	6	14
$Mo_2Br_4(PMe_3)_4$	this work	2
$Mo_2Cl_4(PMe_3)_4$	this work	2
$Mo_2I_4(PMe_3)_4$	this work	2

In the series $[Mo_2(O_2CR)_4]$ as the molybdenum shielding decreases so the ionization energies of the δ and π orbitals of the molybdenum-molybdenum quadruple bond increase, (Figure 8.1.2).

The Mo-Mo bond distances and the Mo-Mo stretching frequencies in Table 8.1.2 suggest a stronger Mo-Mo bond in the tetracarboxylate compounds than in those of the type $[Mo_2X_4(PMe_3)_4]$. So in this comparison a strengthening of the Mo-Mo bond occurs with a decrease in the molybdenum shielding.

Figure 8.1.3 shows the results of SCF-Xα-SW calculations on $[Mo_2Cl_4(PH_3)_4]$ and $[Mo_2(O_2CH)_4]$ and, for comparison, the p.e. results for $[Mo_2Cl_4(PMe_3)_4]$ and $[Mo_2(O_2CH)_4]$. Ligand energy levels have been omitted for clarity. Although direct comparison of the values obtained requires caution, the calculations suggest that the σ-Mo-Mo energy increases with a decrease in ^{95}Mo shielding. Figure 8.1.4 shows that the σ-Mo-Mo energy would also increase as ^{95}Mo shielding increases on coordination of axial ligands. This data is consistent with the Mo-Mo σ or σ^* orbitals being important in the electronic transitions which deshield the molybdenum nucleus.

There is little difference in the ^{95}Mo chemical shifts of $[Mo_2Cl_4(PMe_3)_4]$ and $[Mo_2Br_4(PMe_3)_4]$ in THF or in toluene while the molybdenum in the iodo analogue is more shielded by approximately 80 ppm. It has been proposed that the difference is due to relativistic effects.[17] Decreased shielding in the order I > Br > Cl is that expected if nephelauxetic effects dominated the shielding pattern and Cl > Br > I if spectrochemical effects were dominant. However the nephelauxetic sequence is not normally observed with low shielding. The ordering I > Br > Cl is also that expected because of relativistic effects.

Figure 8.1.2. Ionization Energies versus $\delta^{95}Mo$ for $[Mo_2(O_2CR)_4]$

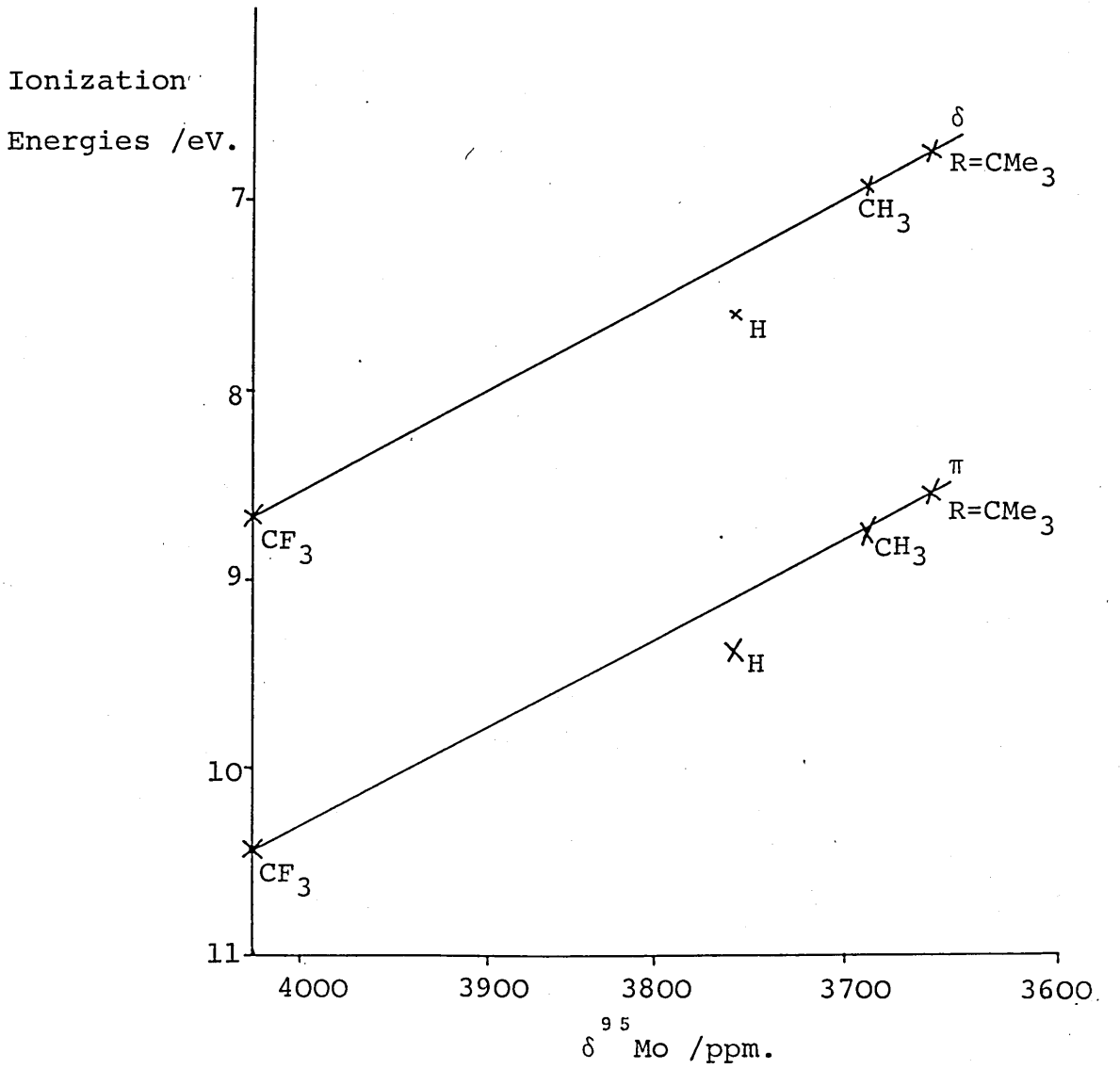

Figure 8.1.3. Results of SCF-Xα-SW Calculations, and P.E.S. Data for Molybdenum-Molybdenum Quadruply Bonded Compounds

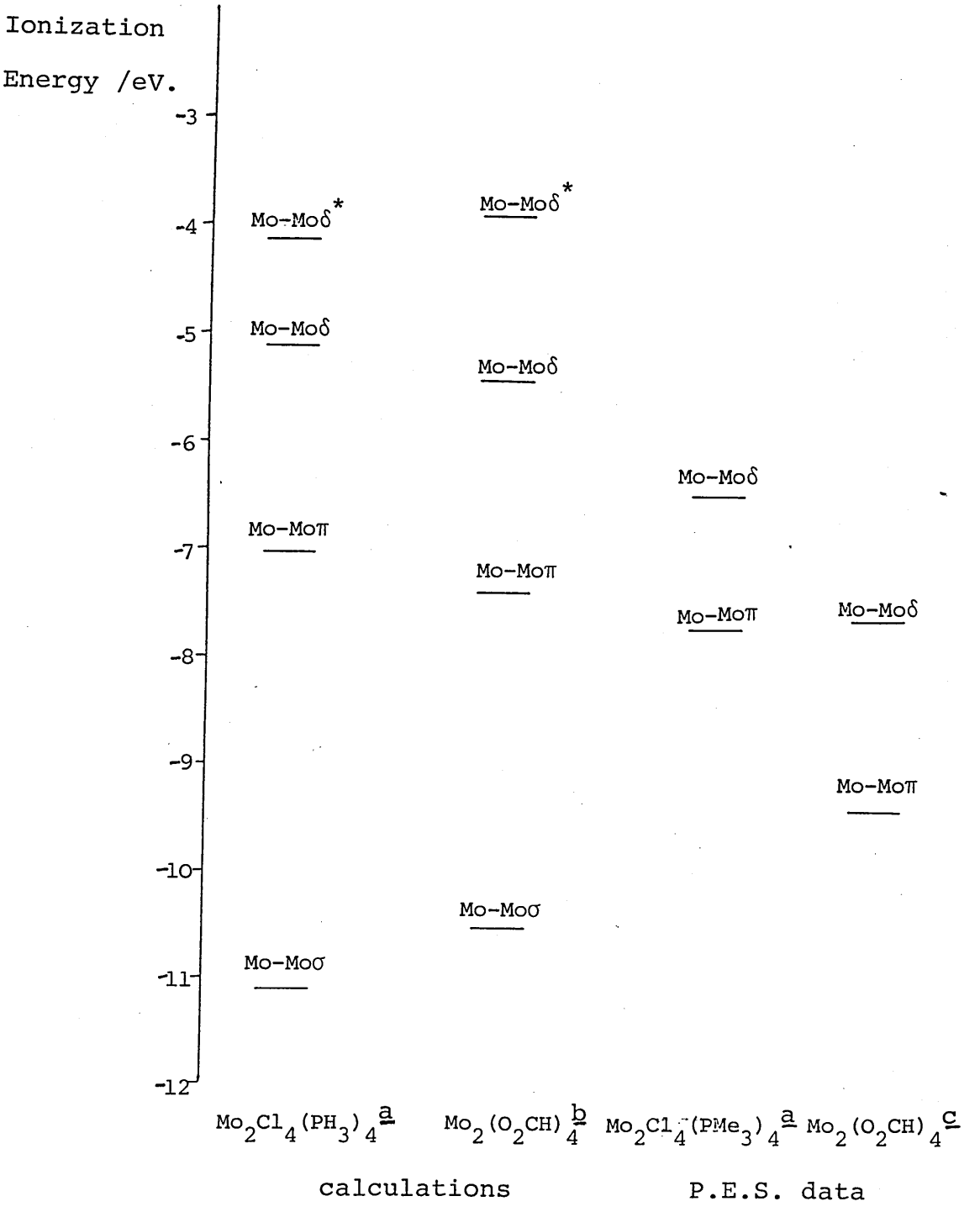

a ref 4, b ref 15, c ref 5,

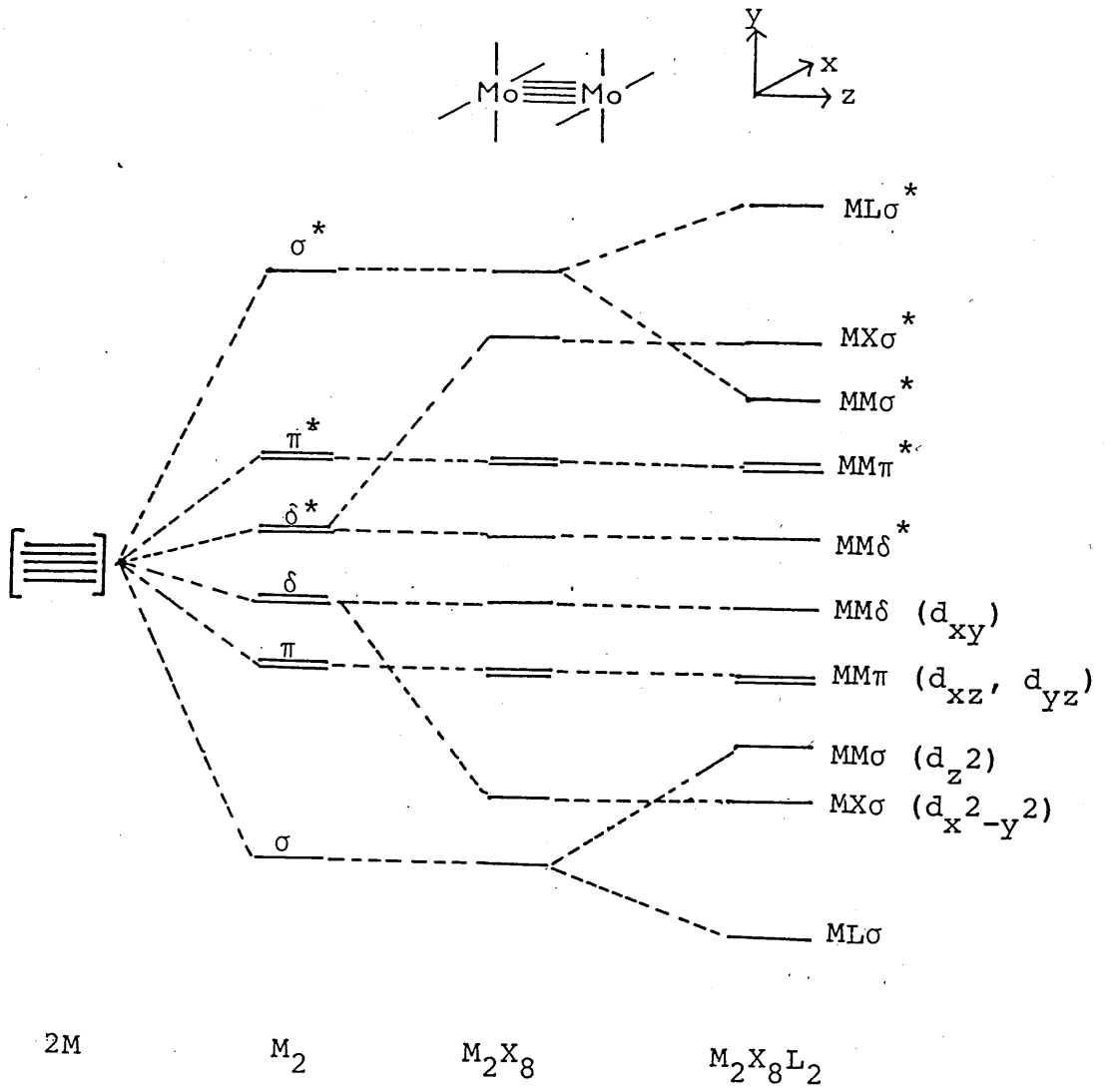

Figure 8.1.4. The Effect of Binding Axial Ligands to a Mo-Mo Quadruply Bonded Compound.[16]

The Mo-Mo σ orbital mixes with the σ orbital of L that contains the donor electron pair resulting in a stabilised orbital of mainly M-L σ character and a destabilised orbital of mainly M-M σ character.

Section 2: ^{95}Mo Chemical Shift and Bond Multiplicity

Table 8.2.1 shows n.m.r. data for molybdenum-molybdenum triply bonded compounds and a related singly bonded compound.

Figure 8.2.1 shows the molybdenum chemical shifts of molybdenum-molybdenum bonded dimers so far measured. The data are far from comprehensive and direct comparisons are complicated by the variety of ligands present. A major problem is the presence of bridging groups which influence the molybdenum-molybdenum separation. The ligands can strongly influence the chemical shift, for example molybdenum-molybdenum quadruply bonded species presently span a range of about 1200 ppm. and molybdenum-molybdenum singly bonded dimers have been found over a very large molybdenum chemical shift range. However, it seems that for compounds with similar types of ligands and taking into account the various shielding series for ligands which have been elucidated for molybdenum there is a trend to decreasing ^{95}Mo shielding with increasing metal-metal bond multiplicity.

Table 8.2.1. N.m.r. Data for Mo—Mo Compounds

Sample	Solvent	δ^{95}Mo / ppm.	$w_{\frac{1}{2}}$ /Hz.	$^{1}J(^{95}Mo-^{31}P)$ /Hz.	δ^{31}P / ppm.	δ^{13}C in $CDCl_3$ /ppm. MeCp	CO
$[Mo(MeCp)(CO)_3]_2$ [a]	CH_2Cl_2	-1831	160			93.2,91.8,14.4	
$[Mo(MeCp)(CO)_2]_2$	CH_2Cl_2	159	150			110.2,93.1,89.8,132	236.8
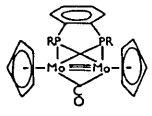 [b] R = Bu^t	CH_2Cl_2	1372	100	214	222		
R = Ph	CH_2Cl_2	1396	170	221	181		

a see chapter 5.1

b compound supplied by Prof. E.Kyba, University of Texas at Austin, U.S.A.

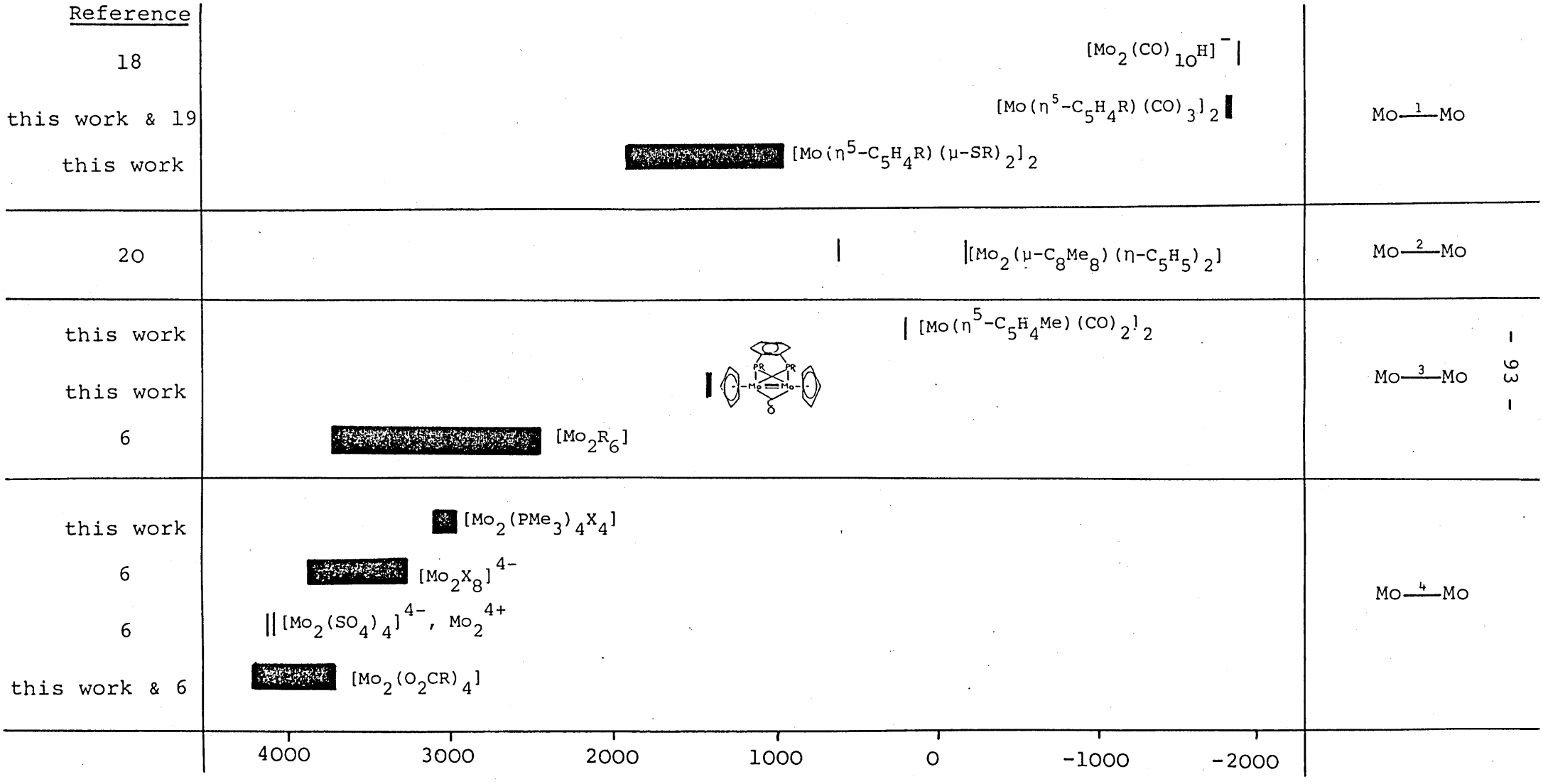

Figure 8.2.1. ^{95}Mo chemical shift and bond multiplicity

References for Chapter 8

1 S.F. Gheller, T.W. Hambley, R.T.C. Brownlee, M.J. O'Connor, M.R. Snow, A.G. Wedd, J. Am. Chem. Soc., 1983, 105, 1527.

2 S.K. Habron, Part II Thesis, Oxford, 1983

3 J.C. Green, personal communication.

4 F.A. Cotton, J.L. Hubbard, D.L. Lichtenberger, I. Shim, J. Am. Chem. Soc., 1982, 104, 679.

5 J.C. Green, A.W. Coleman, A.J. Hayes, E.A. Seddon, D.R. Lloyd, Y. Niwa, J. Chem Soc. Dalton Trans., 1979, 1057.

6 M. Minelli, J.H. Enemark, R.T.C. Brownlee, M.J. O'Connor, A.G. Wedd, Co-ord. Chem. Rev., in press.

7 D.J. Santure, J.C. Huffman, A.P. Sattelberger, Inorg. Chem., 1985, 24, 371.

8 R.T.C. Brownlee, M.J. O'Connor, B.P. Shehan, A.G. Wedd, J. Magn. Reson., 1985, 61, 516.

9 F.A. Cotton, J.G. Norman Jr., J. Am. Chem. Soc., 1972, 94, 5697.

10 F.A. Cotton, M.W. Extine, T.R. Felthouse, B.W.S. Kolthammer, D.G. Lay, J. Am. Chem. Soc., 1981, 103, 4040.

11 F.A. Cotton, Acc. Chem. Res., 1978, 11, 225.

12 J.S. Filippo, H.S. Sniadoch, Inorg. Chem., 1973, 12, 2326.

13 D.S. Martin, R.A. Newman, P.E. Fanwick, Inorg. Chem., 1979, 18, 2511.

14 M.C. Manning, W.C. Trogler, J. Am. Chem. Soc., 1983, 105, 5311.

15 J.G. Norman Jr., H.J. Kolari, H.B. Gray, W.C. Trogler, Inorg. Chem., 1977, 16, 987.

16 F.A. Cotton, G. Wilkinson, "Advanced Inorganic Chemistry", 4th edition, Wiley, 1980.

17 J. Mason, personal communication.

18 A.F. Masters, G.E. Bossard, T.A. George, R.T.C. Brownlee, M.J. O'Connor, A.G. Wedd, Inorg. Chem.,1983, 22, 908.

19 S. Dysart, I. Georgii, B.E. Mann, J. Organomet. Chem., 1981, 213, C10.

20 M. Green, N.C. Norman, A.G. Orpen, C.J. Schaverien, J. Chem. Soc. Dalton Trans., 1984, 2455.

Chapter 9: Molybdenum Sulphur Compounds

Section 1: Molybdenum-sulphur Dimers

Cyclopentadienyl-molybdenum dimers with four sulphur bridges have been shown to exhibit catalytic activity including reduction and dehydrosulphurisation of organic groups under mild conditions.[1-9] Also such dimers sustain more than one reversible one-electron redox process with continuity of structure and as such they resemble the related cubanes and ferredoxins which mediate electron transfer in redox proteins.

Table 9.1.1 shows n.m.r. data for some cyclopentadienyl molybdenum dimers with sulphur ligands.

The linewidths of the ^{95}Mo signals observed for these compounds are relatively small for molecules of their volume and apparent asymmetry so the electronic distribution must cause a low electric field gradient around the molybdenum nucleus. Increase in the molecular tumbling rate by lowering the viscosity of the solvent results in sharper lines as shown by the reduction from 110 to 60 Hz from CH_2Cl_2 to Et_2O solvent for $[Mo(MeCp)(\mu_2\text{-}S)(\mu\text{-}SEt)]_2$. Substitution of the cyclopentadienyl ring increases the linewidth of the molybdenum signal, as illustrated by $[Mo(Pr^iCp)(\mu\text{-}SMe)_2]_2$ versus $[MoCp(\mu\text{-}SMe)_2]_2$.

These dimers may be divided into two types $[Mo^{IV}Cp(\mu\text{-}S)(\mu\text{-}SR)]_2$ and $[Mo^{III}Cp(\mu\text{-}SR)_2]_2$, the latter exhibiting lower shielding of the molybdenum nucleus. Figure 9.1.1a[5] shows the derivation of the orbitals of $[MoCp(\mu\text{-}S)_2]_2$ and Figure 9.1.1b[5] compares the orbitals of $[MoCp(\mu\text{-}S)_2]_2$, $[MoCp(\mu\text{-}S)(\mu\text{-}SH)]_2$ and $[MoCp(\mu\text{-}SH)_2]_2$. These diagrams are derived from extended Hückel calculations. The reduction in ^{95}Mo shielding may

Table 9.1.1 N.m.r. data for some cyclopentadienyl molybdenum sulphur dimers

Sample	Solvent	δ^{95}Mo	$W_{\frac{1}{2}}$	δ^{13}C in $CDCl_3$ Cp carbons		$\underline{C}H_3$-Cp	Other
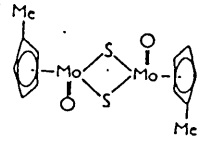 a	CH_2Cl_2	-501	100	104.3	101.8	14.5	
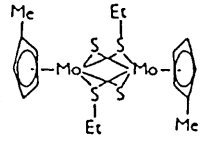 a	CH_2Cl_2 Et_2O	497 513	110 60	98.7	96.2	17.0	31.9, 27.7 (Et)
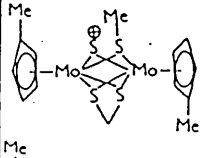 a	CH_2Cl_2	536	50	104.0	102.4	17.0	49.8 (S-CH_2-S) 19.0 (S-Me)
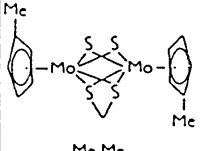 a	CH_2Cl_2	601	40	[c]100.6	97.6	16.9	33.5 (S-CH_2-S)
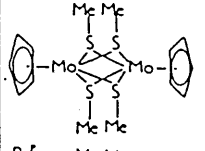 a	C_6H_5Me	937	70				
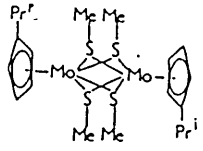 b	C_6H_5Me	1010	550				

continued.....

Table 9.1.1 N.m.r. data for some cyclopentadienyl molybdenum sulphur dimers

Sample	Solvent	δ^{95}Mo	$W_{\frac{1}{2}}$	δ^{13}C in $CDCl_3$ Cp carbons		$\underline{C}H_3$-Cp	Other	
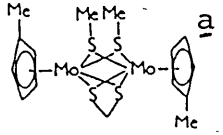 a	CH_2Cl_2	1273	45	93.2	87.5	16.2	74.6 (S-CH_2-S)	22.3 (S-Me)
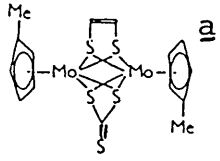 a	CH_2Cl_2	1283	23	98.8	96.1	16.2	147.6 (-CH=CH-)	
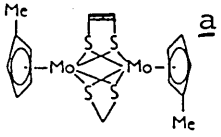 a	CH_2Cl_2	1925	60	[c]95.4	90.1	16.4	92.3 (S-CH_2-S)	147.4 (-CH=CH-)

a compound supplied by C.Casewit and M.Rakowski DuBois, Univ. of Colorado

b compound supplied by D.P.S.Rodgers

c ^{13}C n.m.r. data from ref 7

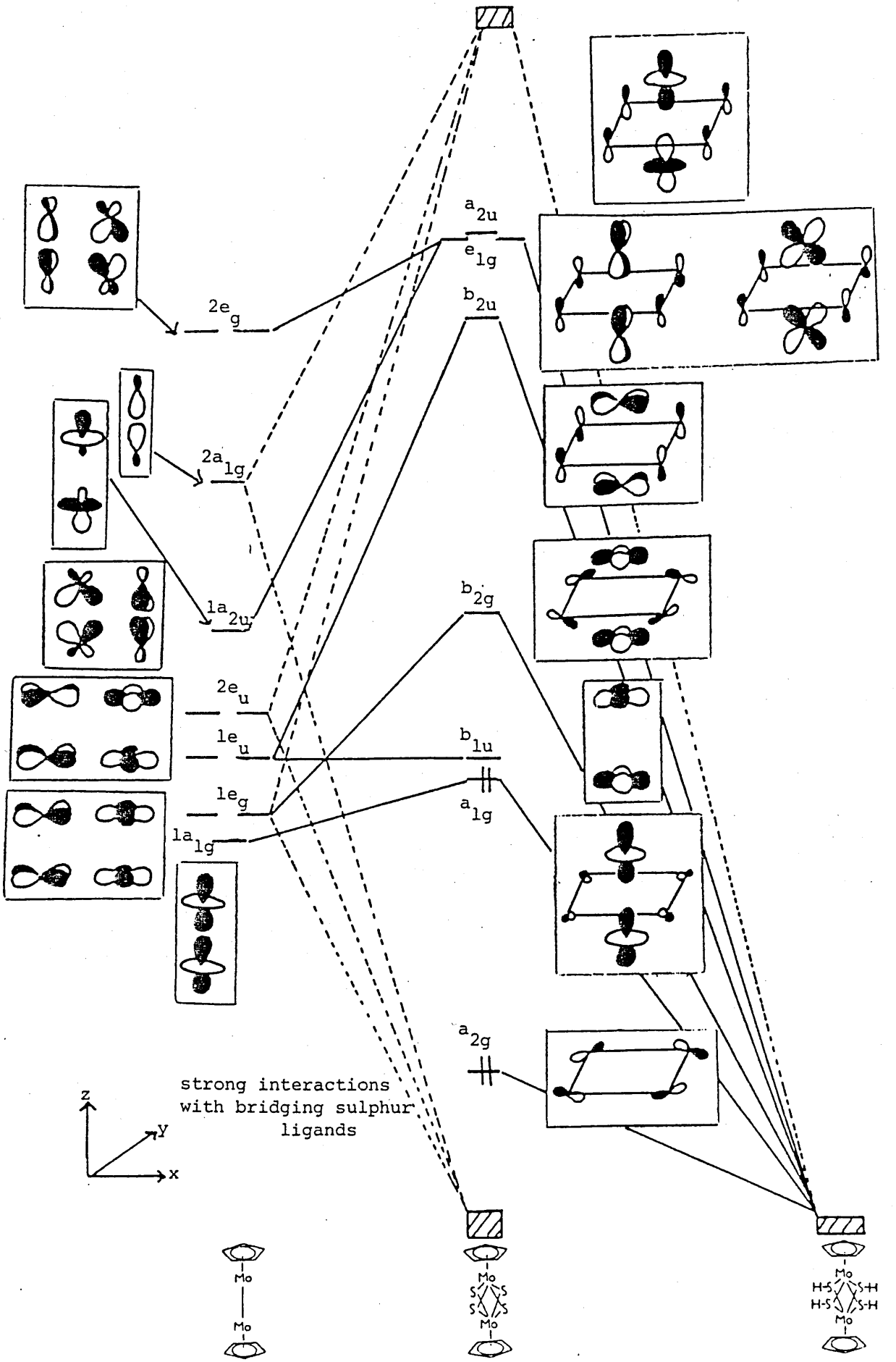

Figure 9.1.1a. Derivation of the Orbitals of $[MoCpS_2]_2^5$

Key to figure 9.1.1.

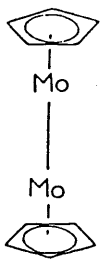

$2e_g$ π^* d_{xz}, d_{yz}

$2a_{1g}$ σ sp hybrid

$1a_{2u}$ σ^* d_{z2}

$2e_u$ π d_{xz}, d_{yz}

$1e_u$ δ^* d_{xy}, $d_{x^2-y^2}$

$1a_{2u} \rightarrow a_{2u}$ destabilised by antibonding interaction of torus of d_{z2} with p_z orbitals of 4 sulphur atoms

$2e_g \rightarrow e_{1g}$ destabilised by antibonding interaction with p_z orbitals of 4 sulphur atoms

$1e_u \rightarrow b_{2u}$ antibonding interaction of d_{xy} with p_z of sulphur atoms

$1e_g \rightarrow b_{2g}$ antibonding interaction of d_{x2-y2} with p_x and p_y of sulphur atoms

$1e_u \rightarrow b_{1u}$ not of proper symmetry to interact with any of the ligand orbitals

$1a_{1g} \rightarrow a_{1g}$ slightly destabilising interaction of d_{z2} bonding contributuion of the dimer with sulphur p_x and p_y orbitals completely localised on the sulpur ligands, S-S antibonding

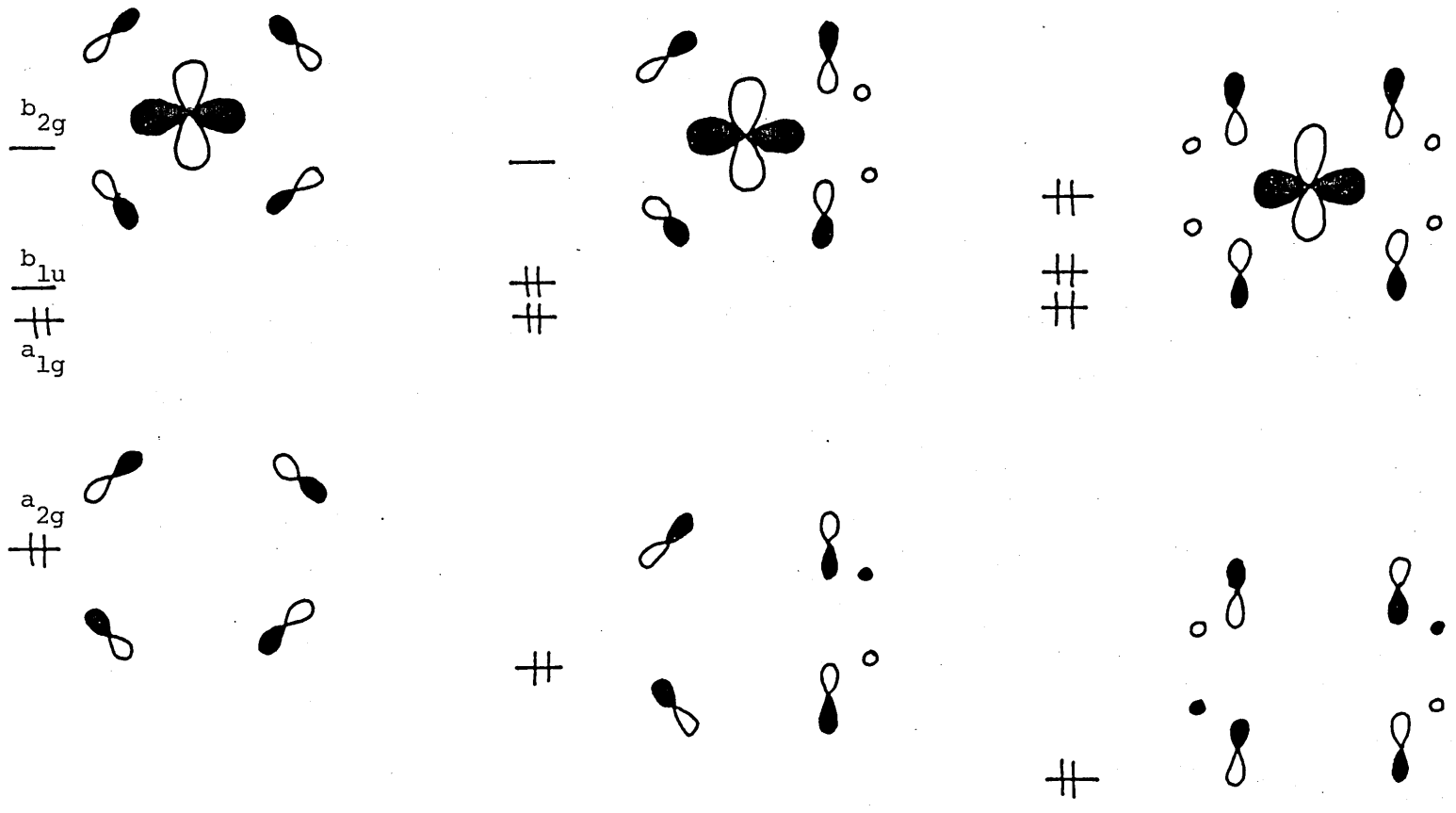

Figure 9.1.1b. Comparison of Orbital Occupancy for $[MoCpS_2]_2$, $[MoCpS(SH)]_2$ & $[MoCp(SH)_2]_2^5$

the molecular orbitals are viewed down the metal-metal vector

perhaps be associated with the increase in the number of electrons for the paramagnetic circulation on filling the b_{2g} orbital (derived from the metal $d_{x^2-y^2}$ orbital) and the destabilisation of the a_{1g} and b_{1u} h.o.m.o.'s (derived from the metal d_{z^2} and $d_{x^2-y^2}$ orbitals).

Distortions of bond angles at the metal can reduce the metal shielding by increasing the imbalance of charge in the valence shell and removing orbital degeneracies, for example in the series $[Mo(CO)_4(Ph_2P(CH_2)_nPPh_2)]$ ^{95}Mo shielding decreases in the order n = 2 > 3 > 1.[10] Cross-linking of two bridging sulphurs by a methylene group reduces the ^{95}Mo shielding within both the Mo(III) and Mo(IV) series. As Table 9.1.2 shows the reduction in ^{95}Mo shielding is accompanied by distortion of the Mo_2S_4 framework. Alkene cross-linking also deshields the metal nucleus. Structural data suggests that in the alkene cross-linked compound the most important distortion occurs at the sulphur.

Table 9.1.3 gives the electronic spectral data that exists for the cyclopentadienyl molybdenum dimers measured. Although the data is limited and the range of $\delta^{95}Mo$ in the compounds is comparatively small there is a trend to longer wavelengths, consistent with there being a smaller h.o.m.o. - l.u.m.o. gap, as the molybdenum shielding decreases.

Table 9.1.4 gives the electrode potentials that have been measured for these cyclopentadienyl molybdenum dimers. In the Mo(III) $(SR)_4$ dimers a decrease in $E_{\frac{1}{2}}^{ox}$, and in the Mo(IV) $S_2(SR)_2$ dimers deshielding of the molybdenum is accompanied by an increase in $E_{\frac{1}{2}}^{red}$ and a decrease in $(E_{\frac{1}{2}}^{red}-E_{\frac{1}{2}}^{ox})$. Assuming that $(E_{\frac{1}{2}}^{red}-E_{\frac{1}{2}}^{ox})$ is related to the h.o.m.o. - l.u.m.o. gap

Table 9.1.2 Structural Parameters for two cyclopentadienyl molybdenum-sulphur dimers

	δ^{95}Mo	MeS---SMe /Å	MeS Mo SMe	CH_2 S---S /Å	Mo S S	Interligand Distance S---S/Å	Mo-Mo	Mo-SMe
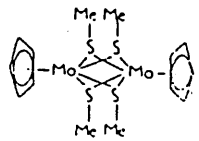 a	937	2.96	74°	-	-	2.96	2.603	2.46
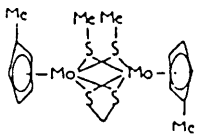 b	1273	2.823	70.3°	2.673	66.1°	3.119	2.596	2.448

a X-ray structural data from ref 11

b X-ray structural data from ref 7

Table 9.1.3 Electronic Spectral Data for some Cyclopentadienyl Molybdenum Sulphur Dimers

	δ^{95}Mo in CH_2Cl_2	Solvent	λ/nm	10^{-3} ε [a] /M^{-1} cm^{-1}
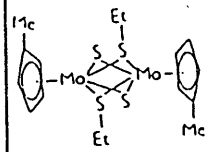	497	$CHCl_3$	687 514 398 320	2.1 3.9 1.6 sh
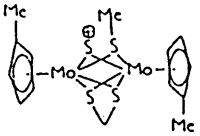	536	CH_2Cl_2	855 537 477	2.1 1.0 sh
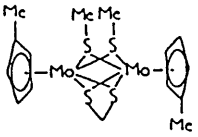	601	THF	727 598 498	2.4 2.1 0.8

a electronic spectral data from ref 3

Table 9.1.4 Electrode Potential Data for some cyclopentadienyl molybdenum-sulphur dimers

	$E_{\frac{1}{2}}^{red}$/V	$E_{\frac{1}{2}}^{ox}$/V	$E_{\frac{1}{2}}^{red} - E_{\frac{1}{2}}^{ox}$	δ^{95}Mo
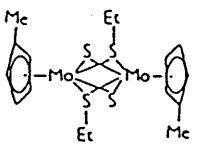	-1.43	-0.57	-0.86 [a]	497
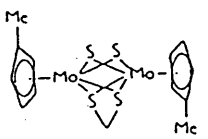	-1.30	-0.27	-1.03 [b]	601
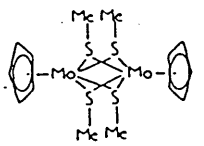		0.15 [c]		937
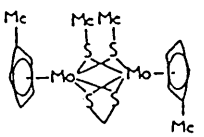		-0.04 [b]		1273
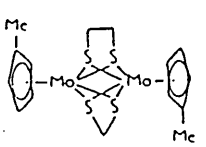		-0.12 [b]		1925

a electrode potential data from ref 3, refers to S-Me compound

b electrode potential data from ref 7

c electrode potential data from ref 26

for rotation of charge an algebraic decrease in its value may be expected to correlate with a decrease in the molybdenum shielding in these compounds.

A linear relationship has been found between ^{13}C and ^{59}Co n.m.r. spectra of substituted cyclopentadienyl cobalt complexes and their catalytic properties in the synthesis of pyridine derivatives suggesting that a direct screening of potential catalysts by n.m.r. spectroscopy is possible.[12] The b_2 l.u.m.o. in the $[Mo^{IV}Cp(\mu\text{-}S)(\mu\text{-}SR)]_2$ compounds is important to the catalytic properties of these dimers as a vacant site for the coordination of $\pi(C{=}C)$ or $\pi(C{\equiv}N)$ electrons, the π^* orbitals of the incoming group accepting electrons from the a_2 sulphur orbitals.[5] The sensitivity of the ^{95}Mo shielding to the changes in the valence orbitals suggests the possibility of a connection between chemical shift and reactivity in these compounds.

Section 2: Clusters

Mo-S clusters are important biologically as described in Chapter 2. It is hoped that ^{95}Mo n.m.r. will provide information on the nature of the reaction site and the solution structure of diamagnetic species just as e.s.r. spectroscopy has aided the study of the paramagnetic species involved in molybdoenzymes.

Table 9.2.1 shows ^{95}Mo n.m.r. data for some Mo-S clusters. The range of linewidths observed is large and illustrates that the electric field gradient is an important factor in determining the linewidth as some of the signals were much sharper than would be expected from considering the size of the molecule.

Table 9.2.1 ^{95}Mo n.m.r. Data for Molybdenum-sulphur Clusters

Sample	$\delta^{95}Mo$ / ppm	$w_{\frac{1}{2}}$ / Hz.	$\delta^{13}C$ in $CDCl_3$ / ppm.			Ref.
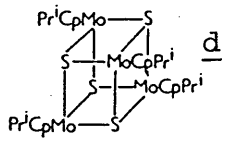 d	-1643	60				this work[c]
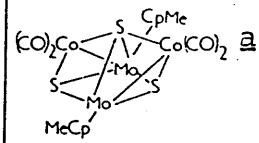 a	-431	100	99.5	97.0	16.0	this work[e]
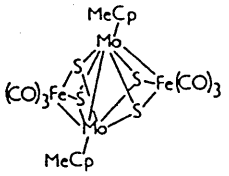 a	14	28	95.5	89.7	16.4	this work[e]
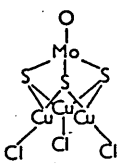 a	474	20				f
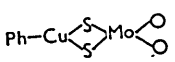 c	611	70				f
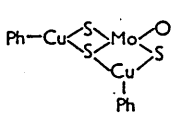 c	892	100				f
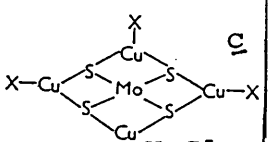 c X=Cl, Br.	886-910	1400				f
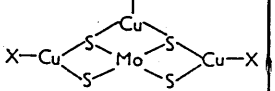 X=Cl[c], Br[c], I[b]	1234-1282	170-250				f
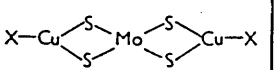 X=Cl[c], Br[c], CN[b], Ph[b']	1616-1700	250-600				f
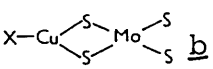 b X=CN, Ph	1864-1903	30-50				f

a CH_2Cl_2 solvent

b CH_3CN solvent

c DMF solvent

d C_6D_6/C_6H_5Me solvent, compound supplied by D.P.S. Rodgers

e compound supplied by Prof. M. Rakowski-DuBois and Dr. C. Casewit, University of Colorado at Boulder.

f ref 13

$[Mo(Pr^{i}Cp)S]_4$ undergoes one and two electron oxidation with continuity of structure[14] but unfortunately the species formed are paramagnetic and so could not be studied by ^{95}Mo n.m.r. spectroscopy.

This initial work on mixed-metal clusters demonstrates that these compounds show a large dispersion of ^{95}Mo chemical shifts and can give sharp signals which suggests that ^{95}Mo n.m.r. spectroscopy may be a useful tool for their study.

References for Chapter 9

1 M. Rakowski DuBois, R.C. Haltiwanger, D.J. Miller, G. Glatzmaier, J. Am. Chem. Soc., 1979, 101, 5245.

2 M. Rakowski DuBois, D.J. Miller, J. Am. Chem. Soc., 1980, 102, 4925.

3 M. Rakowski DuBois, M.C. VanDerveer, D.L. DuBois, R.C. Haltiwanger, W.K. Miller, J. Am. Chem. Soc., 1980, 102, 7456.

4 M. Rakowski DuBois, D.L. DuBois, M.C. VanDerveer, R.C. Haltiwanger, Inorg. Chem., 1981, 20, 3064.

5 D.L. Dubois, W.K. Miller, M. Rakowski DuBois, J. Am. Chem. Soc., 1981, 103, 3429

6 M. Rakowski DuBois, J. Am. Chem. Soc., 1983, 105, 3710.

7 M. McKenna, L.L. Wright, D.J. Miller, L. Tanner, R.C. Haltiwanger, M. Rakowski DuBois, J. Am. Chem. Soc., 1983, 105, 5329.

8 W.K. Miller, R.C. Haltiwanger, M.C. VanDerveer, M. Rakowski DuBois, Inorg. Chem., 1983, 22, 2973.

9 C.J. Casewit, R.C. Haltiwanger, J. Noordik, M. Rakowski DuBois, Organometallics, 1985, 4, 119.

10 G.T. Andrews, I.J. Colquhoun, W. McFarlane, S.O. Grim, J. Chem. Soc. Dalton Trans., 1982, 2353.

11 N.G. Connelly, L.F. Dahl, J. Am Chem. Soc., 1970, 92, 7470.

12 H. Bonnemann, W. Brijoux, R. Brinkman, W. Meurers, R. Mynott, W. van Philipsborn, T. Egolf, J. Organomet. Chem., 1984, 272, 231.

13 M. Minelli, J.H. Enemark, J.R. Nicholson, C.D. Garner, Inorg. Chem., 1984, 23, 4384.

14 J.A. Bandy, C.E. Davies, J.C. Green, M.L.H. Green, K. Prout, D.P.S. Rodgers, J. Chem. Soc., Chem. Commun., 1983, 1395.

Chapter 10: Molybdenum Compounds with Mixed Ligands

Table 10.1 gives ^{95}Mo n.m.r. data for molybdenum compounds with mixed ligands. While the variety of ligands involved makes overall comparisons impossible, there are some points to note concerning individual compounds or groups of compounds.

The ^{95}Mo chemical shift obtained for $[Mo(dppe)_2H_4]$ (-1865 ppm) resembles that of $[Mo(dptpe)_2H_4]$ (-1805 ppm)[1] (dptpe = $(C_6H_4Me\text{-}4)_2PCH_2CH_2P(C_6H_4Me\text{-}4)_2$). Similarly, in the compounds trans-$[Mo(dArpe)_2(N_2)_2]$ the molybdenum is deshielded when Ar = C_6H_4Me-4 relative to C_6H_5.[2] Whereas ^{95}Mo-^{31}P coupling is resolved in these dinitrogen compounds none is seen in the tetrahydrides (which are fluxional[7]).

$[Mo(CO)_4(4,4'\text{-}(CMe_3)_2\text{-}2,2'\text{-bpy})]$ was measured in ^{95}Mo and ^{15}N resonance by B.E. Mann for J.A. Connor.[3] More compounds $[Mo(CO)_4(4,4'\text{-}X_2\text{-}2,2'\text{-bpy})]$ were studied as far as solubility allowed. The ^{95}Mo chemical shift varied only slightly with X for the compounds measured and there were no obvious correlations observed between $\delta^{95}Mo$ and either $\delta^{15}N$ or λ_{max} from electronic spectra.[3] The bands in question had been assigned as containing a major metal to ligand charge transfer component and some metal localised d-d character. This study was undertaken as it had been found that the variations in the spectroscopic properties of the complexes (i.r., electronic absorption and emission and ^1H and ^{13}C n.m.r.) were strongly correlated with the electronic substituent parameters of the group X. However, it was also noted that the nature of the metal atom (Mo or W) has no significant influence on the spectroscopic properties reported.[3] The deshielding of the nitrogens in the ligating $(4,4'\text{-}Cl_2\text{-}2,2'\text{-bpy})$ relative to the methyl analogue is a well known para effect.

Table 10.1 ^{95}Mo n.m.r. Data for Molybdenum Compounds with Mixed Ligands

Sample	Solvent	$\delta^{95}Mo$ /ppm.	$W_{\frac{1}{2}}$ /Hz.
$[Mo(dppe)_2H_4]$ a	C_6H_5Me/C_6H_6	-1865	320
$[Mo(Pr^iCp)dmpe_2H]^{2+}PF_6^-$ b	$(CH_3)_2CO$	-1584	broad
$[Mo(\eta^5\text{-}C_7H_9)(\eta^3\text{-}C_7H_7)dmpe]$ d	C_6H_5Me	-1535 j	40
$[Mo(CO)_4(4,4'\text{-}Me_2\text{-}2,2'bpy)]$ f	DMSO	-1195	180
$[Mo(CO)_4(2,2'bpy)]$ f,n	DMSO	-1186	
$[Mo(CO)_4(4,4'\text{-}Cl_2\text{-}2,2'\text{-}bpy)]$ f	DMSO	-1173 k	250
$[Mo(CO)_4(4,4'\text{-}(CMe_3)_2\text{-}2,2'bpy)]$ l	$CDCl_3$	-1173 m	
$[Mo(CO)_2(2,2'bpy)_2MeCN]^{2+}[BF_4^-]_2$ f	$(CH_3)_2CO$	-1175	<60
$[Mo(CO)_4(Me_2NCH_2CH_2NMe_2)]$ e	CH_2Cl_2	-1018	80
$[Mo(\eta\text{-}C_7H_7)dppe(MeCN)]^+PF_6^-$ b	MeCN	-582	600
$\{[MoCp(O)I_2](\mu\text{-}O)\}$ c	$CH_2Cl_2/CDCl_3$	-355	80
$[Mo_3O_2(OAc)_6(H_2O)_3]^{2+}\ [BF_4^-]_2$ g	D_2O	1076	680
$[Mo(CO)_4(\mu\text{-}AsMe_2)(\mu\text{-}As_2Me_4)(MoCp(CO)_2]$ h	THF	-1457 -1726	200 100
$\{[MoCp(CO)_2]_2(\mu\text{-}AsMe_2)(\mu\text{-}H)\}$ h	THF	-1881	150

a compound supplied by author

b compound supplied by M.L.H. Green laboratory

c compound supplied by D.P.S. Rodgers

d compound supplied by P. Newman

e compound supplied by E.C. Alyea

f compound supplied by Prof. J. Connor and J.M.A. Walshe, Chemistry Dept., University of Kent.

g compound supplied by Prof. F.A. Cotton, Texas A & M University, U.S.A.

h compound supplied by Prof. R.A. Jones, University of Texas at Austin, U.S.A.

j $^{1}J(^{95}Mo-^{31}P)$ = 129,173 Hz.

k $\delta^{15}N$ = -124 ppm (in DMSO)

l $\delta^{15}N$ = -155 ppm, ref 3.

m ref 3

n $\delta^{95}Mo$ = -1186 ppm (in DMF), ref 5.

$[Mo(\eta\text{-}C_7H_7)dppe(MeCN)]^+$ gives a ^{95}Mo signal in a position consistent with those resonances found for compounds containing an $(\eta\text{-}C_7H_7)$ ring.

The trimer $[Mo_3O_2(OAc)_6(H_2O)_3][BF_4]_2$ has a structure involving a triangle of molybdenum atoms and two capping oxygen atoms.[4] Its ^{95}Mo chemical shift compares with those of $[Mo_3O_4(\overset{\frown}{LL})_3]^{2-}$ (1024-1162 p.p.m.)[5]. This anion involves a triangle of molybdenum atoms with one capping oxygen atom and an oxygen atom bridging each side of the molybdenum triangle.

References for Chapter 10

1 A.F. Masters, G.E. Bossard, T.A. George, R.T.C. Brownlee, M.J. O'Connor, A.G. Wedd, Inorg. Chem., 1983, 22, 908.

2 S. Donovan-Mtunzi, M. Hughes, G.J. Leigh, H. Modh. Ali, R.L. Richards, J. Mason, J. Organomet. Chem., 1983, 246, C1.

3 J.A. Connor, C. Overton, J. Organomet. Chem., 1983, 249, 165.

4 F.A. Cotton, M. Ardon, A. Bino, Z. Dori, M. Kaftory, G. Reisner, Inorg. Chem., 1982, 21, 1912.

5 S.F. Gheller, T.W. Hambley, R.T.C. Brownlee, M.J. O'Connor, M.R. Snow, A.G. Wedd, J. Am. Chem. Soc., 1983, 105, 1527.

6 A.F. Masters, R.T.C. Brownlee, M.J. O'Connor, A.G. Wedd, J.D. Cotton, J. Organomet. Chem.,1980, 195, C17.

7 P. Meakin, L.J. Guggenberger, W.G. Peet, E.L. Muetterties, J.P. Jesson, J. Am. Chem. Soc., 1973, 95, 1467.

Chapter 11 ^{183}W N.m.r.

Section 1 Results

One of the aims of this work was to extend the use of direct ^{183}W n.m.r. observation in the field of organometallic and co-ordination chemistry. The problems associated with direct observation of the ^{183}W nucleus include

1 Low sensitivity (receptivity 0.6 relative to ^{13}C)

2 Low frequency (Ξ 4.161733 MHz)

3 Long relaxation times

4 Large chemical shift range allied with sharp signals

Therefore direct observation is time consuming. The effects of probe ringing, arising from the low frequency may be reduced by using a pre-aquisition delay of 0.95 ms on the JEOL FX90Q. Relaxation times may be shortened by the addition of a relaxation agent such as $[Cr(acac)_3]$[1] or the use of viscous solvents, the latter having been used with success in ^{15}N n.m.r. studies for example.[2] The INEPT (Insensitive nucleus enhancement by polarisation transfer) pulse sequence has been employed making use of ^{183}W-^{1}H couplings obtainable from ^{1}H spectra.[3]

An adapted DEPT(distortionless enhancement by polarisation transfer) pulse sequence, courtesy of Drs R. Goodfellow and M. Murray, Bristol University, was used to obtain ^{183}W resonances for tungsten hydride compounds on the JEOL FX90Q. The adaption was necessary as one of the parameters required in the original program was $(\pi_{1_H} - \pi/2_{183_W})$ which is negative for the JEOL FX90Q at the Open University. It was suggested that the π_{1_H} used (44 μs in this case) was incorrect as it was the value for the multinuclear probe of the JEOL FX90Q

which is not necessarily the correct value for the low frequency probe used for observing ^{183}W signals directly. However the only way to obtain the correct value would be very time consuming involving use of the DEPT program with varying π_{1_H}. Therefore the signals obtained using (π_{1_H} = 44 μs) are not necessarily optimised. However, a preliminary experiment using a very concentrated solution of $[W(PMe_3)_3H_6]$ suggested that our value of π_{1_H} was not greatly in error.

Figure 11.1.1 shows the improved sensitivity possible using the DEPT sequence. Table 11.1.1 shows the ^{183}W n.m.r. data obtained using the DEPT sequence.

In attempting to extend the use of the DEPT sequence to different types of tungsten compounds $[W(\eta\text{-}C_7H_7)(CO)_3]^+[BF_4^-]$ was synthesised. $^2J(^{183}W\text{-}^1H)$ was found to be 2.45 Hz, from the ^1H n.m.r. spectrum. From a comparison of $\delta^{95}Mo$ and $\delta^{183}W$ for the series $M(CO)_nL_{6-n}$ (n = 3,4,5,6)[5] $\delta^{183}W$ for this compound was predicted to be about -3348 ppm.

The chemical shift range searched was -3257 to -3525 ppm. However after 9,836 scans no signal had been observed. One possible explanation may be that the DEPT sequence includes the value $\frac{1}{2J}$ and, when J is small relatively large errors may be introduced into $\frac{1}{2J}$ through any uncertainty in J.

The lack of resonance obtained for $W(PMe_3)_3H_5K$ has not been satisfactorily explained. Coupling to ^{39}K was ruled out on the grounds that the ^{39}K nucleus would relax too fast if there were a W-K bond and effectively decouple itself from the tungsten. The chemical shift range covered in total was -6440 to -1620 ppm in sections of 2000 Hz and ca. 6 000 scans.

Figure 11.1.1. ^{183}W n.m.r. spectra of $[W(PMe_3)_3H_6]$

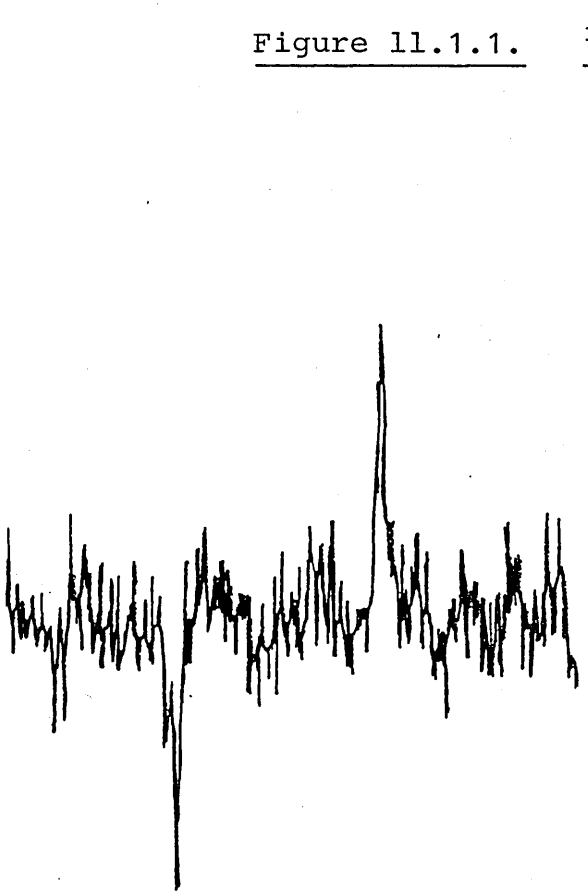

JEOL FX90Q

^1H decoupled

11 096 scans

(pre-aquisition delay of 0.95 ms.
may be responsible for phasing difficulties)

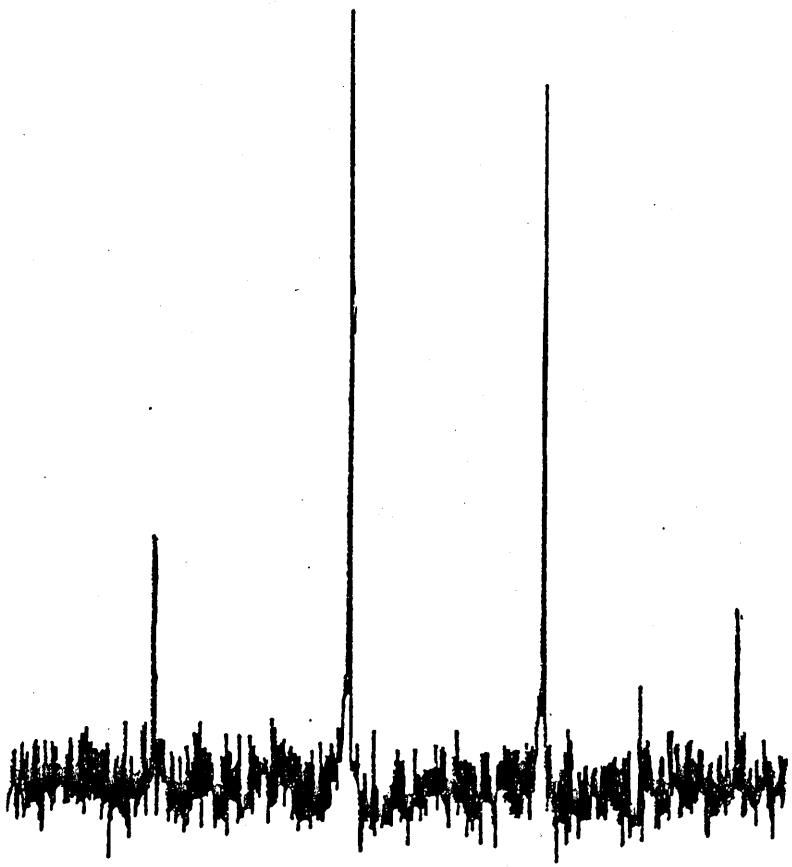

JEOL FX90Q

DEPT sequence

9 819 scans

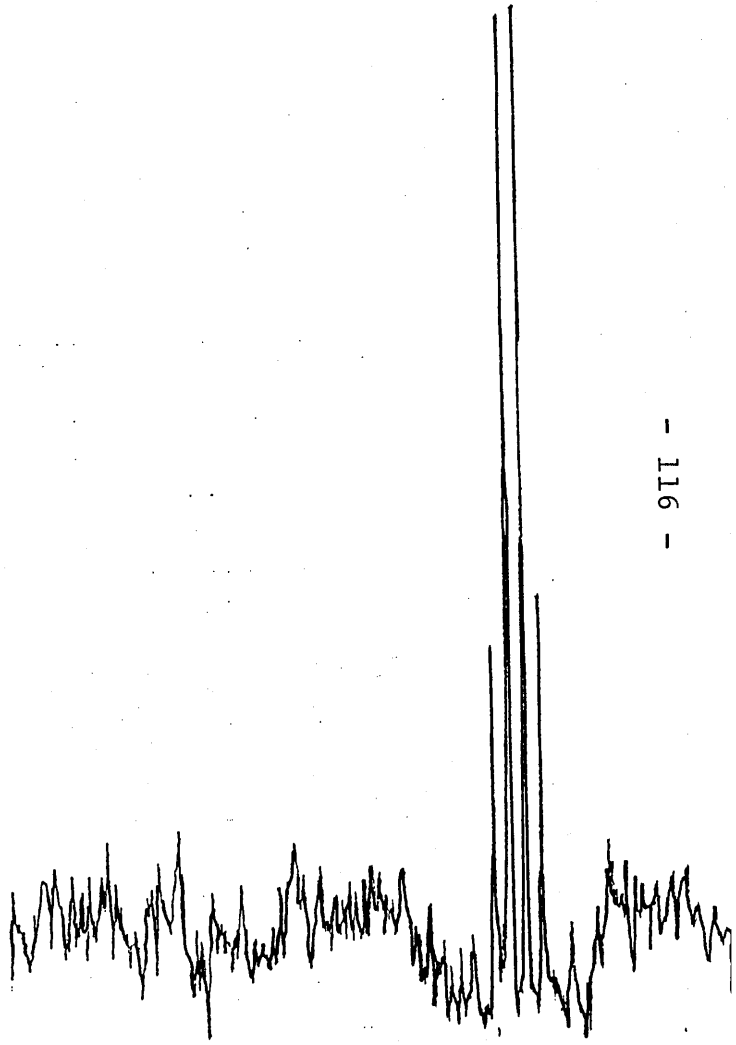

BRUKER WH400

^1H decoupled

20 063 scans

Table 11.1.1

	Solvent	Approximate [W] molar	$\delta^{183}W$	Value $^1J(^{183}W-^1H)$ used/Hz	$^1J(^{183}W-^{31}P)$ /Hz	No. of scans	Approximate S/N ratio
$[W(\eta-C_5H_5)H_2]$ [a]	PhMe	0.1 (sat. soln)	-4672	72 [b]	-	10 213	2:1
$[W(PMe_3)_3H_6]$ [g]	C_6D_6/ PhMe	1.0	-3760	30 [b]	71	9 819	10:1
$[W(PMe_3)_3H_5-SnBu^n_3]$ [d,h]	C_6H_6	0.3	-3718	22 [c]	106 [e]	56 649	3:1
$[W(PMe_3)_3H_5K]$ [h]	THF	1.0	-	18 [c]	166 [c]	ca. 6 000	-
$[W(C_7H_7)(CO)_3]^+[BF_4]^-$ [f]	$(CH_3)_2CO$	sat. soln.	-	2.45		9836	-

a -4667 ppm from double resonance $^1H\{^{183}W\}$ ref 7. Compound supplied by G.Parkin

b ref 7, c ref 8,

d $\delta^{119}Sn$ = 49 (quartet), $^1J(^{183}W-^{119}Sn)$ = 116 Hz. $^2J(^{119}Sn-^{31}P)$ = 164 Hz.

e only central 2 peaks of quartet visible above noise, $^1J(^{183}W-^{31}P)$ = 102 Hz. from ^{31}P spectrum.

f compound supplied by author, g compound supplied by C.Clayton,

h compound supplied by A.Berry,

The value of $^{1}J(^{183}W - ^{119}Sn)$ of 116 Hz obtained for $[W(PMe_3)_3H_5SnBu^n_3]$ may be compared with that of $[Me_3SnW(CO)_3(\eta\text{-}C_5H_5)]$ where $^{1}J(^{183}W - ^{119}Sn) = 150 \pm 5Hz$, found by $^{1}H\{^{183}W\}$ double resonance.[6] ^{183}W shielding decreases $[W(PMe_3)_3H_6] > [W(PMe_3)_3H_5SnBu^n_3]$ but $[W(\eta\text{-}C_5H_5)(CO)_3SnMe_3] > [W(\eta\text{-}C_5H_5)(CO)_3H]$[6].

Table 11.1.2 lists the results of direct observation of the ^{183}W with broad band ^{1}H decoupling and without resort to polarisation transfer experiments. Compounds in this group are generally not amenable to such methods as ^{183}W-^{1}H couplings are not easily obtainable. The most likely reasons for the failure to obtain signals are

(1) too short a delay allowed resulting in saturation, the relaxation time for $[W(CO)_6]$ has been found to be greater than 80s.[1]

(2) insensitivity of the nucleus.

Table 11.1.2. ^{183}W n.m.r. Results using ^{1}H Decoupling Only.

Sample	Solvent	$\delta^{183}W$ / ppm.	Chemical Shift Range Searched / ppm.	Hz/Pt	Repetition Rate /s.	Approximate [W] /Molar.	No. of Scans	Spectrometer Frequency MHz.
$[W(\eta\text{-}C_6H_5Me)_2]$ a	d^6-benzene	n.o.	-2462 → -2194 e	0.12	9.1	0.1	7294	3.72
$[W(PMe_3)_3H_6]$ b	benzene-d^6 /toluene	-3756		6.1	2.7	1.0	20 063	16.65
$[W(PMe_3)_3H_6]$ b	benzene-d^6 /toluene	-3754	-3627 → -3895	0.12	6.6	1.0	11 096	3.70
$[W_2(PMe_3)_4Cl_4]$ c	THF/d^6-acetone	n.o.	1000 → 6000 f	6.1	2.7	1.2	22 301	16.65
$[W(\eta\text{-}C_7H_8)(CO)_3]$ d	CH_2Cl_2 + $[Cr(acac)_3]$	n.o.	-3735 → -2761 g	0.12	4.2	0.5	ca.9000	3.72

a compound supplied by G.Parkin

b compound supplied by C.Clayton

c compound supplied by S.K.Habron

d compound supplied by author

e $\delta^{95}Mo$ $[Mo(\eta\text{-}C_6H_5Me)_2$ = -1270 ppm.

f $\delta^{95}Mo$ $[Mo_2(PMe_3)_4Cl_4]$ = 3008 ppm.

g $\delta^{95}Mo$ $[Mo(\eta\text{-}C_7H_8)(CO)_3]$ = -1694 ppm.

Section 2 Comparison of $\delta^{183}W$ and $\delta^{95}Mo$

Figure 11.2.1 is a plot of $\delta^{183}W$ and $\delta^{95}Mo$ using results from the literature and this work. This covers a wide range of types of molecule yet there is good correlation between the molybdenum and tungsten chemical shifts. The slope of the plot is 1.7, the same as that obtained from a study of molybdenum and tungsten carbonyl compounds.[5]

The slope of the plot should be given by[5]

$$\frac{\Delta\delta(^{183})}{\Delta\delta(^{95})} = \frac{\Delta E(Mo)}{\Delta E(W)} \quad \frac{\langle r^{-3}\rangle_{5d\ W}\ D_i(W)}{\langle r^{-3}\rangle_{4d\ Mo} D_i(Mo)}$$

It has been proposed that the ΔE values for completely analgous molybdenum and tungsten compounds may be similar; it has been found from electronic spectra for many complexes of molybdenum and tungsten that the ratio $\Delta E(Mo)/\Delta E(W)$ is close to unity.[5] $\langle r^{-3}\rangle_{nd}$ terms for molybdenum and tungsten free atoms are available from spectroscopy and by calculation. The values $\langle r^{-3}\rangle_{5d}(W) = 9.32\ a_o^{-3}$

and $\langle r^{-3}\rangle_{4d}(Mo) = 4.42\ a_o^{-3}$ $\quad (a_o = 0.529\ \text{Å})$

have been given[13] yielding $\dfrac{\langle r^{-3}\rangle_{5d}(W)}{\langle r^{-3}\rangle_{4d}(Mo)} = 2.1$

It is reasonable to suppose that the differences in the radial terms for analogous molybdenum and tungsten compounds with respect to their free atom terms would be comparable giving a similar value for the ratio

$\dfrac{\langle r^{-3}\rangle_{5d}(W)}{\langle r^{-3}\rangle_{4d}(Mo)}$ to that quoted above for any given pair of

corresponding molybdenum and tungsten compounds.

Figure 11.2.1.

$\delta^{183}W$ versus $\delta^{95}Mo$

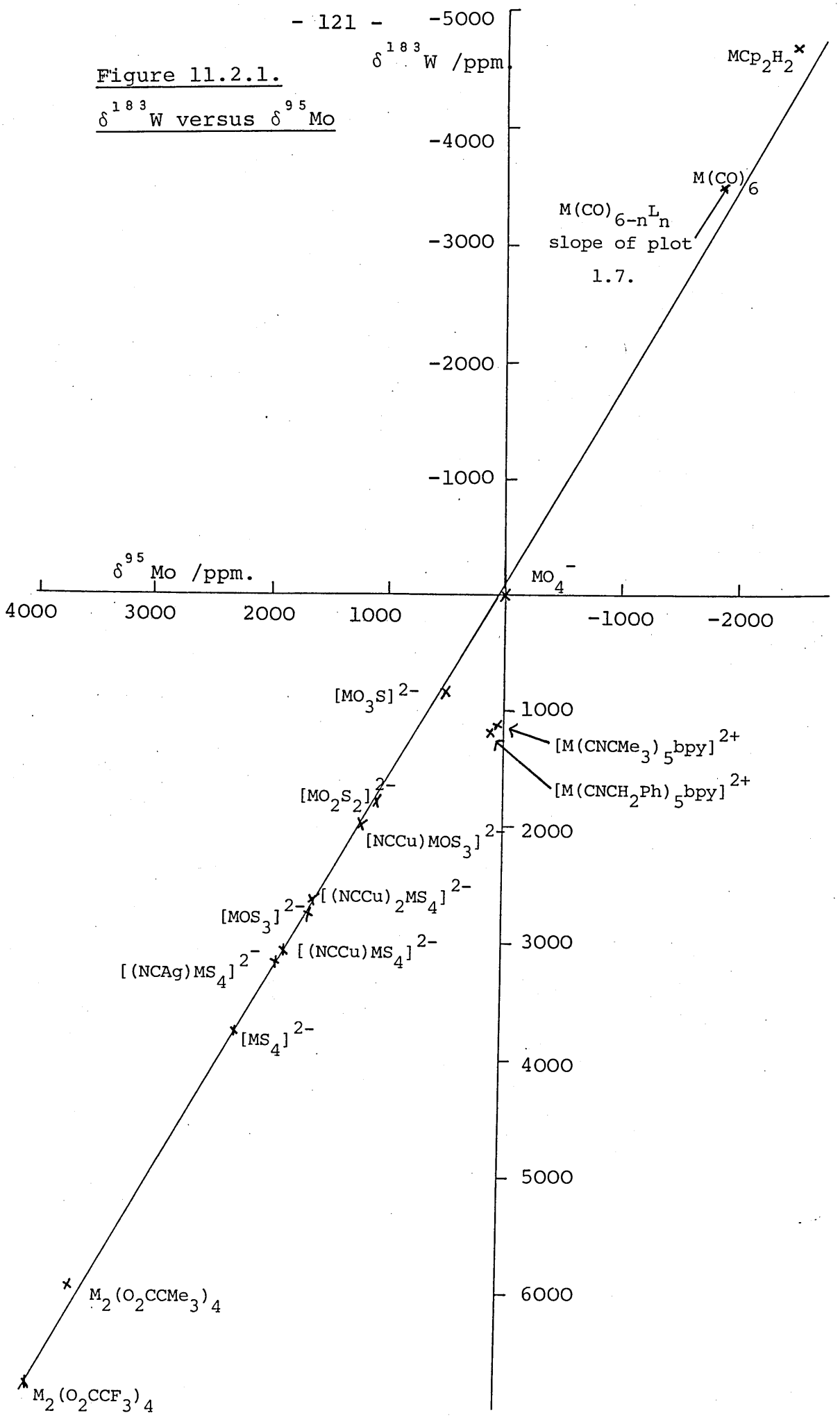

Key to Figure 11.2.1.

Compound	δ^{95}Mo reference	δ^{183}W reference
$[MCp_2H_2]$	this work	6
$[M(CO)_{6-n}L_n]$ n = 1,2,3	5	5
$[MO_nS_{4-n}]^{2-}$ n = 0-4	9	9
$[M_2(O_2CR)_4]$	this work	10,12
$[M(CNR)_5bpy]^{2+}$	11	11

The relative values of the charge imbalance terms for molybdenum and tungsten in corresponding compounds would be difficult to quantify but the differences are unlikely to be great. From these considerations the value of the slope obtained is not inconsistent with the theoretical treatment.

It has been noted[14,15] that there is a periodicity in the chemical shift range of the elements. An increase in the chemical shift range of elements across a period is accompanied by an increase in the radial terms of the free atoms. Also the same increases are seen down a group. Generally, it is observed in comparisons of elements in the same group the shifts for the heavier element are larger than the increase in the free atom radial term would suggest.[14,15] However in the case of Mo and W this does not appear to be so.

References for Chapter 11

1 R.L. Keiter, D. Vander Velde, J. Organomet. Chem., 1983 258, C34.

2 B.P. Bammel, R.F. Evilia, Anal. Chem., 1982, 54, 1318.

3 C. Brevard, R. Schimpf, J. Magn. Reson., 1982, 47, 528.

4 D.M. Doddrell, D.T. Pegg, M.R. Bendall, J. Magn. Reson., 1982, 48, 323.

5 G.T. Andrews, I.J. Colquhoun, W McFarlane, S.O. Grim, J. Chem. Soc. Dalton Trans., 1982, 2353.

6 H.C.E. McFarlane, W. McFarlane, D.S. Rycroft, J. Chem. Soc. Dalton Trans., 1976, 1616.

7 G. Parkin, personal communication.

8 A. Berry, personal communication.

9 S.F. Gheller, T.W. Hambley, J.R. Rodgers, R.T.C. Brownlee, M.J. O'Connor, M.R. Snow, A.G. Wedd, Inorg. Chem., 1984, 23, 2519.

10 D.J. Santure, K.W. McLaughlin, J.C. Huffman, A.P. Sattelberger, Inorg. Chem., 1983, 22, 1877.

11 M. Minelli, J.H. Enemark, A. Bell, R.A. Walton, J. Organomet. Chem., 1985, 284, 25.

12 D.J. Santure, J.C. Huffman, A.P. Sattelberger, Inorg. Chem., 1985, 24, 371.

13 T.A. Carlson, C.C. Lu, T.C. Tucker, C,W. Nestor, F.B. Malik, Oak Ridge National Laboratory, 1970, pp 1-29.

14 H.S. Gutowsky, C.J. Jameson, J. Chem. Phys., 1964, 40, 1714.

15 C.J. Jameson, J. Mason, Chapter 3 in "Multinuclear NMR", Plenum, 1986.

Chapter 12: Temperature Independent Paramagnetism Studies

Section 1: Introduction

Temperature independent paramagnetism arises by a coupling of the ground state of the system with excited states under the influence of a magnetic field.[1] It is of the order of 0-500 emu mol^{-1}. So, nuclear magnetic shielding and diamagnetic susceptibility depend on the same paramagnetic and diamagnetic currents.

The magnetic susceptibility χ is the sum of the diamagnetic and paramagnetic contributions.[2]

$$\chi = \chi_d + \chi_p$$

$$\sigma = \sigma_d + \sigma_p$$

$$\chi_d = \left(\frac{-N\mu_o}{4\pi}\right)\left(\frac{2e^2\langle r^2\rangle}{3m}\right)$$

$$\sigma_d = \frac{\mu_o}{4\pi}\frac{e^2}{3m}\langle O|\Sigma_j r_j^{-1}|O\rangle$$

$$\chi_p = \frac{N\mu_o}{4\pi}\frac{2\mu_B^2}{3}\Sigma\left[\frac{\langle O|L|n\rangle\langle n|L|O\rangle}{E_n - E_o}\right]$$

$$\sigma_p = \frac{-\mu_o\mu_B^2}{3\pi\hbar^2}\Sigma_j\left[\frac{\langle O|\Sigma_j L_j|n\rangle\langle n|\Sigma_j (L_j r_j^{-3})O\rangle + cc}{(E_n - E_o)}\right]$$

Therefore[3] $\sigma_d \cong -2\langle r^{-3}\rangle\chi_d/N$

$\sigma_p \cong -2\langle r^{-3}\rangle\chi_p/N$

where N is the Avogadro constant

The radical factor $\langle r^{-3}\rangle$ appears only in the nuclear magnetic shielding because the nucleus samples the magnetic field from its vantage point. Therefore, it was hoped that a correlation would be found between the temperature independent paramagnetism and the molybdenum chemical shift.

Section 2: Results and Discussion

The magnetic susceptibilities in emu g^{-1}, of a variety of molybdenum compounds were measured by Dr. S. Swithenby, Physics Department, The Open University using a superconducting quantum interference device (SQUID). Values of the TIP for the molybdenum atom were calculated using the Pascal empirical scheme

$$\chi_M = \sum_A n_A \chi_A + \lambda_p$$

χ_M = molar susceptibility

χ_A = contribution characteristic of atom A

n_A = number of atoms A in the molecule

λ_p = constitutive correction depending on the chemical nature of the various groups present.

Table 12.2.1 shows the magnetic susceptibility data for the molybdenum compounds measured by Dr. S. Swithenby and their ^{95}Mo chemical shifts. The error involved can be great. One reason is the limited amount of sample available, commonly less than half a gram, ideally 2g sample masses should be used.[4] The high molecular masses of some of the samples can act to increase the error involved in the measurements. The values of Pascal constants used may be another source of inaccuracy. These may be improved in some cases by a measurement of the ligand, for example dppe which is an air stable white solid. Care must be taken in the handling of the samples for magnetic susceptibility measurements of this type, for example the use of nickel spatulas should be avoided as these may introduce trace ferromagnetic impurities.[4] It may be that the stainless steel cannulae used to transfer air-sensitive solutions can introduce trace impurities. The present method of measurement of the magnetic susceptibility adopted by Dr. Swithenby

Table 12.2.1

Sample	δ^{95}Mo	$10^6\chi$ /emu g^{-1}	$10^6\chi_M$ /emu mol^{-1}	ligand[g] Contribution $10^6\chi_l$ /emu mol^{-1}	$10^6\chi_{Mo}$ /emu mol^{-1}	Mass of Sample/g
$[Mo(dppe)_2H_4]$[a]	-1813	0.6 ± 0.2	-538	-582	44 ± 180	0.25
$[Mo(dppe)(N_2)_2]$[c]	-787	1.9 ± 0.1	1081	-592	2393 ± 94[h]	0.47
$Na_2[MoO_4].2H_2O$ [d] (1)	0	-0.18 ± 0.2	-44	-42	-2 ± 4	1.88
$[Mo_3O_2(OAc)_6(H_2O)_3][BF_4]_2$ [e]	1076	0.5 ± 0.1	451	-268	90 ± 30	0.41
$[Bu^n_4]_2[MoS_4]$[c] (2)	2260	-0.4 ± 0.2	-283	-474	191 ± 71[k]	0.47
$[Mo_2(O_2CH)_4]$[g] (5)	3768	0.23 ± 0.15	86	-63	75 ± 27	
$[Mo_2(PMe_3)_4Br_4]$[b,j] (4)	3008	-0.3 ± 0.02	-245	-405	80 ± 9	
$[Mo_2(PMe_3)_4Cl_4]$[a,j] (3)	3008	-0.37 ± 0.02	-236	363	64 ± 7	
$[Mo_2(O_2CCF_3)_4]$[a] (6)	3874	-0.13 ± 0.04	-84	-150	33 ± 13	0.90

Notes for Table 12.2.1.

General note: emu are not S.I. units but are in common use, including in the published tables (ref 5).

a compound supplied by author

b compound supplied by S.K.Habron

c compound supplied by Dr.R.Richards and M.Hughes, ARC Unit of Nitrogen Fixation.

d commercial sample recrystallised from water.

e compound supplied by Prof.F.A.Cotton, Texas A and M University U.S.A.

f compound supplied by V.C.Gibson; sample gave dubious ^{95}Mo signal.

g values of Pascal constants from ref 5

h probably contains ferromagnetic impurity

j samples recrystallised from toluene/light petroleum

k sample had ferromagnetic moment in zero field so the quoted value of χ should be treated with suspicion

required the samples to be air stable in the solid state, which is a limitation on the type of compound that can be studied in this way.

Table 12.2.2 shows magnetic susceptibility data and metal chemical shifts of molybdenum compounds, collected from the literature.

Figure 12.2.1 is a plot of $10^6\chi_{Mo}$/emu mol^{-1} versus δ^{95}Mo/ppm for the compounds listed in tables 12.2.1 and 12.2.2. Although there is considerable scatter a general trend to an increase in χ_{Mo} with a decrease in ^{95}Mo shielding is discernable. It must be remembered that the metal shielding is dependent upon the radial term, which is linked with nephelauxetic effects of ligands (see Chapter 3, Section 1), whereas the TIP is not so a linear plot would only be expected if the radial term is constant.

Table 12.2.2

Compound	δ^{95}Mo	$10^6\chi_M$ /emu mol^{-1}	Ligand[f] Contribution $10^6\chi_l$	$10^6\chi_{Mo}$ /emu mol^{-1}
$[Mo(\eta\text{-}C_5H_5)(CO)_3H]$ (7)	-2047[a]	-130	-62	-62
$[Mo(CO)_6]$ (8)	-1857[b]	-74	-26	-48
$[Mo(CO)_3(PF_3)_3]$ (9)	-1857[b]	-185	-149	-36
$[Mo(PF_3)_6]$ (10)	-1857[b]	-288	-271	-17
$K_4[Mo(CN)_8]$ (11)	-1309[c]	-220	-173	-47
$[MoO_2(acac)_2]$ (12)	-45[d]	-80	-122	42
$Na_2[MoO_4]$ (13)	0[c]	-21	-32	11
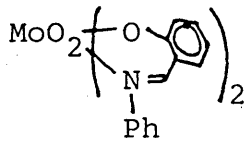 (14)	ca.100	-202	-230	28
$H_2[Mo_3O_4(ox)_3(H_2O)_3]$	1044[e]			
$K_2[Mo_3O_4(ox)_3(H_2O)_3]$ (15)				176.5[g]

a ref 6, b ref 7, c ref 8, d ref 9, e ref 10,

f calculated from Pascal constants from ref 5,

g ref 5.

Figure 12.2.1. $10^6\chi_{Mo}$ versus $\delta^{95}Mo$

Numbers in parentheses refer to the numbering system used in tables 10.2.1 and 10.2.2.

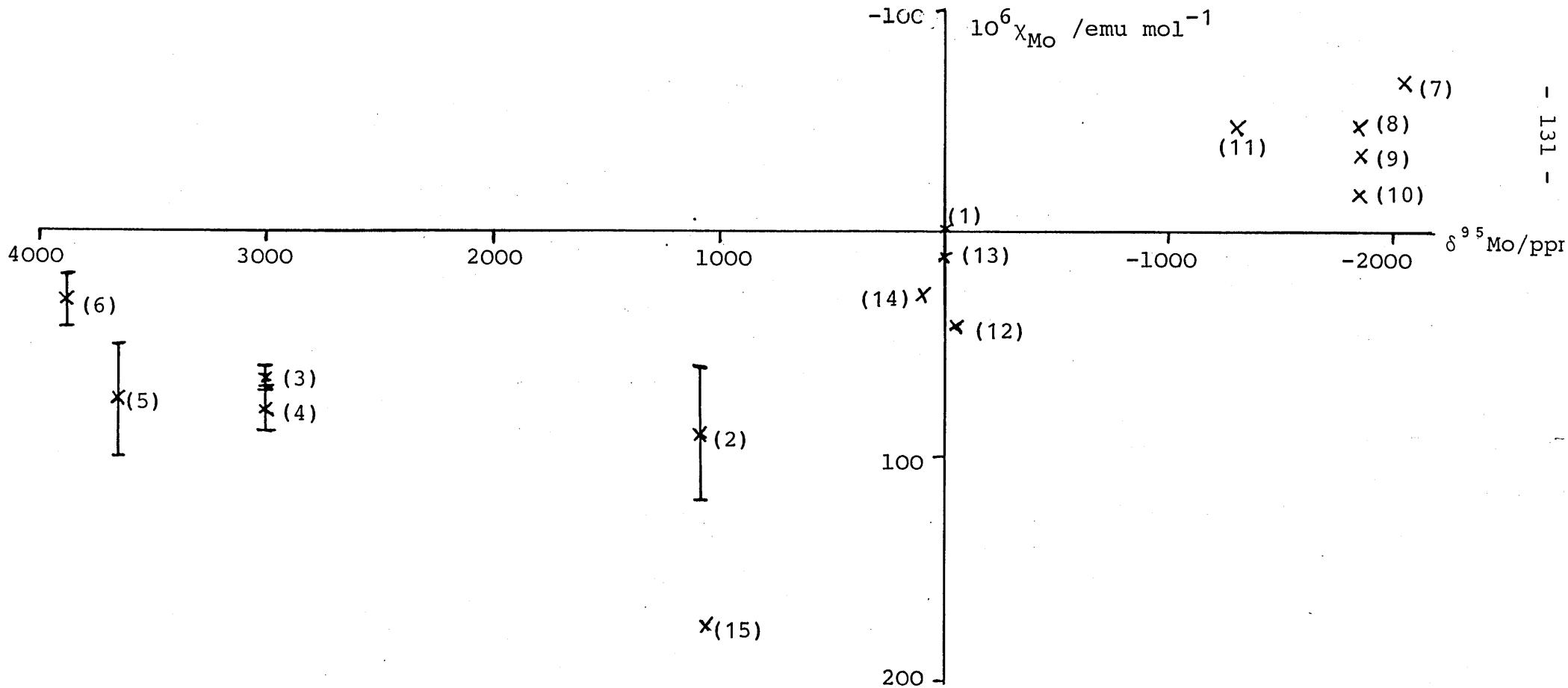

References for Chapter 12

1 F.A. Cotton, G. Wilkinson "Advanced Inorganic Chemistry" 4th edition, Wiley 1980.

2 F.E. Mabbs, D.J. Machin, "Magnetism and Transition Metal Complexes", Chapman & Hall, 1973.

3 J. Mason, Adv. in Inorg. Chem. Radiochem., 1979, 199.

4 S. Swithenby, personal communication.

5 Landolt-Börnstein, Physikalisch-Chemische Tabellen, New Series Magnetic Properties of Transition Metal Compounds, Volumes II/2,8,10,11.

6 J.Y. Le Gall, M.M. Kubicki, F.Y. Petillon, J. Organomet. Chem. 1981, 221, 287.

7 J.T. Bailey, R.J. Clark, G.C. Levy, Inorg. Chem., 1982, 21, 2085.

8 O. Lutz, A. Nolle, P. Kroneck, Z. Naturforsch., 1976, 31a, 454.

9 K.A. Christensen, P.E. Miller, M. Minelli, T.W. Rockway, J.H. Enemark, Inorg. Chim. Acta, 1981, 56, L27.

10 S.F. Gheller, T.W. Hambley, R.T.C. Brownlee, M.J. O'Connor, M.R. Snow, A.G. Wedd, J. Am. Chem. Soc., 1983, 105, 1527.

Chapter 13: Experimental

Section 1: Synthesis

Most of the compounds studied were air sensitive so manipulations were carried out in an inert atmosphere using a dual vacuum/nitrogen line and Schlenk-glassware, the latter flame-dried when strict anhydrous conditions were necessary. Solutions and solvents were transferred through stainless steel transfer tubes using a positive pressure of nitrogen. Mixtures were filtered in a similar way using a modified transfer device which could be fitted with either filter paper or glass fibre filter discs. All solvents were deoxygenated prior to use by repeated pumping followed by saturation with nitrogen. When required, solvents were dried by refluxing over appropriate drying agents (hydrocarbon solvents and THF, molten K, Na or an alloy of the two; CH_2Cl_2, P_2O_5; MeCN, CaH_2).

For the synthetic methods used please see the tables at the end of the Chapter.

N.m.r. samples were prepared under N_2 in a 10 mm n.m.r. tube fitted with a screwcap and rubber septum. Alternatively, especially in the case of extremely air and/or moisture sensitive samples, the solution was transferred to a 10 mm n.m.r. tube and frozen at -196^{o} C, then the tube was sealed under vacuum.

Section 2: Spectroscopy

N.m.r. spectra were obtained on a JEOL FX90Q fitted with a multinuclear 10 mm insert (6.5 - 36.2 MHz and 84 - 90 MHz) or a low frequency 10 mm insert (2.75 MHz - 6.5 MHz) at the Open University, Milton Keynes or on a WH400 Bruker, SERC high field service, Warwick University.

When running ^{95}Mo n.m.r. spectra on the JEOL FX90Q a pre-aquisition delay of 0.5 ms was used to reduce the effects of probe ringing. When broad signals were expected the number of sampling points used was reduced and zero filling employed resulting in faster accumulation, without loss of signal intensity as all the information is contained in the early part of the F.I.D. When the signals were sharp this treatment resulted in distortion and broadening of the lines. Where the sample was poorly soluble or available in small quantity only but was expected to give a reasonably sharp line accuracy in linewidth was sacrificed for more rapid data accumulation. In these cases the linewidth is given as $\leqslant$ x Hz. Typical repetition times used were in the range 0.1 - 0.2 secs. Generally, 8K data points were used with a frequency range of 20 000 Hz. ^{95}Mo chemical shifts are given relative to 1M aqueous $[Na_2MO_4]$ at PH 11 and ^{183}W chemical shifts are given relative to 1M aqueous $[Na_2WO_4]$. The standard used for ^{31}P n.m.r. is external 85% H_3PO_4 and for ^{13}C n.m.r. tetramethylsilane. All chemical shifts are quoted in ppm relative to the standard, high frequency being positive.

For a discussion of the n.m.r. techniques used for observing ^{183}W resonances please see Chapter 11.

Electronic spectra were run using cells adapted for air sensitive work, with a teflon tap and cone on a Perkin Elmer 552 spectrometer.

Compound	Chapter	Synthetic Method	Reference
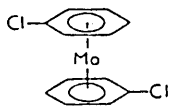	4	Metal vapour synthesis. Mo atoms + C_6H_5Cl	1
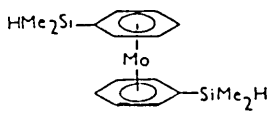	4	Metal vapour synthesis. Mo atoms + $C_6H_5SiMe_2H$	2
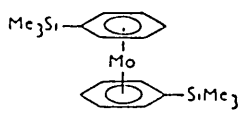	4	Treatment of $[Mo(C_6H_5Cl)_2]$ with Bu^tLi followed by Me_3SiCl	1
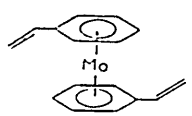	4	Treatment of $[Mo(C_6H_5Cl)_2]$ with $CH_2CHMgCl$, work up under strictly anhydrous conditions	2
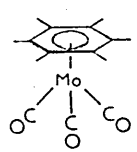	4	$[Mo(CO)_6]$ and C_6Me_6 in refluxing hexane	17
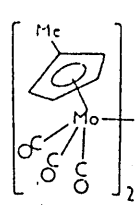	5	$[Mo(CO)_6]$ in refluxing methylcyclopentadiene	3

continued.....

Compound	Chapter	Synthetic Method	Reference
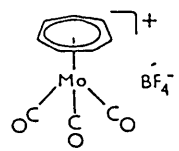	5	$[Mo(\eta^6\text{-}C_7H_8)(CO)_3]$ with $[Ph_3C]^+[BF_4]^-$	4
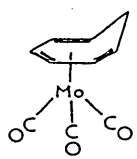	5	$[Mo(CO)_6]$ and C_7H_8 in refluxing n-butyl ether	5
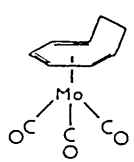	5	C_8H_{10} prepared by refluxing together C_8H_8, Zn dust and KOH followed by steam distillation. $[Mo(CO)_3(MeCN)_3]$ from $[Mo(CO)_6]$ in refluxing MeCN. C_8H_{10} and $[Mo(CO)_3(MeCN)_3]$ in refluxing hexane gives product.	6 7
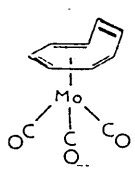	5	$[Mo(CO)_3(MeCN)_3]$ and C_8H_8 in refluxing hexane.	8
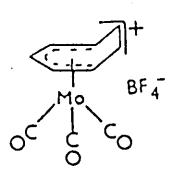	5	$[Mo(\eta^6\text{-}C_7H_8)(CO)_3]$ with aqueous HBF_4.	9

continued.....

Compound	Chapter	Synthetic Method	Reference
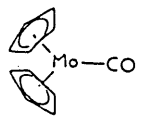	6	Reduction of $[MoCp_2Cl_2]$ with Na/Hg alloy under CO	10
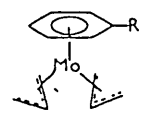	7	$[Mo(\eta\text{-}C_6H_5R)(\eta\text{-}C_3H_5)Cl]_2$ and $[C_3H_5MgCl]$. $[Mo(\eta\text{-}C_6H_5R)(\eta\text{-}C_3H_5)Cl]_2$ from $[Mo(\eta\text{-}C_6H_5R)_2]$ and $[C_3H_5Cl]$.	11
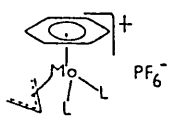	7	$[Mo(\eta\text{-}C_6H_6)(\eta\text{-}C_3H_5)Cl]_2$ and the appropriate ligand in refluxing ethanol. Precipitation of the product using aqueous $[NH_4PF_6]$.	12
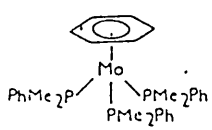	7	$[Mo(\eta\text{-}C_6H_6)_2]$ and $[PMe_2Ph]$ in xylene at 140 C.	13
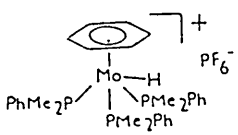	7	$[Mo(\eta\text{-}C_6H_6)(PMe_2Ph)_3]$ and hydrochloric acid. Precipitation of the product using aqueous $[NH_4PF_6]$.	13

continued.....

Compound	Chapter	Synthetic Method	Reference
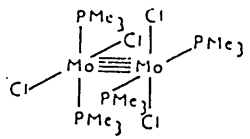	8	$[Mo_2(O_2CCH_3)_4]$, Me_3SiCl and PMe_3 in THF. $[Mo_2(O_2CCH_3)_4]$ from $[Mo(CO)_6]$ in refluxing glacial acetic acid.	14,15
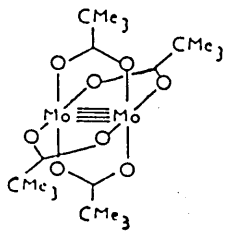	8	$[Mo(CO)_6]$ and CMe_3CO_2H in refluxing 1,2-dichlorobenzene.	16
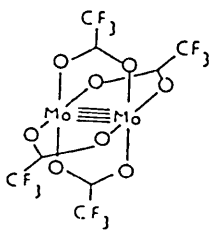	8	$[Mo_2(O_2CCH_3)_4]$, CF_3CO_2H and $[(CF_3CO_2)_2O]$ refluxed together.	18
$[Mo(MeCp)(CO)_2]_2$	8	N_2 bubbled through $[MoMeCp(CO)_3]_2$ in refluxing diglyme.	19
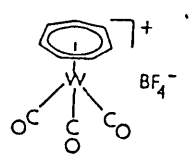	11	As for corresponding molybdenum compound, starting from $[W(CO)_6]$.	20

References for Chapter 13.

1 P.R. Brown, D. Phil. Thesis, Oxford, 1982.

2 I. Treurnicht, D. Phil. Thesis, Oxford, 1984.

3 R.B. King, "Organometallic Syntheses", Academic Press, New York, 1965, p.109.

4 H.J. Dauben Jr., L.R. Hornen, J. Am. Chem. Soc., 1958, 80, 5570.

5 F.A. Cotton, J.A. McCleverty, J.E. White, Inorg. Syn., 1969, 9, 121.

6 British Patent, 773, 225
Chem. Abstr. 1957, 51, 13915c.

7 R. Aumann, S. Winstein, Tetrahedron Lett., 1970, 903.

8 S. Winstein, H.D. Kaesz, C.G. Kreiter, E.C. Frederich, J. Am. Chem. Soc., 1965, 87, 3267.

9 A. Salzer, H. Werner, J. Organomet. Chem., 1975, 87, 101.

10 J.L. Thomas, J. Am. Chem. Soc. 1973, 95, 1838.

11 M.L.H. Green, L.C. Mitchard, W.E. Silverthorn, J. Chem. Soc., Dalton Trans., 1973, 1952.

12 M.L.H. Green, L.C. Mitchard, W.E. Silverthorn, J. Chem. Soc. Dalton Trans., 1973, 2177.

13 M.L.H. Green, L.C. Mitchard, W.E. Silverthorn, J. Chem. Soc. 1971, 2929.

14 S.K. Habron, Part II Thesis, Oxford, 1983.

15 T.A. Stephenson, E. Bannister, G. Wilkinson, J. Chem. Soc., 1964, 2538.

16 F.E. McCanley, J.L. Templeton, T.J. Colburn, V. Katovic. R.J. Hoxmeier, Adv. Chem. Ser., 1976, 150, 318.

17 A. Pidcock, J.D. Smith, B.W. Taylor, J. Chem. Soc. (A), 1967, 872.

18 F.A. Cotton, J.G. Norman Jr., J. Co-ord. Chem., 1971, 1, 161.

19 M.D. Curtis, N.A. Fotinos, L. Messerle, A.P. Sattelberger, Inorg. Chem., 1983, 22, 1559.

20 R.B. King, A. Fronzaglia, Inorg. Chem., 1966, 5, 1837.